MOLECULAR MECHANISMS OF MOUSE ADENOVIRUS TYPE 1 PATHOGENESIS

by

LEI FANG

(Under the direction of Robert Ivarie)

ABSTRACT

Both viral genes and host factors contribute to the final outcome of mouse adenovirus type 1 (MAV-1) infection. MAV-1 early region 1A (E1A) encodes a virulence gene in viral infection of mice. An unbiased experimental approach, a GST pull-down, was used to screen for cellular proteins that interact with E1A protein. We identified mouse Sur2 (mSur2), a subunit of Mediator complex, as a protein that binds to MAV-1 E1A. Conserved region 3 (CR3) of MAV-1 E1A was mapped as the region required for Sur2-E1A interaction. Studies on the functions of Sur2 using mouse embryonic fibroblasts (MEFs) showed that there was a multiplicity-dependent growth defect of MAV-1 in $Sur2^{-/-}$ MEFs compared to $Sur2^{+/+}$ MEFs. The viral replication defects in $Sur2^{-/-}$ MEFs appeared to be due at least in part to a defect in viral early gene transcription.

Further study of the contributions of E1A to mSur2 function in MAV-1 replication using E1A mutant viruses suggests that mSur2 functions through E1A CR3 interaction-dependent and -independent pathways in cell culture. Moreover, titrations of viral yields from infected brains of four inbred strains of mice showed that E1A null (*pm*E109) and CR3Δ (*dl*E106) mutant viruses had a significant defect in viral replication compared to wt MAV-1 in all these strains of mice.

This result supports the hypothesis that MAV-1 E1A-mSur2 interaction is important in MAV-1 replication in mice.

MAV-1 infects only brain microvascular endothelial cells (ECs), and causes dose-dependent encephalomyelitis and inflammatory cell accumulation in the brain blood vessels. The expression of cell adhesion molecules such as ICAM-1, VCAM-1, and E-selectin on ECs mediates the adhesion and permeation of lymphocytes and leucocytes into the inflammatory lesions. The expression levels of VCAM-1, ICAM-1, and E-selectin were tested on one established cell line, mouse brain microvascular endothelial cells (MBMECs). Wt MAV-1 infection did not alter expression of these cellular adhesion molecules, whereas cytokines TNF-α and IFN-γ induced VCAM-1 and ICAM-1 expression. Our data suggest that MAV-1 infection may not directly induce the expression of cellular adhesion molecules on endothelial cells in mouse brain, but could do so through an indirect mechanism, such as by inducing cytokine expression.

INDEX WORDS: Mouse adenovirus type 1, pathogenesis, E1A, mSur2, viral replication, protein-protein interaction, GST pull-down, cellular adhesion molecules, MBMEC, endothelial cells

MOLECULAR MECHANISMS OF MOUSE ADENOVIRUS TYPE 1 PATHOGENESIS

by

LEI FANG

M.D., Shanghai Medical University, P. R. China, 1996

M. S., Shanghai Medical University, P. R. China, 1999

A Dissertation Submitted to the Graduate Faculty of the University of Georgia in Partial Fulfillment of the Requirements for the Degree

DOCTOR OF PHILOSOPHY

ATHENS, GA

2004

MOLECULAR MECHANISMS OF MOUSE ADENOVIRUS TYPE 1 PATHOGENESIS

by

LEI FANG

Major Professor: Robert Ivarie

Committee: Katherine Spindler
Richard Meagher
Mary Bedell
Zhen Fang Fu
Sidney Kushner

Electronic Version Approved:

Maureen Grasso
Dean of the Graduate School
The University of Georgia
December 2004

ACKNOWLEDGMENTS

I thank Kathy Spindler, Marty Moore, Gwen Hirsch, Adriana Kajon, Caroline Ingle, Carla Sturkie, Amanda Welton, Bob Ivarie, Sidney Kushner, Mike Terns, Wei Zhang, Mike Imperiale, Jason Weinberg, Mary Lutzke, Maria Ow, Ivan Mott, Libby McKinney, Muthugapatti Kandasamy, Anne Marie, Lucia Pawloski, Yujing Li, Liqin Zhou who trained and helped me at the bench. I am grateful to my committee members, Kathy Spindler, Bob Ivarie, Rich Meagher, Mary Bedell, Zhen Fu, Massimo Palmarini and Sidney Kushner for suggestions and encouragement. I also thank the great attention of my ad hoc University of Michigan committee members, Mike Imperiale, Gary Huffnagle, and Rosemary Rochford. I am grateful for the efforts of the monoclonal antibody facility at the University of Georgia and the Michigan Proteomics Consortium. Many thanks go to the office staffs of both the Genetics Department at the University of Georgia and the Microbiology and Immunology Department at the University of Michigan.

I am especially grateful to Kathy Spindler for being my mentor and advisor on not only scientific training, but also cultural exploring. Without her enormous amount of time, great patience, consistent encouragement, constructive suggestions, I would not have gotten this far.

I would like to thank Marty Moore, Carla, Amanda, Maggie, Chenoo, Anne Marie, Liqin, Yujing, Scott Lu Bin, David Zhang, Weicheng Zhang, Wenduo Zhou, Xuehe Li, Ye Feng and Yan Xu, Kai Yang and Xuelin Bian for their friendship.

And last but not least, I dedicate this work to my parents, brother and sister. It is with their understanding and unconditional support that I was able to complete this work.

TABLE OF CONTENTS

Page

CHAPTER 1

INTRODUCTION AND LITERATURE REVIEW

Members of the family *Adenoviridae* are non-enveloped, icosahedral viruses that replicate in the nucleus. Their linear, double-stranded genome DNA molecules are 26-45 kbp in size and rank as medium-sized among the DNA viruses (26, 99). In addition to four accepted genera, there is a partial genome sequence of a fish adenovirus, implying a fifth genus (5). Adenoviruses infect vertebrates from fish to humans. *Mastadenovirus* and *aviadenovirus* originate from mammals and birds, respectively. *Atadenovirus* and *siadenovirus* have a broader range of hosts, including various ruminants, birds and reptiles. The similarities between phylogenetic trees for adenovirus protease and the small subunit of host mitochondrial rRNA indicate that adenoviruses have largely co-speciated with their hosts (5). The species-specific nature of adenoviruses is demonstrated by the facts that mastadenoviruses infect mammalian hosts exclusively and that aviadenoviruses have been found only in birds (5).

Human adenoviruses (hAds) are the most extensively studied adenoviruses. They were first isolated from patients with respiratory illness by Rowe et al. (94) and Hilleman and Werner (53) in 1953. They have been established as a model system to study DNA replication, mRNA transcription and processing, cell cycle regulation, and apoptosis in molecular biology. Moreover, hAds are being used to develop vectors for gene therapy and vaccines (43, 50, 58, 108). However, little is known about the pathogenesis of hAd infections. There are at least two reasons why study of pathogenesis of adenovirus infection is becoming more and more critical. First, hAd has emerged as important pathogen in immunocompromised patients (20, 55, 110). There are currently more than 51 distinct hAd serotypes (99). hAd infections generally have few pathognomonic signs and symptoms in immunocompetent adults. However, in immunocompromised hosts, including AIDS patients and pediatric bone marrow transplant patients, hAds can cause serious infections with a high mortality rate (69, 110). Adenoviruses are

associated with acute pneumonia in children in developing countries, where they are a major cause of illness and death (65). Second, design of more effective gene therapy vectors and therapeutic vaccines requires a deeper understanding of hAd pathogenesis. One problem in using hAd as gene therapy vectors is host immune responses to hAd vectors. hAds have immunoregulatory properties (55, 99). The host immune system limits the efficiency of adenovirus-mediated gene therapy (130). The immunogenicity of adenoviruses has been used in immunotherapy and generating therapeutic vaccines (80). However, an understanding of host immune response to hAd is essential to improve the safety and effectiveness of hAd vectors and vaccines.

The limited knowledge of hAd pathogenesis is due in part to the strict species-specificity of adenoviruses. A productive infection does not typically occur in a nonpermissive host. Infections of mice and cotton rats with nonphysiological doses of hAds have had limited success in developing an animal model (41, 109). In contrast, the use of mouse adenovirus type 1 (MAV-1) in its natural host, mice, is an excellent model to study adenovirus pathogenesis. The availability of mouse genome sequence and the various genetic and immunological tools for mouse study also facilitates our understanding of adenovirus pathogenesis.

A. hAd E1A and its interacting proteins

There are many advantages of adenovirus that make it an ideal model in molecular virology. The virus is easily propagated to produce high titer stocks, and the viral genome is readily manipulated, facilitating the study of adenovirus gene functions by mutational analysis. Studies of adenovirus-infected cells have made numerous contributions to our understanding of viral and cellular gene expression and regulation, DNA replication, cell cycle control, and cell growth regulation (99). Viral early genes are responsible for establishment of an optimal

environment for viral replication, setting up viral systems that protect the infected cells from various antiviral defenses of the host organism and synthesizing viral gene products needed for viral DNA replication. Although the early genes in human adenovirus (hAd) have been demonstrated to be involved in a variety of cellular processes, such as transformation, oncogenesis, the cell cycle, mRNA splicing and transport, transcriptional activation and repression and apoptosis (55, 99, 121, 123), little is known about their roles in the course of pathogenesis.

hAd E1A is the most thoroughly studied adenovirus gene, mainly because of its transformation and transcriptional activation propertites. It is required for transformation of non-permissive cells and induction of tumors in animals (14). E1A activates transcription of other viral early genes (8, 62), and is important for viral replication (49, 99, 127). hAd2/5 E1A produces two closely related, alternatively spliced transcripts, which give two major proteins of 243 and 289 amino acids (aa), respectively (8, 98). Three conserved regions (CR1, CR2, CR3) have been identified within the first exon of E1A gene when comparing a variety of human serotypes (86). E1A is the first viral transcription unit to be expressed after the viral chromosome reaches the nucleus. Transcription of hAd E1A gene is controlled by a constitutively active promoter that includes two enhancer elements (99). The E1A proteins do not exhibit sequence-specific DNA binding (99), but they function as transcription regulators by various strategies involving both direct and indirect binding to cellular proteins.

The three conserved regions as well as the N-terminus and C-terminus of the E1A proteins are all involved in protein-protein interactions. Different proteins that interact with hAd E1A protein continue to be identified and illustrate the complexity of the molecular basis of viral-host interactions. The well-established interactions of E1A-pRb and E1A-p300 illustrate

how hAd E1A regulates the cell cycle of host cells (49, 99). Adenovirus propagation depends on the transcription, translation, and DNA replication machineries of host cells for its own replication cycle. Regulation of cell cycle by pulling cells from G0/G1 to S phase is therefore critical for adenovirus to get access to the host machineries, thereby creating an optimal environment for viral replication. The key to understanding how hAd E1A proteins manipulate cell cycle regulation came from the observation that a set of cellular proteins can be coimmunoprecipitated with the E1A proteins (49, 99). E1A can drive resting cells into S phase by either binding Rb through CR1 and CR2 (23, 32, 119) or by binding the transcription coactivator CBP/p300 through CR1 and the poorly-conserved N-terminus (105, 128). The D-L-X-C-X-E motif in the CR2 domain is essential for binding to pRb, with an auxiliary role from the N-terminal portion of CR1 domain to stabilize the interaction (56, 114, 120).

In addition to Rb, E1A binds to the related pocket proteins such as p107 and p130. Recent reviews of the Rb-E2F pathways and CBP/p300 functions illustrate the importance of those factors in cell cycle control and other processes (31, 44, 48). By liberating E2F transcription factors and preventing their re-association with Rb, E1A disrupts the normal cell cycle, pulling cells from G_0/G_1 phase to S phase. The released E2F is then able to bind to and activate transcription of its target genes important for DNA replication and entry into S phase. These include genes that contain E2F binding sites in their promoters, such as thymidine kinase, thymidylate synthetase, dihydrofolate reductase (DHFR), ribonuleotide reductase, DNA polymerase α, c-myb, cdc2, c-myc, and N-myc (87).

E1A proteins also facilitate cell cycle progression by binding to p300/CBP. The p300 binding sites on E1A include the N-terminus and the C-terminus of the CR1 domain (113). The E1A mutants that contain intact p300/CBP binding sites but lack CR2 and therefore are unable to

bind to pRb can still stimulate cellular DNA synthesis. This suggests that there are at least two independent pathways by which hAd E1A can stimulate host cells from G0/G1 to S phase. p300 and CBP are two closely related proteins, functioning as transcription co-activators. They contain intrinsic histone acetylase activity. P/CAF, which interacts with p300/CBP, is a histone acetyltransferase. Therefore, p300/CBP functions to facilitate gene transcription at least in part by modifying chromatin structure. E1A binds to p300/CBP to inhibit function of the latter, including acetyltransferase activity. However, the genes responsible for entry into S phase have not been identified yet.

In summary, two different regions of the E1A proteins can stimulate host cell progress from G0/G1 to S phase through two independent pathways, those involving p300/CBP and pRB family members. It is reasonable to postulate that this might provide a fail-proof mechanism for the virus to replicate in cultured cells. Alternatively, both pathways may be important for adenovirus to replicate efficiently, particularly in animal hosts, in which adenovirus presumably encounters a more complicated environment for its replication.

It has been known for a long time that hAd E1A can transactivate transcription of viral early genes, including E1B, E2, E3, and E4 (8, 62, 89). The transactivation function of E1A depends largely on the CR3 domain of the 289 aa E1A protein (42, 81, 82, 92, 122). There are two domains in the CR3 region, a zinc finger (aa 140-178) and a carboxyl (aa 180-188) domain. The zinc finger domain was defined as a transactivation domain by its ability to activate transcription when fused to a DNA-binding domain (73, 78). There is some evidence that the terminal ~10 aa in the carboxyl domain of CR3 region can bind to several cellular transcription factors (74), which might contribute to the transcription activation function of CR3.

Since E1A protein itself does not bind to DNA directly, its transactivation function must involve recruitment of one or more cellular transcription factors. By analyzing the cis-acting region of hAd5 E1B promoter, it was shown the TATA box alone in E1B responds to activation by the 289 aa E1A protein (124, 125). The TATA box is the binding site for the general transcription factor TFIID (27, 91, 96). Therefore, it was proposed that hAd E1A targets a general transcription factor to transactivate viral early genes (124, 125). The identification of TBP as an interacting protein that directly binds to the CR3 domain (54, 72) suggested that the interaction between E1A CR3 and TBP was at least in part the basis of E1A CR3 transactivation mechanism (39, 116). However, there are several pieces of experimental evidence that argue against this proposed model. First, the single amino acid mutants (V147L and C137S) of a Gal4-E1A fusion protein are severely defective in transcription activation in cultured cells and in a cell-free system (117), but they show little or no defects in E1A-TBP interaction (7). Second, a Gal4-E1A fusion protein does not interact with the pre-assembled TBP-TATA DNA complex (7). Third, systematic mutations of TBP surface residues did not support the model that the interaction between E1A CR3 and TBP is the primary mechanism for E1A CR3 transactivation (7).

Recently, Sur2 was identified as an E1A CR3-specific binding protein (15). Sur2 is a subunit of a large complex known as *Srb/Mediator* or *TRAP*, which is conserved from yeast to humans (13). E1A also binds the Mediator complex, including the Sur2 subunit, in adenovirus-infected cells and transformed cells (111). In addition, single-amino-acid mutations in the CR3 domain that show defects in transcriptional activation are also defective in binding Sur2. Therefore, it has been proposed that the recruitment of Mediator complex to DNA promoter

regions via an interaction between E1A CR3 and Sur2 is the primary mechanism for E1A CR3 transactivating transcription of viral early genes (15, 19, 107, 111).

There is evidence that E1A can remodel chromatin structure through direct and indirect binding to cellular protein complexes. Both p300/CBP and its associated protein P/CAF have histone acetyltransferase activity. Acetylation of histones weakens their interaction with DNA, producing a chromatin structure that facilitates transcription. The inhibition of some cellular enhancer elements such as IL-6 (59) and rat insulin (105, 106) by E1A (93) is thought to inhibit p300/CBP activity and simultaneously displace P/CAF (47, 105, 115, 126). Recently, p400 (37) and TRRAP (29, 71) were found to interact with the N-terminus of E1A. p400 contains a region that is homologous to SWI/SNF2 in yeast, which has intrinsic ATP-dependent DNA helicase activity that remodels chromatin to modulate transcriptional activation and repression (37). The p400 complex has been shown to have ATPase and helicase activities (37). TRRAP is a component of various large histone acetyltransferase (HAT) complexes, including TIP60 complex, SAGA complex containing GCN5 or P/CAF (36). The interaction between E1A and TRRAP/GCN5 complex during adenovirus infection in cells has been demonstrated (71), suggesting that E1A may modulate cellular transcription programs to facilitate viral replication by recruiting HAT activity to viral and cellular promoter regions. However, more definitive experiments are needed to address the biologically relevant functions of HAT complexes in adenovirus replication. Since the N-terminus of E1A is the region required for interacting with p300/CBP (112), p400 (37), and TRRAP (29), the contribution from each interaction for adenovirus infection remains a challenge because E1A mutants that distinguish these protein-protein interactions have not yet been isolated.

B. E1A function in MAV-1 infection in vitro (in cell culture) and in vivo (in mice)

MAV-1 was first isolated by Hartley and Rowe (1960) (51). The DNA genome sequence of MAV-1 has been determined (79). The overall viral gene organization of MAV-1 is very similar to that of hAds (Fig. 1.1). MAV-1 DNA synthesis was observed as early as 20 h post infection (p.i.) in L929 cells infected at an MOI of 10 (104). An increase in virus titer relative to input virus in 3T6 cells and mouse brain microvascular endothelial cells (MBMECs) is observed at 36-48 h p.i. (21, 129). Cytopathic effects (CPE) are first detected at 36-48 h p.i at an MOI of 5 and are similar to other adenoviruses: infected cells round up, become refractile and eventually detach from the cell culture plates (104). The pathogenicity of MAV-1 infection in mice is dependent on viral doses, viral strains, and mouse strains (45, 70, 84, 85, 103). MAV-1 infects endothelial cells and cells of the monocyte-macrophage lineage in outbred (64), C57BL/6 (B6) mice (22, 84), and SJL/J mice (103), whereas hAds infect epithelial cells in humans (55). Mouse spleen and brain are two major organs targeted by MAV-1 infection, yielding the highest levels of infectious viruses (103). MAV-1 causes acute and persistent infection in mice (84, 101). Depending on the viral dose, the disease signs observed range from hunched posture, ruffled coat, and abdominal breathing to mild ataxia, hyperreflexia, posterior paralysis and neurological disease signs (70), which are correlated with encephalomyelitis in mouse brains and spinal cords (22, 45, 64, 84).

Most MAV-1 gene functions have not been studied except for MAV-1 E1A and E3. E1A is the focus of this dissertation, and Chapters 2 and 3 will address a particular E1A function. There are certain similarities and differences in protein structure between MAV-1 E1A and hAd E1A. In contrast to the hAds that encode two major E1A mRNAs, MAV-1 encodes only a single major E1A mRNA composed of three exons. The MAV-1 E1A protein is equivalent to the hAd

289-aa protein and is 200 aa long, containing CR1, CR2, and CR3 (3, 4) (Fig. 1.2). MAV-1 E1A is approximately 40% similar to the hAd4, hAd5, and hAd7 289-aa E1A proteins within the three conserved regions. In particular, the zinc finger domain (Cys-X_2-Cys-X_n-Cys-X_2-Cys) in CR3 and the pRb-binding motif (D-L-X-C-X-E) in CR2 are present in both hAd5 and MAV-1 E1A (3, 6, 25). Significant similarities with MAV-1 were not found outside these conserved regions. However, there are other sequences conserved in hAd E1As that are not found in the MAV-1 E1A protein coding sequence. The Arg-2 in hAds, which was shown to be important in rapid E1A turnover (100) and cooperativity with the ras oncogene in transformation (119), is not in MAV-1 E1A, although MAV-1 E1A does have an Arg at position 3. A basic pentapeptide sequence at the hAd E1A carboxy terminus, which was shown to be important for nuclear localization (76), is not present in MAV-1 E1A. Even though it has been noted that hAd E1A is present in both the nucleus and cytoplasm of cells, the significance of cytoplamic E1A protein has not been studied in detail. The single MAV-1 E1A may fulfill the functions of both the 243- and 289-aa E1A proteins of hAd2. Alternatively, MAV-1 may be deficient in particular activities of the 243-aa protein. For example, no MAV-1 transformation activity has been detected (30) (K. R. Spindler, unpublished data).

Although MAV-1 E1A conserves several functions of hAd E1A, some differences are observed in cultured cells infected with MAV-1 compared to hAds. MAV-1 E1A binds to mouse pRb and p107 as shown in an in vitro mixing experiment (102), but prior to the research in this dissertation, an interaction between MAV-1 E1A viral protein and endogenous cellular pRb and p107 proteins had not been demonstrated, nor was it known whether MAV-1 E1A bound to the other Rb family protein, p130. Surprisingly, there are no replication defects for wt MAV-1 in $Rb^{+/-}$ or $Rb^{-/-}$ mouse embryonic fibroblasts (MEFs) compared to $Rb^{+/+}$ MEFs, at least at an MOI

of 5 (129). Moreover, the biological significance of these interactions between MAV-1 E1A and Rb family proteins in MAV-1 infection has not been tested in mice. In cell culture, MAV-1 E1A is not absolutely required for viral replication, at least at an MOI of 5 (129). In fact, hAd E1A is not absolutely required for hAd replication either (38, 57, 88, 98). There is no significant difference in growth between wt MAV-1 and E1A mutant viruses, including pmE109 (E1A null mutant), dlE105 (CR1Δ mutant), dlE102 (CR2Δ mutant), and dlE106 (CR3Δ mutant) when mouse 3T6 cells or 37.1 cells (complementing cell line for E1A mutant viruses) are infected at an MOI of 5 (129). In addition, there are no replication defects for these E1A mutants in $Rb^{+/-}$ or $Rb^{-/-}$ mouse embryonic fibroblasts (MEFs) compared to wt MAV-1 at an MOI of 5 (129).

Surprisingly, the steady-state mRNA levels of several viral early genes (E1B, E3, and E4) are not reduced but rather slightly higher in E1A mutant virus-infected 3T6 cells compared to wt MAV-1-infected cells at MOIs of 1, 5, or 10 (129). Note that all the above experiments were done at a relatively high input MOIs (MOIs of 1 to 10), experimental conditions under which those E1A mutants might not show any replication defects. Interestingly, *dl*312, an E1A null mutant of hAd, shows a multiplicity-dependent phenotype (38, 57, 88, 98). At low MOIs, there is a delay and reduced expression of viral early genes, but at higher MOIs the expression of viral early genes can be enhanced (88). The multiplicity-dependent phenotype is not unique to adenoviruses. It has been observed for many viruses, including hAds (38, 57, 88, 98), herpes simplex virus type 1 (HSV-1) (18, 24, 34), cytomegalovirus (CMV) (16, 90) and African swine fever virus (ASFV) (83). Therefore, it is of interest to test those E1A mutant viruses at a low input MOI that might show replication defects in cell culture. In addition, since endothelial cells and mononuclear/macrophage lineage cells are cell types targeted by MAV-1 in mice (22, 64), using 3T6 (fibroblast cells) may not accurately reflect E1A function in MAV-1 infection.

Similar to hAd infections, MAV-1 replication in cell culture is resistant to interferon (IFN) (66). MAV-1 E1A is the primary viral gene responsible for counteracting the IFN response (66), as is hAd E1A (1, 46, 67). Like hAds, the anti-IFN effects of MAV-1 E1A are at least in part mediated by inhibiting the expression of IFN-stimulated genes. However, CR1 of hAd E1A is required for antagonizing the IFN response (1), whereas all three conserved regions (CR1, CR2, and CR3) of MAV-1 E1A are required (66). Despite this difference, the anti-IFN function of E1A is clearly conserved in hAds and MAV-1.

Functions of MAV-1 E1A have also been studied in mice. The E1A gene product is a virulence factor in MAV-1 infection in Swiss outbred mice (101) and inbred SJL/J mice, as determined by LD_{50} experiments (103). There is no difference in tissue (brain, spleen, and spinal cord) or cell type (endothelial cells and mononuclear/macrophage lineage) tropism between pmE109 (E1A null mutant virus) and wt MAV-1 (101). This suggests that E1A is not critical for establishing the tropism in MAV-1 infection in mice. There is also no significant difference in viral DNA levels between wt MAV-1 and pmE109 at 5 days p.i. in Swiss mice infected at a high dose (10^4 PFU). However, reduced levels of viral DNA are found in the brains and spleens at 14 days p.i in mice infected with pmE109 compared to wt MAV-1 at a low dose (1 PFU) (101). Hence, the viral DNA replication defect seen at a low input dose can be overcome by a high input viral dose. This suggests a multiplicity-dependent effect in MAV-1 infection in mice. However, one critical question that has not been addressed is whether the viral DNA represents newly replicated progeny viruses or simply disseminated viruses from injection. Viral yields by plaque assays or expression of viral early genes (mRNA or protein) will be more informative to elucidate the possible contributions of E1A in MAV-1 pathogenesis in mice.

C. Host factors in MAV-1 infection

The outcome of MAV-1 infections in mice is dependent on viral genes and also host factors. On one hand, identification of virulence genes, such as E1A and E3 genes in MAV-1 helps us to understand viral pathogenesis. On the other hand, there is different susceptibility to MAV-1 infection among different strains of mice. SJL/J mice are the most susceptible strain with a LD_{50} of $10^{-3.2}$ PFU (103). Other strains, such as C3H/HeJ, 129/J, BALB/cJ, and C57BL/6J (B6), are resistant to MAV-1 infection with LD_{50} of $> 10^{4.4}$ PFU (103). The mouse strain-dependent susceptibility to MAV-1 infection clearly demonstrates that host factors play critical roles in the outcome of MAV-1 infection. Different host susceptibility to a variety of viruses has been observed, including retroviruses (9), poxviruses (28), papovaviruses (75), rhabdoviruses (61), and herpesviruses (33, 97). The viral yields in brains from SJL/J mice are higher than those in C3H/HeJ mice (103), indicating a correlation between brain viral yields and susceptibility. This in turn suggests that control of MAV-1 replication by mouse host factors might be correlated with their susceptibility to MAV-1 infection. Sublethal irradiation of resistant C3H/HeJ mice renders them susceptible (103), suggesting a requirement of the immune system for control of MAV-1 replication. However, genetic mapping will eventually identify host genes that account for the different susceptibility.

Study of MAV-1 infection in immunodeficient mice also suggests critical roles of the immune system in MAV-1 pathogenesis (84, 85). B cells but not T cells are required for mice to survive an acute MAV-1 infection (84, 85). The protection of B cells against MAV-1 infection may be due to the role of an early T-cell-independent antiviral IgM (85). However, T cells contribute to MAV-1-induced encephalomyelitis in mice and are required for long-term (15 weeks p.i.) survival for MAV-1 infected mice (84). Strikingly, mice lacking Bruton's tyrosine

kinase (Btk) are extremely susceptible to MAV-1 infection, with a LD_{50} of 0.1 PFU (85). $Btk^{-/-}$ mice show a X-linked immunodeficiency phenotype and have reduced levels of serum immunoglobulin (natural antibody), conventional B cells, and peritoneal B-1 cells compared to control mice (68). $Btk^{-/-}$ mice are on a mixed B6 and 129 genetic background, but both B6 and 129 strain mice are resistant to MAV-1 infection (LD_{50}s $>10^{4.4}$ PFU) (103). Therefore, Btk gene is required for survival of MAV-1 infection in mice. It will be interesting to see whether the Btk gene also accounts for the different susceptibility of SLJ/J and C3H/HeJ mice to MAV-1 infection.

C1. Brain microvascular endothelial cells and cell adhesion molecules

MAV-1 is an endotheliotropic virus, infecting brain microvascular endothelial cells (ECs) and not any other cell types in the brain (22, 63). Until this result was obtained, all in vitro experiments had been carried out in mouse fibroblasts. Therefore, understanding the nature of the viral-host interaction in ECs will help to elucidate mouse adenoviral pathogenesis. The endotheliotropism is consistent with observed signs of MAV-1 disease. MAV-1 infected mice show signs of neurologic disease such as tremors, seizures, ataxia, and paralysis. Brain tissue examination shows vascular injury such as fibrinogen in perivascular spaces and inflammation such as edema and inflammatory cells within and around the vessel walls (22, 63, 84, 103).

The endothelium forms a continuous lining of the cardiovascular system, strategically positioned as an interface between the blood and all other tissues. It serves and participates in highly active metabolic and regulatory functions including control of primary hemostasis, blood coagulation and fibrinolysis, platelet and leukocyte interactions with the vessel wall, interaction with lipoprotein metabolism, and regulation of vascular tone (11). More importantly, endothelial

cells (ECs) represent by themselves a large immunologically active system (95). They are known to produce a variety of cytokines, chemokines, and cell surface adhesion molecules that are capable of inducing inflammatory processes and homing leukocytes. The major histocompatibility complex (MHC) molecules, a critical component in immune system function, are also expressed on the EC surface (12, 60, 118).

Vascular ECs are not homogeneous throughout the body. Endothelial cells derived from different vessels are phenotypically and functionally different (11). The large- and small-vessel ECs differ not only in their growth requirements, tube-forming ability, and prostaglandin secretion, but also most importantly in the production, expression, regulation and function of the cell surface adhesion molecules. Factor VIII-related antigen, alkaline phosphatase, CD31, endoglin, specific binding to lectins, uptake of acetylated LDL, and prostacyclin synthesis are generally regarded as endothelial cell markers (95), although there are some variations due to different species, tissues and/or cell culture in vitro.

Unlike most organ systems, the central nervous system (CNS) is separated from the blood by a protective cellular barrier, the blood-brain barrier (BBB). The BBB is one of the crucial factors that maintain the CNS as an immunologically privileged site. The function of the BBB has been described as a complex interaction between microvascular ECs, the underlying basement membrane and associated cells such as smooth muscle cells, pericytes, microglia, and astrocytes (12, 35, 52). ECs of brain capillaries are connected together by tight junctions with extremely high electrical resistance. Under physiological conditions, the BBB enables only the diffusion of water, ions, and some metabolites, but is highly restrictive for the passage of large molecular compounds, including immunoglobulins and all cell types. Therefore, brain microvascular ECs are important for maintaining the integrity of the BBB.

At present, it is unclear which mechanisms are responsible for the development of an immunopathological disease of the brain and how inflammation of the CNS begins. Considerable evidence has accumulated that BBB function is altered under pathological conditions, including virus infection (12). Most viruses infect the CNS via the bloodstream during viremia, although they can reach the CNS via other pathways, such as olfactory nerve and intraaxonal transport, as seen for polio and rabies viruses. Coronavirus has been found to enter the CNS of primates via the brain ECs (17). The presence of specific viral receptors on target cells is a key factor in determining the susceptibility to viral infection. In addition, cellular factors and the accessibility of the specific type of cells also contribute the permissiveness of the viral infection (2). However, the MAV-1 receptor and mechanisms of endotheliotropism of MAV-1 are unknown. It is not known how MAV-1 disseminates inside of the mouse body after injection of virus by an intraperitoneal route.

Cell adhesion molecules play a central role in cell-to-cell and cell-matrix interactions. ECs express cell adhesion molecules, which play a critical role in the inflammatory response (10, 77). ICAM-1, which belongs to the immunoglobulin gene superfamily, is a major ligand for lymphocyte function-associated antigen 1 (LFA-1, CD18/CD11a). ICAM-1 is responsible for leukocyte binding to endothelial cells via LFA-1, playing a central role in the inflammatory reaction as a signaling and co-stimulatory molecule on T-lymphocytes. Another important adhesion molecule receptor-ligand pair involved in inflammatory brain reactions is vascular cell adhesion molecule 1 (VCAM-1) and β1-integrin very late antigen 4 (VLA-4). Endothelial VCAM-1 can mediate adhesion of lymphocytes and macrophages via their integrin receptors. Selectins seem to be critically important in inflammation, and their lectin domain is responsible for adhesion (40). E-selectin is not constitutively expressed by resting endothelial cells, but its

membrane expression and synthesis may be induced by pro-inflammatory cytokines such as TNF-α and IL-1. It is mainly involved in endothelial-neutrophil interactions.

The observation of accumulated inflammatory cells in the vicinity of brain blood vessels of MAV-1 infected mice (21, 84, 85) suggests that cellular adhesion molecules might play a role in MAV-1-induced encephalomyelitis. More interestingly, an E3 null mutant virus (*pm*E314) causes less inflammatory reactions in brain than wt MAV-1 infection at a dose of 10^3 PFU at 8 days p.i. in outbred Swiss mice (21), suggesting an anti-inflammatory role of E3 gene products. In Chapter 4 we describe an investigation of expression of cellular adhesion molecules in MAV-1 infected cells.

REFERENCES

1. **Ackrill, A. M., G. R. Foster, C. D. Laxton, D. M. Flavell, G. R. Stark, and I. M. Kerr.** 1991. Inhibition of the cellular response to interferons by products of the adenovirus type-5 E1A oncogene. Nucl. Acids Res. **19:**4387-4393.
2. **Andino, R., N. Böddeker, D. Silvera, and A. V. Gamarnik.** 1999. Intracellular determinants of picornavirus replication. Trends in Microbiology **7:**76.
3. **Ball, A. O., C. W. Beard, S. D. Redick, and K. R. Spindler.** 1989. Genome organization of mouse adenovirus type 1 early region 1: A novel transcription map. Virology **170:**523-536.
4. **Ball, A. O., M. E. Williams, and K. R. Spindler.** 1988. Identification of mouse adenovirus type 1 early region 1: DNA sequence and a conserved transactivating function. J. Virol. **62:**3947-3957.
5. **Benko, M., and B. Harrach.** 2003. Molecular evolution of adenoviruses. Curr. Top. Microbiol. Immunol. **272:**3-35.
6. **Berg, J. M.** 1986. Potential metal-binding domains in nucleic acid binding proteins. Science **232:**485-487.
7. **Berk, A. J., T. G. Boyer, A. N. Kapanidis, R. H. Ebright, N. N. Kobayashi, P. J. Horn, S. M. Sullivan, R. Koope, M. A. Surby, and S. J. Triezenberg.** 1998. Mechanisms of viral activators. Cold Spring Harb. Symp. Quant. Biol. **63:**243-252.
8. **Berk, A. J., F. Lee, T. Harrison, J. Williams, and P. A. Sharp.** 1979. Pre-early adenovirus 5 gene product regulates synthesis of early viral messenger RNAs. Cell **17:**935-944.

9. **Best, S., P. Le Tissier, G. Towers, and J. P. Stoye.** 1996. Positional cloning of the mouse retrovirus restriction gene *Fv1*. Nature **382:**826-829.

10. **Bevilaqua, M. P.** 1993. Endothelial-leukocyte adhesion molecules. Annu. Rev. Immunol. **11:**767-804.

11. **Bicknell, R.** 1993. Heterogeneity of the endothelial cell. Behring Inst. Res. Commun. **92:**1-7.

12. **Bilzer, T., and L. Stitz.** 1996. Immunopathogenesis of virus diseases affecting the central nervous system. Crit. Rev. Immunol. **16:**145-222.

13. **Boube, M., L. Joulia, D. L. Cribbs, and H.-M. Bourbon.** 2002. Evidence for a mediator of RNA polymerase II transcriptional regulation conserved from yeast to man. Cell **110:**143-151.

14. **Boulanger, P. A., and G. E. Blair.** 1991. Expression and interactions of human adenovirus oncoproteins. Biochem. J. **275:**281-299.

15. **Boyer, T. G., M. E. D. Martin, E. Lees, R. P. Ricciardi, and A. J. Berk.** 1999. Mammalian Srb/Mediator complex is targeted by adenovirus E1A protein. Nature **399:**276-279.

16. **Bresnahan, W. A., and T. E. Shenk.** 2000. UL82 virion protein activates expression of immediate early viral genes in human cytomegalovirus-infected cells. Proc. Natl. Acad. Sci. USA **97:**14506-14511.

17. **Cabirac, G. F., K. F. Soike, and J. Y. Zhang.** 1994. Entry of coronvirus into primate cns following peripheral infection. Microb. Pathogen. **16:**349-359.

18. **Cai, W., and P. A. Schaffer.** 1992. Herpes simplex virus type 1 ICP0 regulates expression of immediate-early, early, and late genes in productively infected cells. J. Virol. **66:**2904-2915.

19. **Cantin, G. T., J. L. Stevens, and A. J. Berk.** 2003. Activation domain-mediator interactions promote transcription preinitiation complex assembly on promoter DNA. Proc. Natl. Acad. Sci. USA **100:**12003-12008.

20. **Carrigan, D. R.** 1997. Adenovirus infections in immunocompromised patients. Am. J. Med. **102:**71-74.

21. **Cauthen, A. N., C. C. Brown, and K. R. Spindler.** 1999. In vitro and in vivo characterization of a mouse adenovirus type 1 early region 3 mutant. J. Virol. **73:**8640-8646.

22. **Charles, P. C., J. D. Guida, C. F. Brosnan, and M. S. Horwitz.** 1998. Mouse adenovirus type-1 replication is restricted to vascular endothelium in the CNS of susceptible strains of mice. Virology **245:**216-228.

23. **Chellappan, S., V. B. Kraus, B. Kroger, K. Munger, P. M. Howley, W. C. Phelps, and J. R. Nevins.** 1992. Adenovirus E1A, simian virus 40 tumor antigen, and human papillomavirus E7 protein share the capacity to disrupt the interaction between transcription factor E2F and the retinoblastoma gene pronuct. Proc. Natl. Acad. Sci. USA **89:**4549-4553.

24. **Chen, J., and S. Silverstein.** 1992. Herpes simplex viruses with mutations in the gene encoding ICP0 are defective in gene expression. J. Virol. **66:**2916-2927.

25. **Culp, J. S., L. C. Webster, D. J. Friedman, C. L. Smith, W.-J. Huang, F. Y.-H. Wu, M. Rosenberg, and R. P. Ricciardi.** 1988. The 289-amino acid E1A protein of

adenovirus binds zinc in a region that is important for trans-activation. Proc. Natl. Acad. Sci. USA **85:**6450-6454.

26. **Davison, A. J., M. Benko, and B. Harrach.** 2003. Genetic content and evolution of adenoviruses. J. Gen. Virol. **84:**2895-908.

27. **Davison, B. L., E. R. Mulvihill, J. M. Egly, and P. Chambon.** 1983. Interaction of eukaryotic class-B transcription factors and chick progesterone-receptor complex with conalbumin promoter sequences. Cold Spring Harb Symp Quant Biol **47 Pt 2:**965-75.

28. **Delano, M. L., and D. G. Brownstein.** 1995. Innate resistance to lethal mouse pox is genetically linked to the NK gene complex on chromosome 6 and correlates with early restriction of virus replication by cells with an NK phenotype. J. Virol. **69:**5875-5877.

29. **Deleu, L., S. Shellard, K. Alevizopoulos, B. Amati, and H. Land.** 2001. Recruitment of TRRAP required for oncogenic transformation by E1A. Oncogene **20:**8270-8275.

30. **Dussaix, E., N. Faucon-Biguet, D. Samolyk, C. Boni, and P. Tournier.** 1982. Restricted replication of mouse adenovirus strain FL in mouse Balb/c cells transformed by simian adenovirus 7. Virology **116:**641-645.

31. **Dyson, N.** 1998. The regulation of E2F by pRb-family proteins. Genes Dev. **12:**2245-2262.

32. **Egan, C., T. N. Jelsma, J. A. Howe, S. T. Bayley, B. Ferguson, and P. E. Branton.** 1988. Mapping of cellular protein-binding sites on the products of early-region 1A of human adenovirus type 5. Mol. Cell. Biol. **8:**3955-3959.

33. **Ellison, A. R., L. Yang, C. Voytek, and T. P. Margolis.** 2000. Establishment of latent herpes simplex virus type 1 infection in resistant, sensitive, and immunodeficient mouse strains. Virology **268:**17-28.

34. **Everett, R. D., C. Boutell, and A. Orr.** 2004. Phenotype of a herpes simplex virus type 1 mutant that fails to express immediate-early regulatory protein ICP0. J. Virol. **78:**1763-1774.

35. **Fabry, Z., C. Neuchrist, K. Kitz, O. Scheiner, D. Kraft, and H. Lassmann.** 1994. Nervous tissue as an immune compartment: The dialect of the immune response in the cns. Immunol. Today **15:**218-228.

36. **Frisch, S. M., and J. S. Mymryk.** 2002. Adenovirus-5 E1A: paradox and paradigm. Nat Rev Mol Cell Biol **3:**441-52.

37. **Fuchs, M., J. Gerber, R. Drapkin, S. Sif, T. Ikura, V. Ogryzko, W. S. Lane, Y. Nakatani, and D. M. Livingston.** 2001. The p400 complex is an essential E1A transformation target. Cell **106:**297-307.

38. **Gaynor, R. B., and A. J. Berk.** 1983. Cis-acting induction of adenovirus transcription. Cell **33:**683-693.

39. **Geisberg, J. V., W. S. Lee, A. J. Berk, and R. P. Ricciardi.** 1994. The zinc finger region of the adenovirus E1A transactivating domain complexes with the TATA box binding protein. Proc. Natl. Acad. Sci. USA **91:**2488-2492.

40. **Geng, J. G., M. P. Bevilaqua, K. L. Moore, and T. M. McIntyre.** 1990. Rapid neutrophil adhesion to activated endothelium mediated by p-selectin. Nature **343:**757-760.

41. **Ginsberg, H. S., L. L. Moldawer, P. B. Sehgal, M. Redington, P. L. Kilian, R. M. Chanock, and G. A. Prince.** 1991. A mouse model for investigating the molecular pathogenesis of adenovirus pneumonia. Proc. Natl. Acad. Sci. USA **88:**1651-1655.

42. **Glenn, G. M., and R. P. Ricciardi.** 1987. An adenovirus type 5 E1A protein with a single amino acid substitution blocks wild-type E1A transactivation. Mol. Cell. Biol. **7:**1004-1011.

43. **Gomez-Roman, V. R., and M. Robert-Guroff.** 2003. Adenoviruses as vectors for HIV vaccines. AIDS Rev. **5:**178-185.

44. **Goodman, R. H., and S. Smolik.** 2000. CBP/p300 in cell growth, transformation, and development. Genes Dev. **14:**1553-1557.

45. **Guida, J. D., G. Fejer, L.-A. Pirofski, C. F. Brosnan, and M. S. Horwitz.** 1995. Mouse adenovirus type 1 causes a fatal hemorrhagic encephalomyelitis in adult C57BL/6 but not BALB/c mice. J. Virol. **69:**7674-7681.

46. **Gutch, M. J., and N. C. Reich.** 1991. Repression of the interferon signal transduction pathway by the adenovirus E1A oncogene. Proc. Natl. Acad. Sci. USA **88:**7913-7917.

47. **Hamamori, Y., V. Sartorelli, V. Ogryzko, P. L. Puri, H.-Y. Wu, J. Y. J. Wang, Y. Nakatani, and L. Kedes.** 1999. Regulation of histone acetyltransferases p300 and PCAF by the bHLH protein Twist and adenoviral oncoprotein E1A. Cell **96:**405-413.

48. **Harbour, J. W., and D. C. Dean.** 2000. The Rb/E2F pathway: expanding roles and emerging paradigms. Genes Dev **14:**2393-2409.

49. **Harlow, E., P. Whyte, B. R. J. Franza, and C. Schley.** 1986. Association of adenovirus early-region 1A proteins with cellular polypeptides. Mol. Cell. Biol. **6:**1579-1589.

50. **Hart, M. K.** 2003. Vaccine research efforts for filoviruses. Int. J. Parasitol. **33:**583-595.

51. **Hartley, J. W., and W. P. Rowe.** 1960. A new mouse virus apparently related to the adenovirus group. Virology **11:**645-647.

52. **Hickey, W. F., B. L. Hsu, and H. Kimura.** 1991. T-lymphocyte entry into the central nervous system. J. Neurosci. Res. **28:**254-264.

53. **Hilleman, M. R., and J. R. Werner.** 1954. Recovery of a new agent from patients with acute respiratory illness. Proc. Soc. Exp. Biol. Med. **85:**183-188.

54. **Horikoshi, N., K. Maguire, A. Kralli, E. Maldonado, D. Reinberg, and R. Weinmann.** 1991. Direct interaction between adenovirus E1A protein and the TATA box binding transcription factor IID. Proc. Natl. Acad. Sci., USA **88:**5124-5128.

55. **Horwitz, M. S.** 2001. Adenoviruses, p. 2301-2326. *In* D. M. Knipe and P. M. Howley (ed.), Fields Virology, 4th ed, vol. 2. Lippincott Williams & Wilkins, Philadelphia.

56. **Howe, J. A., and S. T. Bayley.** 1992. Effects of Ad5 E1A mutant viruses on the cell cycle in relation to the binding of cellular proteins including the retinoblastoma protein and cyclin A. Virology **186:**15-24.

57. **Imperiale, M. J., H.-T. Kao, L. T. Feldman, J. R. Nevins, and S. Strickland.** 1984. Common control of the heat shock gene and early adenovirus genes: evidence for a cellular E1A-like activity. Mol. Cell. Biol. **4:**867-874.

58. **Imperiale, M. J., and S. Kochanek.** 2004. Adenovirus vectors: Biology, design, and production. Curr. Top. Microbiol. Immunol. **273:**335-357.

59. **Janaswami, P. M., D. V. R. Kalvakolanu, Y. Zhang, and G. C. Sen.** 1992. Transcriptional repression of interleukin-6 gene by adenoviral E1A proteins. J. Biol. Chem. **267:**24886-24891.

60. **Jemison, L. M., S. K. Williams, N. Prayoonwiwat, and M. Rodriguez.** 1993. Interferon-gamma-inducible endothelial cell class II major histocompatibility complex

expression correlates with strain- and site-specifc susceptibility to experimental allergic encephalomyelitis. J. Neuroimmunol. **47:**15-25.

61. **Jin, H. K., A. Takada, Y. Kon, O. Haller, and T. Watanabe.** 1999. Identification of the murine *Mx2* gene: Interferon-induced expression of the Mx2 protein from the feral mouse gene confers resistance to vesicular stomatitis virus. J. Virol. **73:**4925-4930.

62. **Jones, N. C., and T. Shenk.** 1979. An adenovirus type 5 early gene function regulates expression of other early viral genes. Proc. Natl. Acad. Sci. USA **76:**3665-3669.

63. **Kajon, A., and G. Wadell.** 1992. Molecular epidemiology of adenoviruses associated with acute lower repiratory disease of children in Buenos Aires, Argentina (1984-1988). J. Med. Virol. **36:**292-297.

64. **Kajon, A. E., C. C. Brown, and K. R. Spindler.** 1998. Distribution of mouse adenovirus type 1 in intraperitoneally and intranasally infected adult outbred mice. J. Virol. **72:**1219-1223.

65. **Kajon, A. E., A. S. Mistchenko, C. Videla, M. Hortal, G. Wadell, and L. F. Avendaño.** 1996. Molecular epidemiology of adenovirus acute lower respiratory infections of children in the south cone of South America (1991-1994). J. Med. Virol. **48:**151-156.

66. **Kajon, A. E., and K. R. Spindler.** 2000. Mouse adenovirus type 1 replication *in vitro* is resistant to interferon. Virology **274:**213-219.

67. **Kalvakolanu, D. V. R., S. K. Bandyopadhyay, M. L. Harter, and G. C. Sen.** 1991. Inhibition of interferon-inducible gene expression by adenovirus E1A proteins - block in transcriptional complex formation. Proc. Natl. Acad. Sci. USA **88:**7459-7463.

68. **Khan, W. N., F. W. Alt, R. M. Gerstein, B. A. Malynn, I. Larsson, G. Rathbun, L. Davidson, S. Muller, A. B. Kantor, L. A. Herzenberg, F. S. Rosen, and P. Sideras.** 1995. Defective B cell development and function in Btk-deficient mice. Immunity **3:**283-299.

69. **Kojaoghlanian, T., P. Flomenberg, and M. S. Horwitz.** 2003. The impact of adenovirus infection on the immunocompromised host. Rev. Med. Virol. **13:**155-171.

70. **Kring, S. C., C. S. King, and K. R. Spindler.** 1995. Susceptibility and signs associated with mouse adenovirus type 1 infection of adult outbred Swiss mice. J. Virol. **69:**8084-8088.

71. **Lang, S. E., and P. Hearing.** 2003. The adenovirus E1A oncoprotein recruits the cellular TRRAP/GCN5 histone acetyltransferase complex. Oncogene **22:**2836-2841.

72. **Lee, W. S., C. C. Kao, G. O. Bryant, X. Liu, and A. J. Berk.** 1991. Adenovirus E1A activation domain binds the basic repeat in the TATA box transcription factor. Cell **67:**365-376.

73. **Lillie, J. W., and M. R. Green.** 1989. Transcription activation by the adenovirus E1a protein. Nature **338:**39-44.

74. **Liu, F., and M. R. Green.** 1994. Promoter targeting by adenovirus E1a through interaction with different cellular DNA-binding domains. Nature **368:**520-525.

75. **Lukacher, A. E., Y. Ma, J. P. Carroll, S. R. Abromson-Leeman, J. C. Laning, M. E. Dorf, and T. L. Benjamin.** 1995. Susceptibility to tumors induced by polyoma virus is conferred by an endogenous mouse mammary tumor virus superantigen. J. Exp. Med. **181:**1683-92.

76. **Lyons, R. H., B. Q. Ferguson, and M. Rosenberg.** 1987. Pentapeptide nuclear localization signal in adenovirus E1a. Mol. Cell. Biol. **7:**2451-2456.

77. **Malik, A. B., and S. K. Lo.** 1996. Vascular endothelial adhesion moleculaes and tissue inflammation. Pharmacological Rev. **48:**213-229.

78. **Martin, K. J., J. W. Lillie, and M. R. Green.** 1990. Evidence for interaction of different eukaryotic transcriptional activators with distinct cellular targets. Nature **346:**147-152.

79. **Meissner, J. D., G. N. Hirsch, E. A. LaRue, R. A. Fulcher, and K. R. Spindler.** 1997. Completion of the DNA sequence of mouse adenovirus type 1: Sequence of E2B, L1, and L2 (18-51 map units). Virus Res. **51:**53-64.

80. **Miller, G., S. Lahrs, V. G. Pillarisetty, A. B. Shah, and R. P. DeMatteo.** 2002. Adenovirus infection enhances dendritic cell immunostimulatory properties and induces natural killer and T-cell-mediated tumor protection. Cancer Res. **62:**5260-5266.

81. **Montell, C., G. Courtois, C. Eng, and A. Berk.** 1984. Complete transformation by adenovirus 2 requires both E1A proteins. Cell **36:**951-961.

82. **Montell, C., E. F. Fisher, M. H. Caruthers, and A. J. Berk.** 1982. Resolving the functions of overlapping viral genes by site-specific mutagenesis at a mRNA splice site. Nature (London) **295:**380-384.

83. **Moore, D. M., L. Zsak, J. G. Neilan, Z. Lu, and D. L. Rock.** 1998. The African swine fever virus thymidine kinase gene is required for efficient replication in swine macrophages and for virulence in swine. J. Virol. **72:**10310-10315.

84. **Moore, M. L., C. C. Brown, and K. R. Spindler.** 2003. T cells cause acute immunopathology and are required for long-term survival in mouse adenovirus type 1-induced encephalomyelitis. J. Virol. **77:**10060-10070.

85. **Moore, M. L., E. L. McKissic, C. C. Brown, J. E. Wilkinson, and K. R. Spindler.** 2004. Fatal disseminated mouse adenovirus type 1 infection in mice lacking B cells or Bruton's tyrosine kinase. J. Virol. **78**:5584-5590.

86. **Moran, E., B. Zerler, T. M. Harrison, and M. B. Mathews.** 1986. Identification of separate domains in the adenovirus E1A gene for immortalization activity and the activation of virus early genes. Mol. Cell. Biol. **6:**3470-3480.

87. **Nevins, J. R.** 1992. E2F: a link between the Rb tumor suppressor protein and viral oncoproteins. Science **258:**424-429.

88. **Nevins, J. R.** 1981. Mechanism of activation of early viral transcription by the adenovirus E1A gene product. Cell **26:**213-220.

89. **Nevins, J. R., and M. C. Wilson.** 1981. Regulation of adenovirus-2 gene expression at the level of transcriptional termination and RNA processing. Nature **290:**113-118.

90. **Oliveira, S. A., and T. E. Shenk.** 2001. Murine cytomegalovirus M78 protein, a G protein-coupled receptor homologue, is a constituent of the virion and facilitates accumulation of immediate-early viral mRNA. Proc. Natl. Acad. Sci. USA **98:**3237-3242.

91. **Parker, C. S., and J. Topol.** 1984. A Drosophila RNA polymerase II transcription factor contains a promoter-region-specific DNA-binding activity. Cell **36:**357-69.

92. **Ricciardi, R. P., R. L. Jones, C. L. Cepko, P. A. Sharp, and B. E. Roberts.** 1981. Expression of early adenovirus genes requires a viral encoded acidic polypeptide. Proc. Natl. Acad. Sci. USA **78:**6121-6125.

93. **Rochette-Egly, C., C. Fromtental, and P. Chambon.** 1990. General repression of enhanson activity by the adenovirus-2 E1A proteins. Genes Dev. **4:**137-150.

94. **Rowe, W. P., R. J. Huebner, L. K. Gilmore, R. H. Parrot, and T. G. Ward.** 1953. Isolation of a cytopathic agent from human adenoids undergoing spontaneous degeneration in tissue culture. Proc. Soc. Exp. Biol. Med. **84:**570-573.

95. **Ruszczak, Z., and R. A. Schwartz.** 1996. Vascular endothelium in the regulation of immune response. Res. Comm. Molec. Pathol. Pharm. **94:**3-21.

96. **Sawadogo, M., and R. G. Roeder.** 1985. Factors involved in specific transcription by human RNA polymerase II: analysis by a rapid and quantitative in vitro assay. Proc. Natl. Acad. Sci. USA **82:**4394-8.

97. **Scalzo, A. A., N. A. Fitzgerald, A. Simmons, A. B. La Vista, and G. R. Shellam.** 1990. *Cmv-1*, a genetic locus that controls murine cytomegalovirus replication in the spleen. J. Exp. Med. **171:**1469-1483.

98. **Shenk, T., N. Jones, W. Colby, and D. Fowlkes.** 1979. Functional analysis of adenovirus-5 host-range deletion mutants defective for transformation of rat embryo cells. Cold Spring Harbor Symp. Quant. Biol. **44:**367-375.

99. **Shenk, T. E.** 2001. Adenoviridae: The viruses and their replication, p. 2265-2300. *In* D. M. Knipe and P. M. Howley (ed.), Fields Virology, 4th ed, vol. 2. Lippincott Williams & Wilkins, Philadelphia.

100. **Slavicek, J. M., N. C. Jones, and J. D. Richter.** 1988. Rapid turnover of adenovirus E1A is determined through a co-translational mechanism that requires an amino-terminal domain. EMBO J. **7:**3171-3180.

101. **Smith, K., C. C. Brown, and K. R. Spindler.** 1998. The role of mouse adenovirus type 1 early region 1A in acute and persistent infections in mice. J. Virol. **72:**5699-5706.

102. **Smith, K., B. Ying, A. O. Ball, C. W. Beard, and K. R. Spindler.** 1996. Interaction of mouse adenovirus type 1 early region 1A protein with cellular proteins pRb and p107. Virology **224:**184-197.

103. **Spindler, K. R., L. Fang, M. L. Moore, C. C. Brown, G. N. Hirsch, and A. K. Kajon.** 2001. SJL/J mice are highly susceptible to infection by mouse adenovirus type 1. J. Virol. **75:**12039-12046.

104. **Spindler, K. R., M. L. Moore, and A. N. Cauthen.** Mouse adenovirus, The mouse in biomedical research, 2nd ed, vol. II. Academic Press, New York. in press.

105. **Stein, R. W., M. Corrigan, P. Yaciuk, J. Whelan, and E. Moran.** 1990. Analysis of E1A-mediated growth regulation functions: binding of the 300-kilodalton cellular product correlates with E1A enhancer repression function and DNA synthesis-inducing activity. J. Virol. **64:**4421-4427.

106. **Stein, R. W., and E. B. Ziff.** 1987. Repression of insulin gene expression by adenovirus type 5 E1A proteins. Mol. Cell. Biol. **7:**1164-1170.

107. **Stevens, J. L., G. T. Cantin, G. Wang, A. Shevchenko, A. Shevchenko, and A. J. Berk.** 2002. Transcription control by E1A and MAP kinase pathway via Sur2 mediator subunit. Science **296:**755-758.

108. **Thomas, C. E., A. Ehrhardt, and M. A. Kay.** 2003. Progress and problems with the use of viral vectors for gene therapy. Nat. Rev. Genet. **4:**346-358.

109. **Tufariello, J. M., S. Cho, and M. S. Horwitz.** 1994. Adenovirus E3 14.7-kilodalton protein, an antagonist of tumor necrosis factor cytolysis, increases the virulence of vaccinia virus in severe combined immunodeficient mice. Proc. Natl. Acad. Sci. USA **91:**10987-10991.

110. **Walls, T., A. G. Shankar, and D. Shingadia.** 2003. Adenovirus: an increasingly important pathogen in paediatric bone marrow transplant patients. Lancet Infect. Dis. **3:**79-86.

111. **Wang, G., and A. J. Berk.** 2002. In vivo association of adenovirus large E1A protein with the human mediator complex in adenovirus-infected and -transformed cells. J. Virol. **76:**9186-9193.

112. **Wang, H.-G. H., Y. Rikitake, M. C. Carter, P. Yaciuk, S. E. Abraham, B. Zerler, and E. Moran.** 1993. Identification of specific adenovirus E1A N-terminal residues critical to the binding of cellular proteins and to the control of cell growth. J. Virol. **67:**476-488.

113. **Wang, H.-G. W., P. Yaciuk, R. P. Ricciardi, M. Green, K. Yokoyama, and E. Moran.** 1993. The E1A products of oncogenic adenovirus serotype 12 include amino-terminally modified forms able to bind the retinoblastoma protein but not p300. J. Virol. **67:**4804-4813.

114. **Wang, H.-W. H., G. Draetta, and E. Moran.** 1991. E1A induces phosphorylation of the retinoblastoma protein independently of direct physical association between the E1A and retinoblastoma products. Molec. Cell. Bio. **11:**4253-4265.

115. **Wang, H. G., Y. Rikitake, M. C. Carter, P. Yaciuk, S. E. Abraham, B. Zerler, and E. Moran.** 1993. Identification of specific adenovirus E1A N-terminal residues critical to the binding of cellular proteins and to the control of cell growth. J. Virol. **67:**476-88.

116. **Webster, L. C., and R. P. Ricciardi.** 1991. *trans*-Dominant mutants of E1A provide genetic evidence that the zinc finger of the *trans*-activating domain binds a transcription factor. Mol. Cell. Biol. **11:**4287-4296.

117. **Webster, L. C., K. Zhang, B. Chance, I. Ayene, J. S. Culp, W. J. Huang, F. Y. H. Wu, and R. P. Ricciardi.** 1991. Conversion of the E1A cys4 zinc finger to a nonfunctional his2, cys2 zinc finger by a single point mutation. Proc. Natl. Acad. Sci. USA **88:**9989-9993.

118. **Welsh, J., B. Sapatino, B. Rosenbaum, R. Smith, and S. Linthicum.** 1993. Correlation between susceptibility to demyelination and interferon-gamma induction of major histocompatibility complex claas II antigens on murine cerebrovascular endothelial cells. J. Neuroimmunol. **48:**91-100.

119. **Whyte, P., K. J. Buchkovich, J. M. Horowitz, S. H. Friend, M. Raybuck, R. A. Weinberg, and E. Harlow.** 1988. Association between an oncogene and an anti-oncogene: the adenovirus E1A proteins bind to the retinoblastoma gene product. Nature **334:**124-129.

120. **Whyte, P., N. M. Williamson, and E. Harlow.** 1989. Cellular targets for transformation by the adenovirus E1A proteins. Cell **56:**67-75.

121. **Wickham, T. J.** 2000. Targeting adenovirus. Gene Therapy **7:**110-114.

122. **Winberg, G., and T. Shenk.** 1984. Dissection of overlapping functions within the adenovirus type 5 E1A gene. EMBO J. **3:**1907-1912.

123. **Wold, W. S., K. Doronin, K. Toth, M. Kuppuswamy, D. L. Lichtenstein, and A. E. Tollefson.** 1999. Immune responses to adenoviruses: viral evasion mechanisms and their implications for the clinic. Curr. Opin. Immunol. **11:**380-386.

124. **Wu, L., and A. J. Berk.** 1988. Transcriptional activation by the pseudorabies virus immediate early protein requires the TATA box element in the adenovirus 2 E1B promoter. Virology **167:**318-322.

125. **Wu, L., D. S. E. Rosser, M. C. Smith, and A. Berk.** 1987. A TATA box implicated in E1A transcriptional activation of a simple adenovirus 2 promoter. Nature **326:**512-515.

126. **Yang, X.-J., V. V. Ogryzko, J. Nishikawa, B. H. Howard, and Y. Nakatani.** 1996. A p300/CBP-associated factor that competes with the adenoviral oncoprotein E1A. Nature **382:**319-324.

127. **Yee, S.-P., and P. E. Branton.** 1985. Analysis of multiple forms of human adenovirus type 5 E1A polypeptides using an antipeptide antiserum specific for the amino terminus. Virology **146:**315-322.

128. **Yee, S. P., and P. E. Branton.** 1985. Detection of cellular proteins associated with human adenovirus type 5 early region 1A polypeptides. Virology **147:**142-153.

129. **Ying, B., K. Smith, and K. R. Spindler.** 1998. Mouse adenovirus type 1 early region 1A is dispensable for growth in cultured fibroblasts. J. Virol. **72:**6325-6331.

130. **Zotlick, P. W., N. Chirmule, M. A. Schnell, G.-P. Gao, J. V. Hughes, and J. M. Wilson.** 2001. Biology of E1-deleted adenovirus vectors in nonhuman primate muscle. J. Virol. **75:**5222-5229.

Fig. 1.1. Comparison of MAV-1 genome organization map with human adenovirus type 2 (hAd2) genome map. E1A, E1B, E3 and E4 of MAV-1 have been transcriptionally mapped. The other viral regions have been mapped based on DNA sequence and predicted protein similarity. The maps are not drawn to scale.

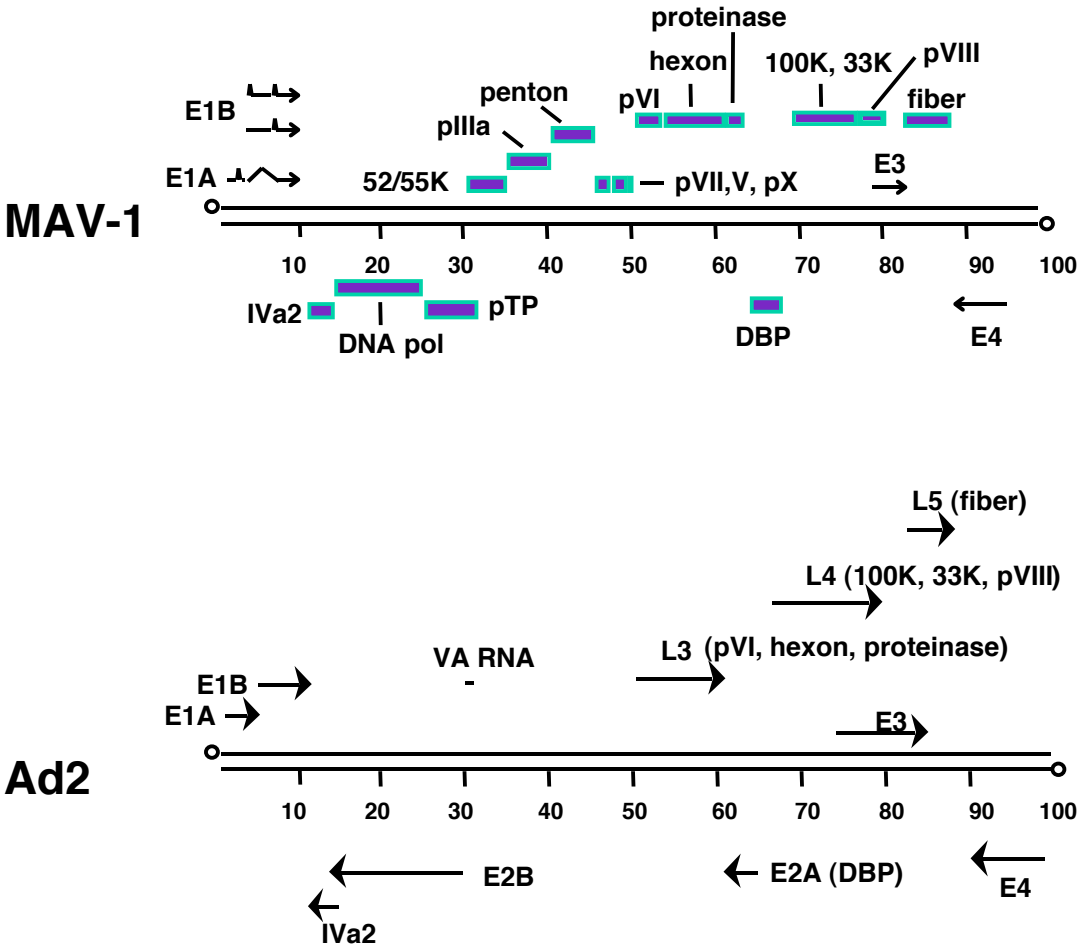
MAV-1
proteinase
hexon
100K, 33K
pVIII
E1B
penton
pVI
fiber
pIIIa
E1A
52/55K
pVII,V, pX
E3
10
20
30
40
50
60
70
80
90
100
IVa2
pTP
DNA pol
DBP
E4
Ad2
L5 (fiber)
L4 (100K, 33K, pVIII)
VA RNA
L3 (pVI, hexon, proteinase)
E1B
E1A
E3
10
20
30
40
50
60
70
80
90
100
E2B
E2A (DBP)
E4
IVa2

Fig. 1.2. Comparison of human adenovirus (hAd) E1A products with MAV-1 E1A product. The lines represent the E1A mRNAs. There are two major hAd E1A transcripts due to alternative splicing. In contrast, MAV-1 only encodes one E1A transcript. The bars represent the E1A protein products. MAV-1 E1A contains all three conserved regions (CR1, CR2, and CR3) as indicated. The maps are not drawn to scale.

Comparison of hAd E1A and MAV-1 E1A

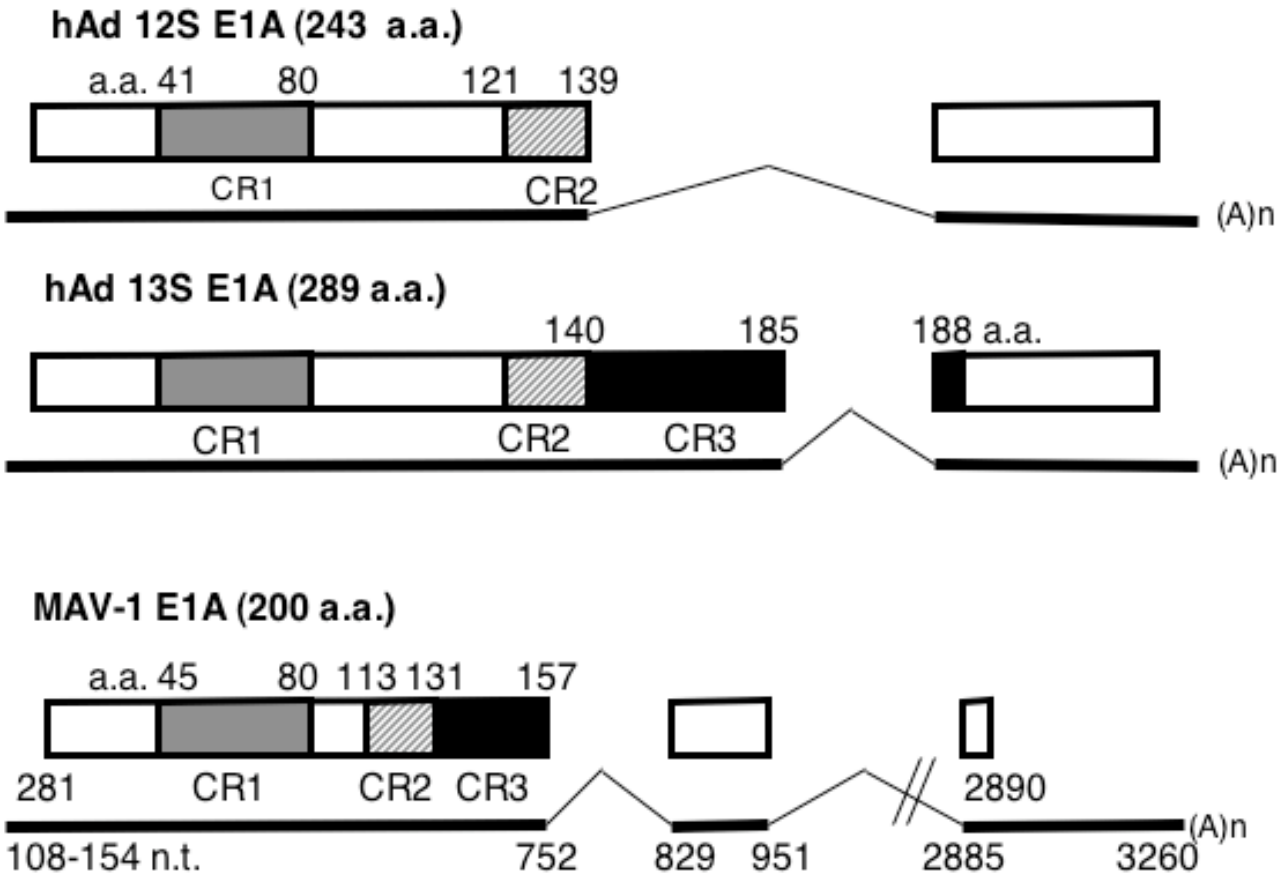

CHAPTER 2

REQUIREMENT OF SUR2 FOR EFFICIENT MOUSE ADENOVIRUS TYPE 1 (MAV-1) REPLICATION[1]

[1]L. Fang, J. Stevens, A. Berk, K. R. Spindler. Journal of Virology. 2004. Reprinted here with permission of publisher.

ABSTRACT

Mouse adenovirus type 1 (MAV-1) early region 1A (E1A) is a virulence gene in viral infection of mice. To broaden our understanding the functions of E1A in MAV-1 pathogenesis, an unbiased experimental approach, GST pull-down, was used to screen for cellular proteins that interact with E1A protein. We identified mouse Sur2, a subunit of Mediator complex, as a protein that binds to MAV-1 E1A. The interaction between Sur2 and MAV-1 E1A was confirmed in virus-infected cells. Conserved region 3 (CR3) of MAV-1 E1A was mapped as the region required for Sur2-E1A interaction, as is the case for human adenovirus (hAd) E1A. Although it has been proposed that hAd E1A recruits the Mediator complex to transactivate transcription of viral early genes, Sur2 function in adenovirus replication has not been directly tested previously. Studies on the functions of Sur2 using mouse embryonic fibroblasts (MEFs) showed that there was a multiplicity-dependent growth defect of MAV-1 in $Sur2^{-/-}$ MEFs compared to $Sur2^{+/+}$ MEFs. Comparison of the viral DNA and viral mRNA levels in $Sur2^{+/+}$ and $Sur2^{-/-}$ MEFs confirmed that Sur2 was important for efficient viral replication. The viral replication defects in $Sur2^{-/-}$ MEFs appeared to be due at least in part to a defect in viral early gene transcription.

INTRODUCTION

The human adenovirus (hAd) early region 1A (E1A) encodes two closely related proteins, 289R and 243R. hAd E1A 289R protein is one of the most extensively studied viral transcriptional regulators. E1A activates transcription of other viral early genes (9, 33), and is important for modulating the cell cycle to facilitate viral replication (27, 51, 54, 59). The E1A 289R and 243R proteins do this by various strategies involving both direct and indirect binding

to cellular proteins. The identification of a set of cellular proteins that can be co-immunoprecipitated with hAd E1A proteins (27, 59), such as retinoblastoma (pRb), the Rb family proteins p107 and p130, and p300/CBP, was critical to understanding how E1A proteins manipulate cell cycle regulation. CtBP is a transcriptional corepressor interacting with the conserved PXDLS motif near the C-terminus of the hAd E1A proteins that was originally identified by GST pull-down assay and later by the yeast two-hybrid system (12, 48). Additional newly identified cellular interacting proteins, such as Sur2 (13), p400 (25), and TRRAP/GCN5 (21, 38), continue to deepen our appreciation of the complexity of the molecular basis of viral-host interactions.

Mouse adenovirus type 1 (MAV-1) specifically targets endothelial cells and cells of the monocyte/macrophage lineage (34, 52), whereas epithelial cells are the main cell type for hAd infection (31). Unlike hAd, MAV-1 only produces a single 200-amino-acid (a.a.) E1A protein (4, 53). Although MAV-1 E1A is not an essential gene for viral replication in cell culture (60), it is a virulence gene in both outbred and inbred mice (52, 55), emphasizing the importance of MAV-1 E1A for viral pathogenesis in vivo. Since hAd E1A itself does not bind to DNA (51), direct and/or indirect association with cellular proteins is essential for E1A to carry out its multiple functions during viral infection. The function of MAV-1 E1A in viral pathogenesis is undoubtedly related to binding to cellular proteins. MAV-1 E1A contains all three conserved regions (CR1, CR2, CR3) (4, 6) found in the hAd 289R E1A protein (42). However the C-terminus of MAV-1 E1A, lacking the conserved motif PXDLS, is completely different from hAd E1A (3), and thus it is unlikely to bind to a mouse homolog of CtBP. Like hAd E1A, MAV-1 E1A interacts with pRb and p107, mainly through the CR1 domain (53). MAV-1 E1A is also similar to hAd E1A in that it plays a major role in antagonizing the antiviral effects of

interferons (IFNs) (35). However, all three conserved regions (CR1, CR2 and CR3) are required for MAV-1 resistance to IFN responses, whereas only CR1 of hAd E1A is needed for the resistance (1). Because of these differences between MAV-1 and hAd E1A, and to broaden our understanding of the roles of E1A in viral pathogenesis, we looked for cellular proteins interacting with MAV-1 E1A. We used an unbiased experimental approach, GST pull-down coupled with mass spectrometry analysis. In the work presented here, we identified mouse Sur2 (mSur2) as a protein that interacts with MAV-1 E1A.

Human Sur2 (hSur2), a subunit of Mediator, binds to CR3 of hAd E1A (13). Mediator complexes function as molecular bridges to link the transcriptional regulators with RNA polymerase II to regulate transcription (11). The interaction between Sur2 and hAd E1A-CR3 is required for recruitment of Mediator and for transcriptional activation by hAd E1A (13, 56), suggesting that recruitment of the Mediator complex transactivates the transcription of other viral early genes. Even though hSur2 interacts with hAd E1A in virus-infected cells (57), the importance of Sur2 in adenovirus replication has not been directly tested because $Sur2^{-/-}$ human cells have not been available. In the work reported here we demonstrated that mSur2 is a critical factor for MAV-1 replication in mouse embryonic fibroblasts (MEFs). Our findings indicate that Sur2 is important for efficient viral replication, providing a new molecular basis to investigate viral pathogenesis in mice.

MATERIALS AND METHODS

Cells and Viruses. Mouse NIH3T6 fibroblast cells were maintained in Dulbecco's modified Eagle's medium (DMEM) supplemented with 5% heat-inactivated calf serum. MAV-1 E1A-expressing 37.1 cells (53) were maintained in DMEM containing 5% heat-inactivated calf

serum and 200 μg/ml G418. Mouse NIH3T3 fibroblast cells were maintained in DMEM with 10% heat-inactivated calf serum. Mouse brain microvascular endothelial cells (MBMECs) were maintained in complete MBMVEC medium purchased from Cell Applications, Inc.

The $Sur2^{-/-}$ and $Sur2^{+/+}$ MEFs were obtained as follows. Sur2 knockout mice were generated by injecting $Sur2^{+/-}$ ES cell clones (Stevens et al. 2002) into C57BL/7 blastocysts. Sur2 heterozygous mice (129SvEV/C57Bl/6) were intercrossed to generate $Sur2^{-/-}$ embryos. Generation and characterization of Sur2 knockout mice will be described in greater detail elsewhere (J. Stevens and A. Berk, in preparation). WT and $Sur2^{-/-}$ MEFs were generated from individual E9.5 littermate embryos. Embryos were dissociated by trypsin digestion and plated in single well of a 24 well plate containing ES growth media (15% FCS [Hyclone], 2 mM L-glutamine [Invitrogen], 50 μg/μl pen/step [Invitrogen], 0.1 mM non-essential amino acids [Cellgro], 10^{-4}M ß-mercaptoethanol, 1000 U/ml LIF [Chemicon]). MEFs were passaged by a 3T3-like protocol until cells escaped replicative senescence. They were then maintained in DMEM containing 10% fetal calf serum.

Wild type (wt) MAV-1 was the standard MAV-1 stock originally obtained from S. Larson (5). *pm*E109 is a MAV-1 E1A null mutant virus; *dl*E105, *dl*E102, *dl*E106 viruses are MAV-1 E1A CR1 deletion, CR2 deletion, CR3 deletion mutants, respectively (53). Mouse gammaherpes virus 68 (MHV-68) was obtained from Dr. Jason Weinberg, University of Michigan.

Plasmid constructions. A plasmid, pAS2E1A, containing the full length MAV-1 E1A cDNA fragment from plasmid Z112.F (4) was generated through several intermediate vectors by using an adaptor (5' GACATGCTCATGAGCATGTCGC 3'). pAS2E1A has the full length E1A cDNA fragment plus an additional 66 nt (5' GAATTCATGG CTTACCCATA CGATGTTCCA

GATTACGCTA GCTTGGGTGG TCATATGGCC ATGAGC 3') at the 5' end of the E1A cDNA sequence. The E1A cDNA and linker was gel purified from *Eco*R I-digested pAS2E1A and ligated to *Eco*R I-digested vector pGEX-4T-1 (Amersham Biosciences) to generate the plasmid pGST-mE1A. The correct open reading frame of pGST-mE1A was confirmed by DNA sequencing. Plasmids pGST-wtE1A, pGST-Nter1, pGST-Nter2, pGST-Cter1, pGST-Cter2 and pGST-Cter3 were made by PCR using primers containing a 5' *Eco*R I site and a 3' *Sal* I site to amplify MAV-1 E1A fragments encompassing full length protein, or residues 1-45, 1-113, 157-200, 125-200 or 90-200, respectively from plasmid pCME1A (53) as a template (Fig. 2.1). The same primers as used in pGST-wtE1A cloning were used to construct pGST-CR1Δ (deletion of 36-77 a.a. of E1A), pGST-CR2Δ (deletion of 112-128 a.a.) and pGST-CR3Δ (deletion of 136-153 a.a.) by PCR using pCMV-CR1Δ, pCMV-CR2Δ and pCMV-CR3Δ as templates (53), respectively (Fig. 2.1). The reaction mix contained the 5' primer (1 ng/μl), 3' primer (1 ng/μl), plasmid template (1 ng/μl), 1.25 unit of *Pfu* polymerase (Stratagene), 1 x *Pfu* reaction buffer, and 200 nM dATP, dCTP, dGTP and dTTP in 100 μl. After 30 cycles (melting at 94ºC for 30 seconds, annealing at 58ºC for 30 seconds, extension at 72ºC for 45 seconds), the PCR reactions were subjected to an additional 7 min incubation at 72ºC (GeneAmplifer 9600, Applied Biosystems). Each PCR reaction yielded a single product that was subsequently purified using a PCR purification kit (Qiagen), digested with *Eco*R I and *Sal* I, gel purified and ligated to pGEX-4T-1 that had been digested with *Eco*R I and *Sal* I. pGST-E3gp11K contains the MAV-1 full length E3 gp11K gene (8).

Purification of glutathione S-transferase (GST) fusion proteins. Plasmid pGST-mE1A was transformed into *E. coli* BL21+ cells (Stratagene). Vector plasmid pGEX-4T-1 was used as a control. A single colony was inoculated into 5 ml 2-YT-G media (1.6% tryptone, 1%

yeast extract, 0.5% NaCl and 2% glucose) with 100 μg/ml ampicillin and cultured overnight at 37ºC. Overnight cultured *E. coli* cells were diluted 1:100 into fresh media. GST-mE1A fusion protein expression was induced by 1 mM IPTG when the optical density (OD_{600}) reached 0.5, and incubation continued for an additional 4 to 6 hours with vigorous agitation at 37ºC. Cells were harvested by centrifuging. Pellets were stored at –70ºC until use.

Pellets were thawed on ice and resuspended (for 200 ml original liquid culture) in 10 ml of ice cold STE buffer (10 mM Tris-HCl, 1 mM EDTA, 150 mM NaCl) with 100 μl of lysozyme solution (30 mg/ml), 1 μl of 100 mM PMSF and 2 μl protease inhibitor cocktail (Sigma). Samples were incubated on ice for 15 min before addition of 100 μl of 1 M DTT and 1.4 ml of 10% Sarkosyl. Samples were sonicated for a total time of 30 seconds and then centrifuged 15,000 xg for 30 min to pellet debris. Supernatants were transferred to a fresh 50 ml tube, and 4 ml of 10% Triton X-100 were added. The samples were diluted with STE buffer to a final 20 ml volume and incubated at room temperature for 30 min. The GST fusion proteins were mixed gently overnight at 4ºC with a 1 ml bed of prepared glutathione Sepharose 4B (Pharmacia Biotech) in PBS. The beads were washed four times with 25 ml of ice cold PBS. The GST fusion proteins were eluted with three successive 1 ml volumes of elution buffer (50 mM Tris-HCl [pH8.0], 10 mM reduced glutathione, 0.1% Sarkosyl). The eluates were pooled and the reduced glutathione and Sarkosyl were removed by overnight dialysis against PBS [pH 7.4]. The purified GST fusion proteins were stored at –70ºC until use.

Large scale GST pull-down assays. Equal amounts of purified GST-fusion proteins or GST proteins were mixed with 100 μl glutathione beads and incubated for 2 hours at 4ºC. Nuclear extraction of $1x10^9$ 3T6 cells or $5x10^8$ MBMECs was performed according to the method of Dignam et al. (22). Fifteen ml of the 3T6 or MBMEC nuclear extracts were pre-

absorbed against 266 µl glutathione beads and then with 500 µl GST-glutathione beads (loaded with 250 µg GST) at 4ºC for 4 hours in GST binding buffer (125 mM NaCl, 50 mM Tris-HCl [pH 7.4], 0.1% NP-40). Equal aliquots of the pre-absorbed nuclear extracts were then added to GST or GST-mE1A-glutathione beads and rocked overnight at 4ºC. The beads were washed twice with GST binding buffer and twice with GST wash buffer (250 mM NaCl, 50 mM Tris-HCl [pH 7.4], 0.1% NP-40). The beads were washed once again with GST binding buffer just before they were eluted with 30 µl 2X sodium dodecyl sulfate-polyacrylamide gel electrophoresis (SDS-PAGE) sample buffer (37) and boiled for 15 min. The bound proteins were separated by 10% SDS-PAGE and either Coomassie stained for mass spectrometry (MS) analysis or transferred to PVDF membranes for immunoblotting.

Mass spectrometry analysis. Bands of interest (see text) were cut out of the Coomassie stained protein gels, digested in-gel with trypsin and used for tandem MS/MS analysis with a MALDI-QTOF machine (Micromass Company) by the Michigan Proteomic Consortium at the University of Michigan. Two search engines, MS-FIT (http://prospector.ucsf.edu) and Mascot (http://www.matrixscience.com), were used to search databases to identify the proteins.

Antibodies. Monoclonal antibody against human Sur2 (BD Pharmingen) cross-reacts with mouse Sur2 and was used at a 1:1000 dilution in Western blot assays. Anti-p107 (sc-318) and anti-p130 (sc-317) polyclonal antibodies were from Santa Cruz Biotechnology. Anti-murine Rb and anti-MAV-1 E1A (AKO7-147) rabbit polyclonal antibodies were as described (53). AKO7-147 and normal rabbit serum (NRS) were purified by DEAE Affi-Gel blue (Bio-Rad) affinity chromatography according to the manufacturer's instructions. Normal rabbit serum (NRS) was used as controls where indicated. Mouse monoclonal antibodies against MAV-1 E1A (mAb10B10) and MAV-1 E3gp11K (mAb11H9) were generated at the University of Georgia

Monoclonal Facility using purified GST-mE1A and GST-gp11K fusion proteins as the antigen, respectively. Both mAb10B10 and mAb11H9 monoclonal antibodies were purified using an Affi-Gel Protein A MAPS II kit (Bio-Rad) according to the manufacturer's instructions. 1:500 dilution of mAb10B10 or 1:1000 dilution of mAb11H9 was used in Western blots. Monoclonal antibody against β-actin was from Sigma (A5441) and used at a 1:5000 dilution in Western blots.

Western blot assays. Samples were dissolved in SDS-PAGE sample buffer and resolved on SDS-polyacrylamide gels. The proteins were electrotransferred onto PVDF membranes at 14 volts for 16 hrs at 4º C, and the membranes were blocked by incubation at room temperature (RT) for 1 h in TBS-Tween (150 mM NaCl, 10 mM Tris [pH 7.4], 0.1% Tween-20) containing 5% nonfat dry milk. Anti-rabbit (1:12,000 from Amersham Biosciences) or anti-mouse (1:12,000 from Amersham Biosciences) IgG-HRP conjugated antibody was used as the secondary antibody. Immunoblots were developed using SuperSignal West Pico Chemiluminescent Substrate (Pierce Biotechnology, Inc.).

Immunoprecipitations. 3T6 cells or MBMECs were lysed in E1A lysis buffer (250 mM NaCl, 50 mM Tris [pH 7.4], 0.1% NP40) containing protease inhibitor cocktail (1: 50)(Sigma). The lysates were diluted to E1A binding buffer (125 mM NaCl, 50 mM Tris [pH 7.4], 0.1% NP40) and then pre-absorbed simultaneously against rabbit normal immunoglobulin G (IgG) and protein A agarose beads (Pharmacia Biotech) by rocking at 4º C for 2 hours. The lysates were then incubated with polyclonal antibody against MAV-1 E1A (AKO7-147) (53) or rabbit normal IgG, followed by incubation with 30 µl of protein A agarose (Oncogene Research Products). The agarose beads were pelleted, washed twice with E1A binding buffer, twice with E1A lysis buffer

and once again with E1A binding buffer. The immunoprecipitated proteins were eluted by boiling in SDS-PAGE sample buffer and subjected to SDS-PAGE and immunoblotting.

Viral growth curves. $Sur2^{+/+}$ and $Sur2^{-/-}$ MEFs were infected with wt MAV-1 at a multiplicity of infection (MOI) of 0.05, 0.1, 1 or 5, or with MHV-68 at an MOI of 0.01. MAV-1 plaque assays were carried out on 3T6 cells as described previously (18). Briefly, cells were harvested at various times post infection (p.i.) by scraping in their medium. The cell suspensions were subjected to three cycles of freezing and thawing and the cell debris was spun out of the supernatant. Tenfold serial dilutions of supernatants were plated in triplicate on 3T6 cells, and plaques were counted at day 9 after plating. For the MHV-68 plaque assay, only supernatants were harvested, and tenfold serial dilutions of supernatants were plated in duplicate on NIH3T3 cells as described (47)

Southern blots. $Sur2^{+/+}$ and $Sur2^{-/-}$ MEFs were infected at an MOI of 0.05, 0.1, 1 or 5 and harvested at various times post infection (p.i.) by scraping the cells off the plates. Viral DNA was isolated by the method of Hirt (28). Equal amounts of DNA samples were digested with *Hin*d III and RNase A and electrophoresed on a 0.7% agarose gel. After staining with ethidium bromide and photography, the gel was soaked in 0.8 M NaCl/0.4 M NaOH for 30 min, rinsed with water and then soaked in 1.5 M NaCl/0.5 M Tris [pH 7.5] for 30 min. The DNA was transferred to a nylon positively charged membrane (Boehringer) by capillary transfer. The DNA was UV crosslinked to the membrane by incubation for 12 seconds in a Fisher UV crosslinker. The membrane was prehybridized in 10 ml of PerfectHyb solution (Sigma) at 65ºC for 2 h. Plasmids pMBA, pMBB and pMBC contain MAV-1 genome sequence from 31.7 to 64.2 m.u., 64.2 to 94.5 m.u. and 6.5 to 31.7 m.u., respectively. They were pooled, digested with *Hin*f I, and labeled using Klenow DNA polymerase with [γ-^{32}P] ATP. The free label was removed by

passage over a G25 Sepharose spin column, and 10^6 to 10^7 cpm of the probe was added to 10 ml PerfectHyb solution to hybridize at 65ºC for 5-18 h. The membranes were washed twice with 2x SSC/0.1% SDS at RT for 15 min, twice with 2x SSC/0.1% SDS at 65ºC for 30 min and once with 0.5x SSC/0.1% SDS at 65ºC for 15 min. A phosphorimager was used to quantify the signals.

Ribonuclease protection assays (RPAs). $Sur2^{+/+}$ and $Sur2^{-/-}$ MEFs were infected at an MOI of 0.05, 0.1, 1 or 5. Total RNA was extracted using TRI reagent (Molecular Research Center, Inc.) following the manufacturer's instructions. An equimolar pool of linearized plasmids were used as templates to make an [α-^{32}P] UTP-labeled multiplex RPA probe set by T7 or T3 polymerase transcription. prK+7, a genomic E1A plasmid containing MAV-1 genome sequence 1-820 nt in a pBluescripts(+) vector, was digested with *Bam*HI at nt 360 in the MAV-1 sequence (GenBank accession no. NC_000942). The full length probe was 489 nt (MAV-1 360-820 nt, plus 29 nt of vector), and the length protected from RNase digestion after hybridization to an E1A mRNA was 392 nt. A genomic hexon plasmid pHEX was constructed by ligation MAV-1 genome sequence 16,432-16,769 nt with a vector pBS2SK$^-$. pHEX was digested at nt 16,432 in the viral sequence at a *Bam*HI site. The full length probe was 395 nt (MAV-1 nt 16,432-16,769, plus 58 nt of vector) and the protected size was 337 nt. The protected length of L32 was 80 nt and was used an internal loading control (29). pZU14 is an E3gp11K cDNA clone used to make an E3 probe (7). The full length probe is 714 nt and the protected E3 signal is 645 nt. pH61 (MAV-1 E2A clone) (60) was digested with *Sma*I and the full length probe is 470 nt. The protected E2A signal is about 440 nt. pZ571 is an E4 cDNA clone (36) and was digested with *Bam*HI. The full length probe is 767 nt and the protected E4 signal is about 700 nt. The linearized plasmid mouse β-actin was from the MAXIscript in vitro transcription kit (Ambion

Inc.). The full length probe of β-actin is 276 nt using T3 transcriptase and the protected length is 245 nt. The RPAs were carried out as described by Hobbs et al. (29). Briefly, 7.5 μg of total RNA was hybridized with the combined MAV-1 probe set and either L32 or β-actin probe overnight at 56ºC. Yeast tRNA was used as a negative control in RPAs. After digestion with RNase A and RNase T1, samples were ethanol precipitated and electrophoresed on 5% polyacrylamide/8M urea gels. After drying, protected mRNA signals were visualized using a phosphorimager, and quantitation was performed by normalizing the mRNA species of interest to L32 or β-actin signals.

RESULTS

Feasibility of GST pull-down assay for screening cellular proteins that interact with MAV-1 E1A. In order to screen for the potential cellular proteins that interact with MAV-1 E1A, we used an unbiased GST pull-down approach. First, we subcloned full length MAV-1 E1A with an additional 66 nt linker at the 5′ end of the E1A sequence into a GST expression vector, resulting in the plasmid pGST-mE1A (Fig. 2.1A). The GST-mE1A fusion protein was overexpressed by inducing the cells with IPTG (Fig. 2.1B, lane 3) and purified using glutathione beads (Fig. 2.1B, lane 4).

Differences in post-translational modifications between proteins expressed in bacterial versus mammalian cells might affect interactions of MAV-1 E1A with cellular proteins. We previously showed that MAV-1 E1A binds to mouse pRb and p107 proteins in an in vitro mixing experiment (53). We reasoned that if the GST-mE1A fusion protein is capable of binding to these known interacting proteins, GST pull-down assays using the GST-mE1A fusion protein would be a valid experimental approach to screen for cellular proteins that interact with MAV-1

E1A. Since the pRb and p107 used in those experiments were in vitro translated proteins, we first further verified that MAV-1 E1A interacts with endogenous Rb family proteins in virus-infected cells. MBMECs were infected with wt MAV-1 at an MOI of 5 and harvested at 40 h post infection (p.i.). Mock and *pm*E109 (E1A null mutant) infection were used as negative controls. Co-immunoprecipitation experiments were carried out using antibodies to the Rb family proteins to show the protein-protein interactions. The immunoprecipitates were electrophoresed, transferred to membranes, and probed with antibody against MAV-1 E1A. As expected, MAV-1 E1A signals were only detected in wt MAV-1-infected samples that had been immunoprecipitated with specific antibodies against p130, p107 or pRb (Fig. 2.2A, lanes 5, 8 and 11), and not with control NRS (lane 2), demonstrating that MAV-1 E1A binds to Rb family proteins in infected cells. Co-immunoprecipitation experiments performed by immunoprecipitation with anti-MAV-1 E1A antibodies (rabbit polyclonal and mouse monoclonal antibodies) and detection on Westsern blots with antibodies against pRb, p107 and p130 confirmed the MAV-1 E1A-pRb, E1A-p107, E1A-p130 interactions (data not shown). The interaction between MAV-1 E1A and p130 had not been previously demonstrated.

Since MAV-1 E1A interacts with pRb, p107 and p130 in virus-infected cells, we tested whether the bacterially expressed GST-mE1A fusion proteins would bind to mouse pRb, p107 and p130. In addition to the full length GST-mE1A protein, we tested a GST fusion construct containing only the C-terminal 157-200 a.a. (GST-Cter1) of E1A (Fig. 2.1A) because we were interested in identifying cellular proteins that specifically bind to MAV-1 E1A C-terminus due to its unique sequence. As controls, we used the GST protein and a GST fusion construct (GST-E3gp11K) containing another MAV-1 early viral protein, E3gp11K (8). As shown in Fig. 2.2B, 2.2C and 2.2D, mouse pRb, p107 and p130, respectively, were bound to GST-mE1A, but

not to GST, GST-Cter1 or GST-E3gp11K fusion proteins. Panel E was a control to show that approximately equivalent amounts of GST-fusion proteins were present in the pull-down assays. Conserved region 2 (CR2) of MAV-1 E1A is critical for binding to pRb and p107 (53). Consistent with those data, the GST-Cter1 fusion protein, lacking the CR2 domain, did not bind to pRb family proteins. The bacterially expressed GST fusion proteins maintained their binding properties like viral E1A, indicating the suitability of screening for E1A-interacting proteins using GST pull-down assays.

Sur2 interaction with MAV-1 E1A CR3 domain. Nuclear extracts from two cell lines, MBMECs and 3T6 cells, were used to screen for potential additional interacting proteins in GST pull-down assays. Approximately $1x10^9$ 3T6 cells or $5x10^8$ MBMECs were used for a single GST pull-down assay with 25 μg of GST fusion protein bound to agarose beads, so that the proteins could be visualized in a Coomassie stained gel (Fig. 2.3A; 3T6 cells data not shown). The GST fusion proteins alone were used as a negative control. The purified GST-Cter1 protein (Fig. 2.1A) was used to screen for proteins that specifically bind to the unique C-terminus of MAV-1 E1A. The protein bands that were only present in the GST-mE1A sample (Fig. 2.3A, lane 6) and not in the GST sample (Fig. 2.3A, lane 5) were considered potential specific MAV-1 E1A binding proteins. Several specific bands were cut out of the gels, and the identification of proteins was carried out by tandem MS/MS analysis. One band, indicated by the arrowhead, was identified as mouse Sur2 (mSur2). We identified mSur2 as a GST-mE1A interacting protein from both cell lines, MBMEC (Fig. 2.3A) and 3T6 (data not shown). Several additional bands were identified by MS/MS analysis. The characterization of these as potential MAV-1 E1A interacting proteins will be described elsewhere following verification using specific antibodies (L. Fang and K. R. Spindler, unpublished data).

We verified the binding specificity of mSur2 to GST-mE1A using Western blots. GST pull-down assays were carried out as in Fig. 2.3A, but instead of staining the protein gel with Coomassie blue, we transferred it to a PVDF membrane and probed for the presence of mSur2 using monoclonal antibody against hSur2. Anti-Sur2 antibody was developed against human protein but cross-reacts with mouse Sur2. Mouse Sur2 protein is almost identical to its human homolog, and human Sur2 can rescue the phenotypic defects in mouse $Sur2^{-/-}$ embryonic stem cells (56). In both MBMECs and 3T6 cells we identified mSur2 specifically bound to the GST fusion protein containing the full length MAV-1 E1A, but not to control GST proteins or C-terminal 157-200 a.a. of E1A in GST-Cter1 (Fig. 2.3B). This demonstrates that mSur2 specifically interacts with GST-mE1A. It is not surprising that mSur2 did not bind to the GST-Cter1 fusion protein, because it has been shown that hSur2 interacts with hAd E1A through CR3 domain (13, 57). The CR3 domain of MAV-1 E1A is absent in the GST-Cter1 construct.

We investigated whether MAV-1 E1A binds to mSur2 in virus-infected cells (Fig. 2.3C). Whole cell lysates from either MAV-1 infected or mock infected cells were subjected to immunoprecipitation using rabbit polyclonal anti-E1A antibody. The anti-E1A immunoprecipitates were analyzed for the presence of mSur2 using anti-Sur2 monoclonal antibody in Western blots. mSur2 was only detected from the MAV-1 infected sample that was immunoprecipitated with anti-E1A antibody (Fig. 2.3C). The results demonstrate that the interaction between MAV-1 E1A and mSur2 occurred in MAV-1-infected cells.

CR3 of hAd E1A is necessary and sufficient for binding to Sur2 (13, 56, 57). Despite the presence of CR3 domain in MAV-1 E1A, there is no significant similarity to hAd E1A outside of the conserved regions (6), making it intriguing to investigate which regions of MAV-1 E1A are important for binding to mSur2. We used two different experimental approaches to map the

interaction region required for MAV-1 E1A interaction with mSur2. First, GST pull-down assays were used. In addition to the GST-mE1A containing a 22 a.a. linker (Fig. 2.1A), we constructed another full length MAV-1 E1A directly downstream of GST, GST-wt E1A (Fig. 2.1A). A series of GST fusion proteins were also prepared that contained either truncated forms or deleted forms of MAV-1 E1A as shown in Fig. 2.1A. GST pull-down assays were carried out using these constructs, and the bound proteins were subjected to Western blots using anti-Sur2 antibody (Fig. 2.4A). The same membrane was stripped and re-probed with anti-GST antibody to verify equivalent loading of GST fusion proteins (Fig. 2.4B). The mSur2 protein was detected in samples with GST-E1A constructs containing the CR3 of E1A (lanes 2-5, 9 and 10), and absent in samples with GST-E1A constructs lacking CR3 (lanes 6-8 and 11). mSur2 did not bind the negative controls, GST (lane 1) or GST-gp11K (lane 12). The results indicate that the CR3 domain is required for the protein-protein interaction.

We tested whether CR3 was required for binding to Sur2 in virus-infected cells using MAV-1 E1A mutant viruses. *dl*E105, *dl*E102 and *dl*E106 viruses are CR1, CR2 and CR3 deletion mutants of E1A, respectively (53). The wt MAV-1 and *pm*E109 (E1A null mutant virus) were used as a postive control and a negative control, respectively. Immunoprecipitation/Western blots were carried out as in Fig. 2.3C. The anti-E1A rabbit polyclonal antibody AKO7-147 is able to recognize all mutant form E1A proteins by immunoprecipitation (53). mSur2 proteins from the cells infected with *dl*E106 (CR3 deletion mutant) failed to co-immunoprecipitate with E1A (Fig. 2.5A, lane 10). This not only confirms the GST pull-down data, but it also demonstrates that CR3 of MAV-1 E1A is required for binding to mSur2 in virus-infected cells. There were slight reductions in the amount of mSur2 co-immunoprecipitated with the CR1 and CR2 deletion mutants relative to wt virus (compare

lanes 6 and 8 to lane 4). The control blots showed that the mSur2 protein levels present in all virus-infected cells were very similar to that in mock infected cells (Fig. 2.5B), indicating that there was no mSur2 protein degradation upon viral infection. There is no growth defect in the E1A mutant viruses at an MOI 5 (60).The viral early gene E3gp11K was monitored to show a comparable efficiency of viral infection by the E1A viral mutants (Fig. 2.5B). E3gp11K protein levels in E1A mutant virus infections were nearly equivalent to those in wt virus infections, as expected since at this multiplicity E3gp11K mRNA levels are not reduced in E1A mutant virus infections relative to wt virus infection (57).

Sur2 is important for MAV-1 replication. We investigated the functional role of mSur2 in MAV-1 infection using $Sur2^{+/+}$ and $Sur2^{-/-}$ MEFs. Cytopathic effects (CPE) after MAV-1 infection were quite different between $Sur2^{-/-}$ and $Sur2^{+/+}$ MEFs. Wt MEFs started to show dramatic CPE at an MOI of 1 or 5 at 3 days p.i., with only slight CPE at MOI of 0.05 (data not shown). At 7 days p.i. the infected wt MEFs showed CPE at all multiplicities, whereas $Sur2^{-/-}$ MEFs showed little or no CPE except at the higher MOIs of 1 and 5 (Fig. 2.6). The results showed that there was a delay of appearance of CPE in $Sur2^{-/-}$ MEFs upon MAV-1 infection compared to wt cells at equivalent MOIs.

We examined MAV-1 replication in $Sur2^{+/+}$ and $Sur2^{-/-}$ MEFs in one-step growth curves (Fig. 2.7A). We observed a multiplicity-dependent virus growth defect upon MAV-1 infection of $Sur2^{-/-}$ MEFs. At an MOI of 5, the viral yields were reduced by a factor of 5 in $Sur2^{-/-}$ MEFs compared with wt cells, whereas at an MOI of 1, the yields were reduced by a factor of 10 to 50. Therefore, at high MOI (1 or 5) MAV-1 was able to replicate and generate mature infectious virions in $Sur2^{-/-}$ MEFs, though less efficiently than in $Sur2^{+/+}$ MEFs (Fig. 2.7A). However, at low MOI (0.05 or 0.1), the viral yields in $Sur2^{-/-}$ MEFs were equivalent to the amount of input

virus, indicating that viral replication was severely reduced. These results indicated that the mSur2 protein was required for MAV-1 replication at a low input MOI and important for efficient viral replication at a high input MOI.

We tested whether this viral replication defect in $Sur2^{-/-}$ MEFs is a general or virus-specific effect. Replication of MHV-68, a mouse gammaherpesvirus, showed no significant differences in growth on $Sur2^{+/+}$ MEFs compared with $Sur2^{-/-}$ MEFs (Fig. 2.7B). The data indicate that mSur2 is not required for MHV-68 replication and suggest that the requirement of mSur2 for viral replication is a relatively specific effect.

The plaque assays measured the final outcome of viral infection. Every step in the infectious process, such as viral early gene expression, viral genome DNA replication, late gene expression, DNA packaging, viral assembly and secretion of mature virions, could affect the final viral yield. We examined some of these steps to determine the potential roles of Sur2 in MAV-1 infection.

We tested whether viral DNA replication differed in $Sur2^{-/-}$ MEFs from $Sur2^{+/+}$ cells by analyzing MAV-1 genome DNA in Southern blots (Fig. 2.8). At MOIs of 1 and 5, MAV-1 DNA was detected at 24 h p.i. in both cell types. The kinetics of viral DNA accumulation during the course of viral infection were shown by the increasing intensity of viral DNA bands in virus-infected $Sur2^{+/+}$ MEFs. In contrast, less DNA accumulation was observed in $Sur2^{-/-}$ MEFs. This indicates that there was no defect in the time of onset of viral DNA synthesis at MOIs of 1 and 5, but the accumulation of viral DNA was substantially decreased in $Sur2^{-/-}$ cells. We did not detect any MAV-1 DNA from $Sur2^{-/-}$ MEFs at MOI of 0.05, whereas in $Sur2^{+/+}$ MEFs it increased to the level comparable to that seen in $Sur2^{+/+}$ MEFs at MOIs of 1 and 5 (Fig. 2.8). The defect in MAV-1 DNA replication in $Sur2^{-/-}$ MEFs, taken together with overall lower virus yield

in these same conditions (Fig. 2.7A), suggested that mSur2 is required for some step at or prior to DNA replication.

We quantitated the steady-state mRNA levels of MAV-1 early genes E1A, E3, E2 and E4, and one viral late gene, hexon, in $Sur2^{-/-}$ and $Sur2^{+/+}$ MEFs using RPAs. Representative RPA gels (Fig. 2.9A) show the mRNA levels of E1A and hexon. The mRNA levels of each viral gene at MOIs of 0.05 and 1 were normalized to the housekeeping gene L32 or to β-actin, and the relative levels are shown in Fig. 2.9B and 2.9C. There was a delay in the onset of detectable transcription of all tested viral early genes, and their steady-state mRNA levels were reduced in $Sur2^{-/-}$ MEFs compared with $Sur2^{+/+}$ MEFs at high MOIs (1 or 5). At an MOI of 0.05, the expression of all viral early genes was severely diminished or not detectable in $Sur2^{-/-}$ MEFs. The viral late gene hexon had essentially the same expression pattern as viral early genes in $Sur2^{-/-}$ MEFs, delayed and reduced relative to $Sur2^{+/+}$ MEFs. However, we also noticed that at high MOIs (1 and 5), the defects in hexon mRNA levels were not as severe as defects in viral DNA levels. Nevertheless, the results indicate that mSur2 is involved in the transcription regulation of the viral early genes, supporting the proposed hAd infection model in which E1A recruits the Mediator complex through stable binding to the Sur2 subunit to transactivate transcription of the other viral early genes (57).

To confirm that the RPA results for mRNA levels were reflected in protein levels, we analyzed the expression of two MAV-1 early proteins, E1A and E3gp11K, and compared them to β-actin (Fig. 2.10). As expected, the levels of MAV-1 E1A and E3gp11K protein accumulation were higher in $Sur2^{+/+}$ MEFs than those in $Sur2^{-/-}$ MEFs when cells were infected at an MOI of 1 (Fig. 2.10). The decreased protein recovery (and loading, see figure legend) of E3 gp11K, E1A, and β-actin seen at 5 and 7 days p.i. in $Sur2^{+/+}$ MEFs (Fig. 2.10A, lane 3 and 4) was

likely due to the CPE at this time in infection (Fig. 2.6). Quantitation (Fig. 2.10B) shows that E1A and E3gp11K protein levels were relatively high even when the CPE were apprarent in the $Sur2^{+/+}$ MEFs. At an MOI of 0.1, E1A or E3gp11K proteins were not detected by Western blots in $Sur2^{-/-}$ MEFs even at 7 days p.i. (data not shown), supporting the hypothesis that mSur2 is required for MAV-1 replication at a low input multiplicity. In contrast, both early viral proteins were readily detected in $Sur2^{+/+}$ MEFs at 3 days p.i. (data not shown). The correlation of Western blot data with the RPA results strongly argues that mSur2 plays a critical role in early phase of MAV-1 replication.

DISCUSSIONS

The identification of multiple cellular proteins that interact with viral proteins has contributed to understanding the physiological functions of those interacting proteins in cells. It is also key to understanding the molecular basis of viral-host interaction during viral infection. MAV-1 E1A is involved in viral pathogenesis, undoubtedly through association with cellular proteins. To better understand the molecular basis of E1A protein in MAV-1 pathogenesis, we used a GST pull-down assay to screen for cellular proteins that interact with MAV-1 E1A. Protein identification was done by proteomic-based MS/MS analysis coupled with a computer database search. Mouse Sur2 protein was identified as one of the specific proteins that interacted with GST-mE1A. The specific binding to MAV-1 E1A was verified by GST pull-down/Western blots (Fig. 2.3B) and was also demonstrated in virus-infected cells by co-immunoprecipitation (Fig. 2.3C). We also demonstrated the feasibility of GST pull-down assays by testing whether the known MAV-1 E1A interactors, pRb and p107 (53), would bind to GST-E1A fusion proteins. Not only pRb and p107 but also p130 specifically bound to GST-mE1A (Fig. 2.3). The

GST-wtE1A construct (Fig. 2.1A) containing no linker gave identical results to the GST-mE1A in GST pull-down assays (data not shown), indicating that the 22 a.a. linker did not affect protein-protein interactions. In addition, here we showed experimentally for the first time that endogenous pRb and p107 proteins interacted with MAV-1 E1A in virus-infected cells, which is consistent with in vitro mixing experiment data (53). In addition, for the first time, p130 was also shown to interact with MAV-1 E1A in virus-infected cells by immunoprecipitation/Western blots. These data indicate that the bacterially expressed GST-mE1A fusion protein maintains the same binding properties as the viral E1A proteins, demonstrating that GST pull-down assays are a valid experimental approach to screen for MAV-1 E1A interacting proteins.

The GST-mE1A fusion protein interacted with many proteins in uninfected cells (Fig. 2.3A, lane 6). We chose several specific GST-mE1A binding protein bands from large-scale GST pull-down gels for MS/MS analysis. Some samples did not generate good quality MS/MS data that could lead to successful protein identification in databases. There were several additional potential interacting proteins identified from the MS/MS analysis, which will be described elsewhere (L. Fang and K. R. Spindler, unpublished data).

CR3 of hAd E1A is known to be necessary and sufficient for binding Sur2 (13, 57). MAV-1 E1A has all three conserved regions with about 40% similarity to hAd E1A conserved regions (6), but no significant similarities are found outside of them (4, 6). Therefore, it was of interest to investigate whether MAV-1 E1A CR3 was essential for binding to mSur2. We used different GST constructs to map the regions of MAV-1 E1A required for binding to mSur2 and showed that CR3 is necessary for this interaction (Fig. 2.4A). Furthermore, using CR1, CR2 and CR3 deletion mutant viruses, we showed that CR3 is also required for the mSur2-E1A interaction in virus-infected cells (Fig. 2.5A). These mutant viruses have no significant growth

defects compared to wt MAV-1 infection in 3T6 cells at an MOI of 5 (60), correlating with similar E3gp11K protein levels (Fig. 2.5B), and E3gp11K mRNA levels (54). The polyclonal antibody against MAV-1 E1A (AKO7-147) can recognize the E1A deletion mutant proteins, including CR3 deletion E1A, in immunoprecipitations (60). Therefore, the absence of mSur2 signal from the CR3 deletion mutant-infected sample immunoprecipitated with anti-E1A antibody was not due to a reduced efficiency of viral infection or failure of antibody recognition. However, we also noticed that there was less mSur2 co-immunoprecipitated with MAV-1 E1A from *dl*E105 and *dl*E102 virus-infected samples than wt MAV-1-infected samples (Fig. 2.5, lane 6, 8). It is possible that the polyclonal E1A antibody does not recognize the deleted forms of E1A protein as efficiently as wt E1A in immunoprecipitations. Another possibility is that the deleted forms of MAV-1 E1A protein might have conformational changes resulting in reduced binding affinity to mSur2. A formal possibility that we believe is less likely is that CR1 and CR2 have direct but small effects on the Sur2-E1A interaction in viral infection.

Using a variety of single amino acid hAd E1A mutations in GST pull-down assays, an intact zinc-finger structure (four cysteine residues that bind a single Zn^{++} ion) in hAd E1A CR3 was shown to be important for Sur2-E1A CR3 interaction (13). MAV-1 E1A CR3 has the same four cysteine residues, but we have not demonstrated the importance of this conserved zinc-finger structure in MAV-1 E1A binding to mSur2. One question that has not been addressed is which regions of Sur2 protein are required for the Sur2-E1A interaction. Human Sur2 protein has been reported to interact with three transcription factors to date, Elk-1 (13, 56), ESX (2) and C/EBPβ (40). Elk-1 is activated by ERK in the MAPK signal transduction pathway and binds serum response elements of targeted genes. The region of Sur2 that binds to Elk-1 is unknown. EXS, an Ets factor, is an epithelial cell type specific transcription factor, and the residues

352-625 a.a. of Sur2 are important for the binding to ESX. It has been suggested that E1A competes with C/EBPβ to bind to Sur2 (40). Mapping the Sur2 region required for binding to E1A will allow us to postulate whether E1A interferes with the binding of Sur2 to these transcription factors. In turn, it will help us understand the physiological functions of Sur2 and address why adenovirus E1A targets Sur2.

The conservation of adenovirus E1A binding to Sur2 in hAd and MAV-1 indicates its importance for adenovirus replication. However, due to adenovirus species-specificity and the availability of only mouse Sur2 knockout cells, Sur2 function in adenoviral replication had not been directly tested prior to this study. There was no detected Sur2 protein in $Sur2^{-/-}$ MEFs by Western blots (data not shown). Expressing hSur2 in $Sur2^{-/-}$ mouse stem cells rescues its defective transcription activation function, showing that Sur2 is the only missing factor in the knockout cells (56). We observed a delay of CPE upon MAV-1 infection in $Sur2^{-/-}$ MEFs compared to wt cells (Fig. 2.6), and viral growth curves demonstrated a defect of MAV-1 replication in $Sur2^{-/-}$ MEFs (Fig. 2.7A). All these data suggest that viral replication in $Sur2^{-/-}$ cells is multiplicity-dependent and that mSur2 is important for efficient MAV-1 replication. More strikingly, we found that at a low input MOI (0.05 or 0.1), MAV-1 replication was severely restricted in $Sur2^{-/-}$ MEFs: the viral yields did not indicate replication above the levels of input virus. Therefore, we suggest that mSur2 is required for viral replication at a low input MOI (0.05 and 0.1), but the requirement is partially overcome at a higher input MOI (1 or 5). The multiplicity-dependent effects in $Sur2^{-/-}$ MEFs was further observed in additional experiments examining the viral DNA, mRNA and protein levels (Fig. 2.8, 2.9, and 2.10) The reduced viral DNA replication in $Sur2^{-/-}$ MEFs correlated well with the lower virus yields. The mRNA levels of viral early genes (Fig. 2.9C) were also markedly reduced in $Sur2^{-/-}$ MEFs compared to $Sur2^{+/+}$

MEFs, which is consistent with E2 transcription deficiency in Sur2$^{-/-}$ mouse embryonic stem cells upon hAd2 infection (56). The data suggest that the viral replication defect is due at least in part to a defect in viral early gene transcription.

We showed that the importance of mSur2 protein for viral replication is specific for MAV-1 because there was no growth defect for MHV-68, a mouse gammaherpesvirus, in Sur2$^{-/-}$ MEFs. The transcription activity of many transcription factors are not affected by hSur2 (2, 13, 56), indicating the narrow target range of Sur2. This raises an interesting question of why the adenovirus E1A protein conserves the ability to bind to such a selective Mediator subunit.

The molecular mechanisms of Sur2 function in MAV-1 infection have not been fully investigated. It has been proposed that the primary mechanism by which E1A recruits the Mediator complex to transactivate transcription of viral early genes is that E1A stimulates and also stabilizes the assembly of a transcription pre-initiation complex on promoter DNA through stable Sur2-E1A CR3 interaction (17, 57). However, the ability of MAV-1 to replicate in Sur2$^{-/-}$ MEFs suggests that there is a Sur2-independent virus replication pathway. This raises many possibilities. First, it is possible that the Mediator complex or transcription pre-initiation complex is recruited to viral gene promoters with a decreased efficiency in the absence of Sur2. It is possible that E1A binds other components of Mediator complex, and it will be interesting to see whether E1A can co-immunoprecipitate other Mediator components in Sur2$^{-/-}$ MEFs. Second, other regions of hAd E1A protein including CR1 and CR2 also have very strong transcriptional activity primarily through binding p300/CBP (10, 58) and Rb family proteins (23), repectively. Binding Rb family members and binding p300/CBP are two independent mechanisms utilized by hAd E1A protein to manipulate the cell cycle from G_1 to S phase (51). MAV-1 E1A protein contains all three conserved regions, and the interactions between MAV-1 E1A and Rb family

members are shown in this work. Another possibility is that E4 gene products may also play a role in MAV-1 replication. The hAd E4 orf6/7 protein has been shown to be able to induce E2F DNA binding to the viral E2A promoter and thus functionally compensate for the loss of E1A in hAd infection (44, 49). MAV-1 E4 orf d (36) has 17% identity and 43% similarity to hAd E4 orf6/7 protein (L. Fang and K. R. Spindler, unpublished data). It is reasonable to speculate that MAV-1 uses one or more mechanisms to replicate if Sur2 is absent in the infected host cells.

Interestingly, *dl*E106 (CR3Δ mutant) virus replicates to comparable level as wt virus in 3T6 cells at an MOI of 5 (60), but its CR3Δ E1A protein does not bind to mSur2 (Fig. 2.5), indicating that MAV-1 E1A-mSur2 interaction itself is not absolutely essential for MAV-1 replication. Moreover, the fact that hAd E1A null mutant virus (*dl*312) can replicate at high MOIs clearly demonstrates that E1A is not an essential gene for hAd replication (26, 32, 43, 50). MAV-1 E1A is dispensable for MAV-1 replication in cell culture, demonstrated by MAV-1 E1A null mutant (*pm*E109) growth at MOIs as low as 1 (60). This indicates the existence of an E1A-independent viral replication pathway and may also explain why MAV-1 is able to replicate in the absence of mSur2-E1A CR3 interaction in $Sur2^{-/-}$ MEFs. We are currently testing the viral replication of E1A null and CR3Δ mutant viruses in $Sur2^{-/-}$ MEFs. However, the data in the work presented here clearly showed that mSur2 is a critical factor for efficient MAV-1 replication.

However, we also note that there are differences between MAV-1 infection in cell culture and in mice. The E1A null mutant *pm*E109 is less virulent than wt MAV-1 in mice (52). The 50% lethal dose (LD_{50}) of *pm*E109 is 2 and 4 logs higher than wt MAV-1 in inbred SJL/J and outbred NIHS mice, respectively (55). Both *pm*E109 and *dl*E106 (CR3Δ) viruses replicated to significantly lower levels in several inbred stains of mice than did wt MAV-1 (L. Fang and K. R.

Spindler, manuscript in preparation). This suggests that mSur2-E1A binding may be more important for MAV-1 replication in mice than cells in culture.

A multiplicity-dependent growth phenotype has been observed for many viruses, including hAds (26, 32, 43, 50), herpes simplex virus type 1 (HSV-1) (16, 20, 24), cytomegalovirus (CMV) (14, 45) and African swine fever virus (ASFV) (41). *dl*312, an E1A null mutant of hAd, shows the multiplicity-dependent phenotype (26, 32, 43, 50). At low MOIs, there is a delay and reduced expression of viral early genes, but at higher MOIs, the expression of viral early genes can be enhanced (43). The UL82-deficient mutant HCMV displays a multiplicity-dependent phenotype in cell culture (14). The defect of severely restricted viral replication of this UL82-deficient mutant virus at low input MOIs can be rescued by higher input MOIs. Very similarly, the severe replication defect of ICP0 null mutant HSV-1 in Vero or BHK cells at low MOIs can be overcome at higher multiplicities (16, 20, 24). A thymidine kinase gene deletion mutant of ASFV shows a growth defect on swine macrophages at low MOIs, but the defect is not apparent at high MOIs (41). It is interesting to note that adenovirus E1A, HSV-1 ICP0 and HCMV UL82 all function in the early phase of viral infection and in gene activation (9, 14, 15, 19, 30, 33, 39), and mutations in these genes all show multiplicity-dependent effects. E1A is the first transcribed gene in adenovirus infection (43, 51) and it transactivates transcription of the other viral early genes including E4 (9, 33). However, E4 gene expression is seen in the absence of E1A when using high MOIs (46), suggesting that there is an E1A-independent pathway to activate the transcription of E4 genes. Therefore, it is possible that E4 gene products may play a role in this multiplicity-dependent effect in MAV-1-infected $Sur2^{-/-}$ MEFs. There might be a threshold in $Sur2^{-/-}$ MEFs for MAV-1 replication. At a relative low MOI, there might not be enough accumulation of E1A or E4 gene products. However, at a higher

MOI, due to the increase of copy number of viral promoters in cells, viral E1A and/or E4 gene products might accumulate to high enough levels to support MAV-1 replication. In any case, MAV-1 does not replicate as well as in $Sur2^{-/-}$ MEFs compared to $Sur2^{+/+}$ MEFs, indicating that Sur2 is important for efficient MAV-1 replication.

ACKNOWLEDGMENTS

We thank Carol Eng, Gwen Hirsch, Carla Pretto, and Amanda Welton for excellent technical assistance. We thank the monoclonal antibody facility at the University of Georgia for assistance with antibody generation. We thank Mary Lutzke, Jason Weinberg, and Martin Moore for assistance with RPAs. We thank Michael Imperiale and members of the Spindler laboratory for critical reviews of the manuscript.

This work was supported by NIH grant R01 AI023762 to K.R.S. and CA25235 to AJB.

1. **Ackrill, A. M., G. R. Foster, C. D. Laxton, D. M. Flavell, G. R. Stark, and I. M. Kerr.** 1991. Inhibition of the cellular response to interferons by products of the adenovirus type-5 E1A oncogene. Nucl. Acids Res. **19:**4387-4393.
2. **Asada, S., Y. Choi, M. Yamada, S. C. Wang, M. C. Hung, J. Qin, and M. Uesugi.** 2002. External control of Her2 expression and cancer cell growth by targeting a Ras-linked coactivator. Proc. Natl. Acad. Sci. USA **99:**12747-12752.
3. **Avvakumov, N., R. Wheeler, J. C. D'Halluin, and J. S. Mymryk.** 2002. Comparative sequence analysis of the largest E1A proteins of human and simian adenoviruses. J. Virol. **76:**7968-7975.

4. **Ball, A. O., C. W. Beard, S. D. Redick, and K. R. Spindler.** 1989. Genome organization of mouse adenovirus type 1 early region 1: A novel transcription map. Virology **170:**523-536.

5. **Ball, A. O., C. W. Beard, P. Villegas, and K. R. Spindler.** 1991. Early region 4 sequence and biological comparison of two isolates of mouse adenovirus type 1. Virology **180:**257-265.

6. **Ball, A. O., M. E. Williams, and K. R. Spindler.** 1988. Identification of mouse adenovirus type 1 early region 1: DNA sequence and a conserved transactivating function. J. Virol. **62:**3947-3957.

7. **Beard, C. W., A. O. Ball, E. H. Wooley, and K. R. Spindler.** 1990. Transcription mapping of mouse adenovirus type 1 early region 3. Virology **175:**81-90.

8. **Beard, C. W., and K. R. Spindler.** 1995. Characterization of an 11K protein produced by early region 3 of mouse adenovirus type 1. Virology **208:**457-466.

9. **Berk, A. J., F. Lee, T. Harrison, J. Williams, and P. A. Sharp.** 1979. Pre-early adenovirus 5 gene product regulates synthesis of early viral messenger RNAs. Cell **17:**935-944.

10. **Bondesson, M., M. Mannervik, G. Akusjarvi, and C. Svensson.** 1994. An adenovirus E1A transcriptional repressor domain functions as an activator when tethered to a promoter. Nucleic Acids Res **22:**3053-3060.

11. **Boube, M., L. Joulia, D. L. Cribbs, and H.-M. Bourbon.** 2002. Evidence for a mediator of RNA polymerase II transcriptional regulation conserved from yeast to man. Cell **110:**143-151.

12. **Boyd, J. M., T. Subramanian, U. Schaeper, M. La Regina, S. Bayley, and G. Chinnadurai.** 1993. A region in the C-terminus of adenovirus 2/5 E1a protein is required for association with a cellular phosphoprotein and important for the negative modulation of T24-*ras* mediated transformation, tumorigenesis, and metastasis. EMBO J. **12:**469-478.

13. **Boyer, T. G., M. E. D. Martin, E. Lees, R. P. Ricciardi, and A. J. Berk.** 1999. Mammalian Srb/Mediator complex is targeted by adenovirus E1A protein. Nature **399:**276-279.

14. **Bresnahan, W. A., and T. E. Shenk.** 2000. UL82 virion protein activates expression of immediate early viral genes in human cytomegalovirus-infected cells. Proc. Natl. Acad. Sci. USA **97:**14506-14511.

15. **Cai, W., and P. A. Schaffer.** 1991. A cellular function can enhance gene expression and plating efficiency of a mutant defective in the gene for ICP0, a transactivating protein of herpes simplex virus type 1. J. Virol. **65:**4078-4090.

16. **Cai, W., and P. A. Schaffer.** 1992. Herpes simplex virus type 1 ICP0 regulates expression of immediate-early, early, and late genes in productively infected cells. J. Virol. **66:**2904-2915.

17. **Cantin, G. T., J. L. Stevens, and A. J. Berk.** 2003. Activation domain-mediator interactions promote transcription preinitiation complex assembly on promoter DNA. Proc. Natl. Acad. Sci. USA **100:**12003-12008.

18. **Cauthen, A. N., and K. R. Spindler.** 1999. Construction of mouse adenovirus type 1 mutants, p. 85-103. *In* W. S. M. Wold (ed.), Adenovirus methods and protocols. Humana Press, Totowa, NJ.

19. **Chau, N. H., C. D. Vanson, and J. A. Kerry.** 1999. Transcriptional regulation of the human cytomegalovirus US11 early gene. J. Virol. **73:**863-870.

20. **Chen, J., and S. Silverstein.** 1992. Herpes simplex viruses with mutations in the gene encoding ICP0 are defective in gene expression. J. Virol. **66:**2916-2927.

21. **Deleu, L., S. Shellard, K. Alevizopoulos, B. Amati, and H. Land.** 2001. Recruitment of TRRAP required for oncogenic transformation by E1A. Oncogene **20:**8270-8275.

22. **Dignam, J. D., R. M. Lebovitz, and R. G. Roeder.** 1983. Accurate transcription initiation by RNA polymerase II in a soluble extract from isolated mammalian nuclei. Nucl. Acids Res. **11:**1475-1489.

23. **Egan, C., T. N. Jelsma, J. A. Howe, S. T. Bayley, B. Ferguson, and P. E. Branton.** 1988. Mapping of cellular protein-binding sites on the products of early-region 1A of human adenovirus type 5. Mol. Cell. Biol. **8:**3955-3959.

24. **Everett, R. D., C. Boutell, and A. Orr.** 2004. Phenotype of a herpes simplex virus type 1 mutant that fails to express immediate-early regulatory protein ICP0. J. Virol. **78:**1763-1774.

25. **Fuchs, M., J. Gerber, R. Drapkin, S. Sif, T. Ikura, V. Ogryzko, W. S. Lane, Y. Nakatani, and D. M. Livingston.** 2001. The p400 complex is an essential E1A transformation target. Cell **106:**297-307.

26. **Gaynor, R. B., and A. J. Berk.** 1983. Cis-acting induction of adenovirus transcription. Cell **33:**683-693.

27. **Harlow, E., P. Whyte, B. R. J. Franza, and C. Schley.** 1986. Association of adenovirus early-region 1A proteins with cellular polypeptides. Mol. Cell. Biol. **6:**1579-1589.

28. **Hirt, B.** 1967. Selective extraction of polyoma DNA from infected mouse cell cultures. J. Mol. Biol. **26:**365-369.

29. **Hobbs, M. V., W. O. Weigle, D. J. Noonan, B. E. Torbett, R. J. McEvilly, R. J. Koch, G. J. Cardenas, and D. N. Ernst.** 1993. Patterns of cytokine gene expression by CD4+ T cells from young and old mice. J. Immunol. **150:**3602-3614.

30. **Homer, E. G., A. Rinaldi, M. J. Nicholl, and C. M. Preston.** 1999. Activation of herpesvirus gene expression by the human cytomegalovirus protein pp71. J. Virol. **73:**8512-8518.

31. **Horwitz, M. S.** 2001. Adenoviruses, p. 2301-2326. *In* D. M. Knipe and P. M. Howley (ed.), Fields Virology, 4th ed, vol. 2. Lippincott Williams & Wilkins, Philadelphia.

32. **Imperiale, M. J., H.-T. Kao, L. T. Feldman, J. R. Nevins, and S. Strickland.** 1984. Common control of the heat shock gene and early adenovirus genes: evidence for a cellular E1A-like activity. Mol. Cell. Biol. **4:**867-874.

33. **Jones, N. C., and T. Shenk.** 1979. An adenovirus type 5 early gene function regulates expression of other early viral genes. Proc. Natl. Acad. Sci. USA **76:**3665-3669.

34. **Kajon, A. E., C. C. Brown, and K. R. Spindler.** 1998. Distribution of mouse adenovirus type 1 in intraperitoneally and intranasally infected adult outbred mice. J. Virol. **72:**1219-1223.

35. **Kajon, A. E., and K. R. Spindler.** 2000. Mouse adenovirus type 1 replication *in vitro* is resistant to interferon. Virology **274:**213-219.

36. **Kring, S. C., A. O. Ball, and K. R. Spindler.** 1992. Transcription mapping of mouse adenovirus type 1 early region 4. Virology **190:**248-255.

37. **Laemmli, U. K.** 1970. Cleavage of structural proteins during the assembly of the head of bacteriophage T4. Nature **227:**680-685.

38. **Lang, S. E., and P. Hearing.** 2003. The adenovirus E1A oncoprotein recruits the cellular TRRAP/GCN5 histone acetyltransferase complex. Oncogene **22:**2836-2841.

39. **Lium, E. K., C. A. Panagiotidis, X. Wen, and S. J. Silverstein.** 1998. The NH2 terminus of the herpes simplex virus type 1 regulatory protein ICP0 contains a promoter-specific transcription activation domain. J. Virol. **72:**7785-7795.

40. **Mo, X., E. Kowenz-Leutz, H. Xu, and A. Leutz.** 2004. Ras induces mediator complex exchange on C/EBP beta. Mol. Cell **13:**241-250.

41. **Moore, D. M., L. Zsak, J. G. Neilan, Z. Lu, and D. L. Rock.** 1998. The African swine fever virus thymidine kinase gene is required for efficient replication in swine macrophages and for virulence in swine. J. Virol. **72:**10310-10315.

42. **Moran, E., and M. B. Mathews.** 1987. Multiple functional domains in the adenovirus E1A gene. Cell **48:**177-178.

43. **Nevins, J. R.** 1981. Mechanism of activation of early viral transcription by the adenovirus E1A gene product. Cell **26:**213-220.

44. **O'Connor, R. J., and P. Hearing.** 2000. The E4-6/7 protein functionally compensates for the loss of E1A expression in adenovirus infection. J. Virol. **74:**5819-5824.

45. **Oliveira, S. A., and T. E. Shenk.** 2001. Murine cytomegalovirus M78 protein, a G protein-coupled receptor homologue, is a constituent of the virion and facilitates accumulation of immediate-early viral mRNA. Proc. Natl. Acad. Sci. USA **98:**3237-3242.

46. **Reichel, R., S. D. Neill, I. Kovesdi, M. C. Simon, P. R. Raychaudhuri, and J. R. Nevins.** 1989. The adenovirus E4 gene, in addition to the E1A gene, is important for *trans*-activation of E2 transcription and for E2F activation. J. Virol. **63:**3643-3650.

47. **Sarawar, S. R., R. D. Cardin, J. W. Brooks, M. Mehrpooya, R. A. Tripp, and P. C. Doherty.** 1996. Cytokine production in the immune response to murine gammaherpesvirus 68. J. Virol. **70:**3264-3268.

48. **Schaeper, U., J. M. Boyd, S. Verma, E. Uhlmann, T. Subramanian, and G. Chinnadurai.** 1995. Molecular cloning and characterization of a cellular phosphoprotein that interacts with a conserved C-terminal domain of adenovirus E1A involved in negative modulation of oncogenic transformation. Proc. Natl. Acad. Sci. USA **92:**10467-10471.

49. **Schaley, J., R. J. O'Connor, L. J. Taylor, D. Bar-Sagi, and P. Hearing.** 2000. Induction of the cellular E2F-1 promoter by the adenovirus E4-6/7 protein. J. Virol. **74:**2084-2093.

50. **Shenk, T., N. Jones, W. Colby, and D. Fowlkes.** 1979. Functional analysis of adenovirus-5 host-range deletion mutants defective for transformation of rat embryo cells. Cold Spring Harbor Symp. Quant. Biol. **44:**367-375.

51. **Shenk, T. E.** 2001. Adenoviridae: The viruses and their replication, p. 2265-2300. *In* D. M. Knipe and P. M. Howley (ed.), Fields Virology, 4th ed, vol. 2. Lippincott Williams & Wilkins, Philadelphia.

52. **Smith, K., C. C. Brown, and K. R. Spindler.** 1998. The role of mouse adenovirus type 1 early region 1A in acute and persistent infections in mice. J. Virol. **72:**5699-5706.

53. **Smith, K., B. Ying, A. O. Ball, C. W. Beard, and K. R. Spindler.** 1996. Interaction of mouse adenovirus type 1 early region 1A protein with cellular proteins pRb and p107. Virology **224:**184-197.

54. **Spindler, K. R., C. Y. Eng, and A. J. Berk.** 1985. An adenovirus early region 1A protein is required for maximal viral DNA replication in growth-arrested human cells. J. Virol. **53:**742-750.

55. **Spindler, K. R., L. Fang, M. L. Moore, C. C. Brown, G. N. Hirsch, and A. K. Kajon.** 2001. SJL/J mice are highly susceptible to infection by mouse adenovirus type 1. J. Virol. **75:**12039-12046.

56. **Stevens, J. L., G. T. Cantin, G. Wang, A. Shevchenko, A. Shevchenko, and A. J. Berk.** 2002. Transcription control by E1A and MAP kinase pathway via Sur2 mediator subunit. Science **296:**755-758.

57. **Wang, G., and A. J. Berk.** 2002. In vivo association of adenovirus large E1A protein with the human mediator complex in adenovirus-infected and -transformed cells. J. Virol. **76:**9186-9193.

58. **Wang, H. G., Y. Rikitake, M. C. Carter, P. Yaciuk, S. E. Abraham, B. Zerler, and E. Moran.** 1993. Identification of specific adenovirus E1A N-terminal residues critical to the binding of cellular proteins and to the control of cell growth. J. Virol. **67:**476-488.

59. **Yee, S. P., and P. E. Branton.** 1985. Detection of cellular proteins associated with human adenovirus type 5 early region 1A polypeptides. Virology **147:**142-153.

60. **Ying, B., K. Smith, and K. R. Spindler.** 1998. Mouse adenovirus type 1 early region 1A is dispensable for growth in cultured fibroblasts. J. Virol. **72:**6325-6331.

Fig. 2.1. Constructs and expression of GST fusion proteins. A, Schematic diagram of GST fusion protein constructs. GST-mE1A contains the full length MAV-1 E1A as well as an additional 22 a.a. linker between GST and E1A protein. Full length MAV-1 E1A protein (1-200 a.a.) without any linker is shown as GST-wt E1A. The fragments of E1A used as GST-fusion proteins were: a.a. 35-78 deletion (GST-CR1Δ), a.a. 111-129 deletion (GST-CR2Δ), a.a. 135-154 deletion (GST-CR3Δ), a.a 1-45 (GST-Nter1), a.a. 1-113 (GST-Nter2), a.a. 90-200 (GST-Cter3), a.a. 125-200 (GST-Cter2), a.a. 157-200 (GST-Cter1). For the deletion constructs the thin lines indicate the portion of the protein contained in the constructs. B, Expression and purification of GST-mE1A fusion proteins from *E. coli*. Samples were electrophoresed on a 10% SDS-polyacrylamide gel and stained with Coomassie blue. Lane 1, molecular weight standards (Rainbow marker from Amersham Biotech); lane 2, crude bacterial extract, without IPTG induction; lane 3, crude bacterial extract, with IPTG; lane 4, purified GST-mE1A fusion protein after elution from glutathione Sepharose 4B beads.

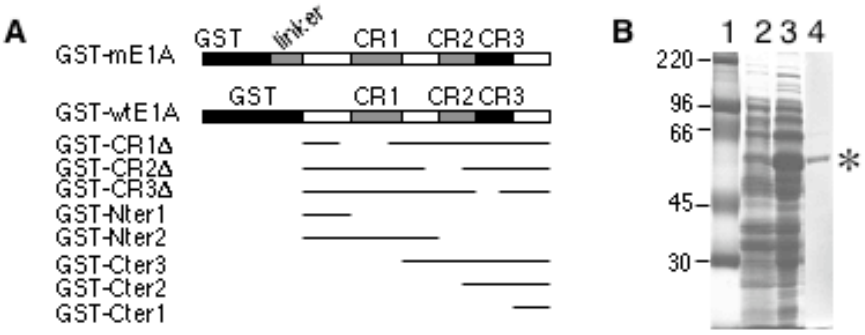
A
GST
linker
CR1
CR2
CR3
GST-mE1A
GST-wtE1A
GST-CR1Δ
GST-CR2Δ
GST-CR3Δ
GST-Nter1
GST-Nter2
GST-Cter3
GST-Cter2
GST-Cter1
B
1 2 3 4
220
96
66
45
30
*

Fig. 2.2. Interactions between MAV-1 E1A and Rb family proteins. A, MBMECs were either mock- (lanes 1, 4, 7 and 10), wt MAV-1- (lanes 2, 5, 8 and 11) or *pm*E109- (lanes 3, 6, 9 and 12) infected at MOI of 5 and harvested at 40 h p.i. Rabbit polyclonal antibody against p130 (lanes 4-6), p107 (lanes 7-9), and Rb (lanes 10-12) was used to immunoprecipitate the whole cell lysates, respectively. Normal rabbit serum (NRS, purified by DEAE Affi-Gel blue chromatography) was used as a negative control (lanes 1-3). Western blots were carried out by probing the membranes with monoclonal antibody against MAV-1 E1A (10B10) (1:1000). The arrowhead indicates the MAV-1 E1A. The asterisk (∗) indicates the IgG heavy chain. B, Equivalent amounts of purified GST, GST-mE1A, GST-Cter1 and GST-gp11K proteins were bound to glutathione beads and then mixed with an equal amount of mammalian whole cell lysates (WCL) from either MBMECs or 3T6 cells as indicated. After washing, bound proteins were eluted and eletrophoresed on 10% SDS-polyacylamide gels and transferred to PVDF membranes. The membrane was probed with polyclonal antiserum against mouse Rb protein. Lane 1, protein molecular weight standards (sizes indicated on the left side); lanes 2-4, proteins bound and eluted from GST-beads, GST-Cter1-beads and GST-mE1A-beads, respectively, mixed with MBMEC lysates; lanes 5-7, proteins bound and eluted from GST-mE1A-beads, GST-Cter1-beads, and GST-beads, respectively, mixed with 3T6 cell lysates. The arrowhead shows the position of mouse Rb. The asterisk shows the detection of GST-mE1A due to the cross-reaction of Rb antibody to GST protein (it was raised against GST-Rb fusion protein). C, GST pull-down assay/Western blot was carried out as B. The membrane was probed with p107 antibody. Lane 1, whole cell lysates from MBMECs; lane 2, protein molecular weight standards; lanes 3-6, proteins bound and eluted from GST-beads, GST-mE1A-beads, GST-Cter1-beads, and GST-gp11K-beads, respectively, mixed with MBMEC lysates. The arrowhead shows the p107

position. D, GST pull-down assay/Western blot was carried out as B. The membrane was probed with p130 antibody. Lane 1, protein molecular weight standards (the size is shown at the left in kDa); lane 2, whole cell lysates from MBMECs; lanes 3-6, proteins bound and eluted from GST-beads, GST-mE1A-beads, GST-Cter1-beads, and GST-gp11K-beads, respectively, mixed MBMEC lysates. The arrowhead showes the p130 position. E, Western blot probed with antibody against GST fusion protein. Same loading order as D.

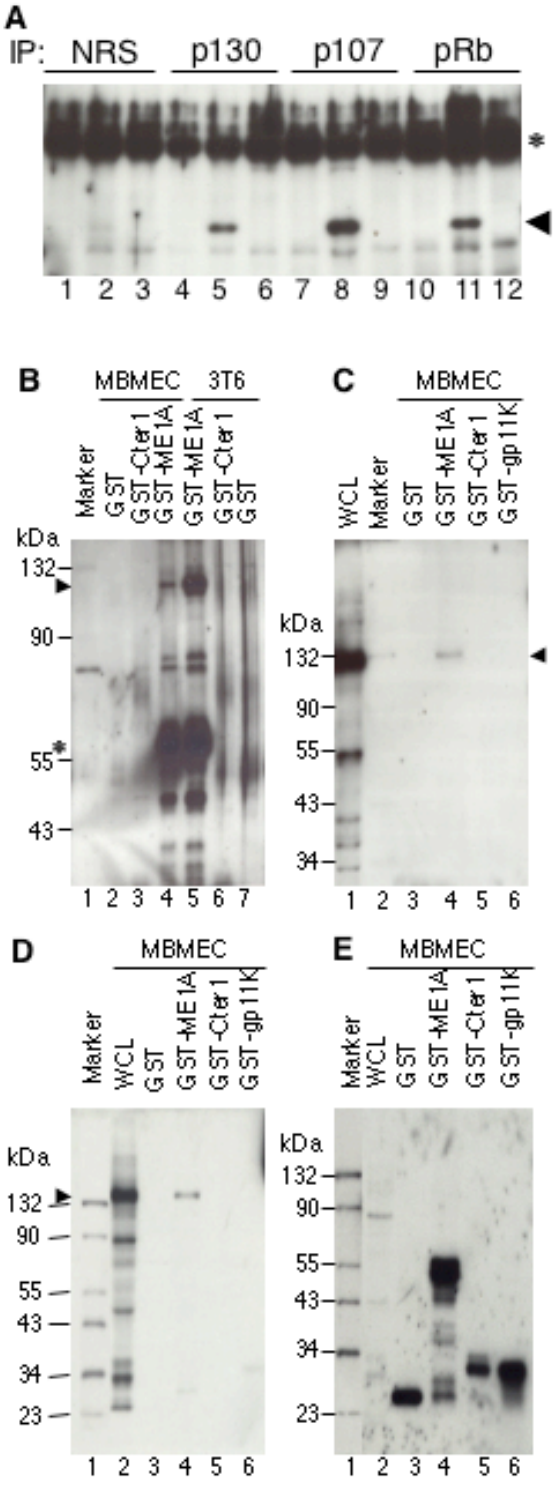
A
IP: NRS p130 p107 pRb
1 2 3 4 5 6 7 8 9 10 11 12
B
MBMEC 3T6
Marker
GST
GST-Cter1
GST-ME1A
GST-ME1A
GST-Cter1
GST
kDa
132
90
55
43
1 2 3 4 5 6 7
C
MBMEC
WCL
Marker
GST
GST-ME1A
GST-Cter1
GST-gp11K
kDa
132
90
55
43
34
1 2 3 4 5 6
D
MBMEC
Marker
WCL
GST
GST-ME1A
GST-Cter1
GST-gp11K
kDa
132
90
55
43
34
23
1 2 3 4 5 6
E
MBMEC
Marker
WCL
GST
GST-ME1A
GST-Cter1
GST-gp11K
kDa
132
90
55
43
34
23
1 2 3 4 5 6

Fig. 2.3. Identification of mSur2 as a specific MAV-1 E1A interacting protein. A, Large scale GST-mE1A pull-down assay. Lane 1, protein molecular weight standards; lanes 2-4, purified GST, GST-mE1A, and GST-Cter1 fusion proteins, respectively, were bound to glutathione Sepharose beads without mixing with any mammalian cell nuclear extracts (-); lanes 5-7, nuclear extracts from 5 x 10^8 mouse MBMECs were precleared sequentially against glutathione Sepharose beads and GST-beads, then an equal amount of the precleared mammalian nuclear extracts were added (+) to GST-beads, GST-mE1A-beads, and GST-Cter1-beads, respectively. Beads were washed and the bound proteins were eluted off the beads by boiling in a protein loading buffer. Proteins binding specificically to GST-mE1A were identified by comparing lane 6 with lanes 3 and 5. Sur2 protein is shown by the arrowhead. An independent duplicate analysis of both MBMEC and 3T6 cell lines gave similar results, with identification of Sur2 (data not shown). B, Sur2 protein interacts with GST-mE1A (full length E1A) in GST pull-downs. GST pull-down assays were performed by incubating the nuclear extracts from 3T6 cells (lanes 1-3) or MBMECs (lanes 4-6) with GST-beads, GST-Cter1-beads or GST-mE1A-beads as indicated. Monoclonal antibody against Sur2 (BD Pharmingen) (1:1000) was used for Western blots. Whole cell lysates (WCL) were used as positive control (lane 8). m, protein molecular weight standards. The arrowhead shows the Sur2 position. C, MAV-1 E1A protein interacts with Sur2 in virus-infected cells. MBEMCs were mock- or MAV-1-infected at an MOI of 5 and harvested at 40 hours p.i. Normal rabbit serum (NRS) or AKO7-147 (E1A) (both purified by DEAE Affi-Gel blue chromatography) was mixed with whole cell lysates of MBMECs to carry out the immunoprecipitation. The immunoprecipitates were electrophoresced on 8% polyacrylamide SDS-PAGEs and transferred to PVDF membranes. Monoclonal antibody against Sur2 was used in Western blots. The arrowhead shows the Sur2 position.

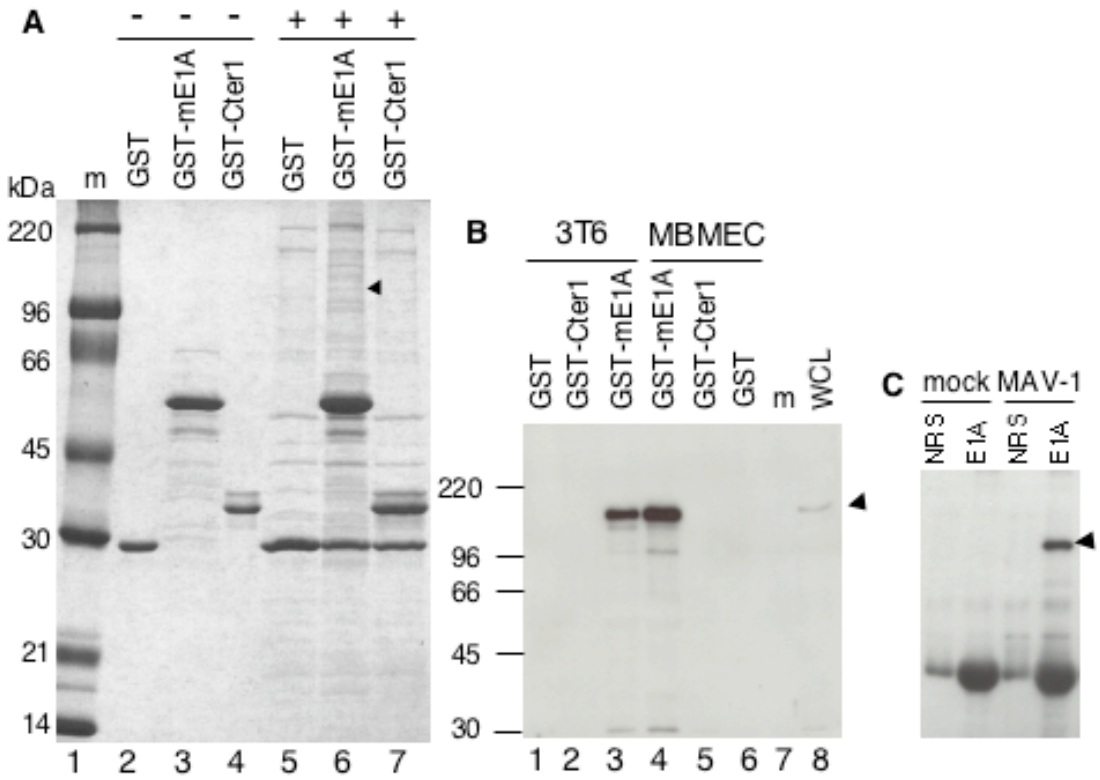
A
-
-
-
+
+
+
kDa
m
GST
GST-mE1A
GST-Cter1
GST
GST-mE1A
GST-Cter1
220
96
66
45
30
21
14
1 2 3 4 5 6 7
B
3T6
MBMEC
GST
GST-Cter1
GST-mE1A
GST-mE1A
GST-Cter1
GST
m
WCL
220
96
66
45
30
1 2 3 4 5 6 7 8
C
mock
MAV-1
NRS
E1A
NRS
E1A

Fig. 2.4. MAV-1 E1A CR3 is required for binding to Sur2. The GST fusion proteins were purified from induced *E. coli*. cells. Whole cell lysates of MBMECs were incubated with different regions of MAV-1 E1A as GST-fusion proteins bound to the glutathione beads. A, the bound proteins were analyzed by Western blotting using monoclonal anti-Sur2 antibody. B, the membrane was stripped and re-probed with anti-GST antibody to show the equivalent loading of various GST fusion proteins.

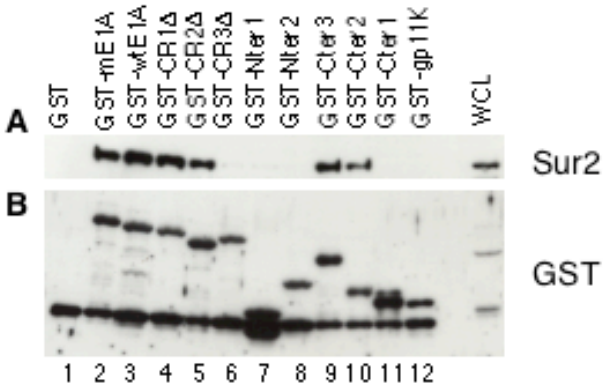
A
B
GST
GST-mE1A
GST-wtE1A
GST-CR1Δ
GST-CR2Δ
GST-CR3Δ
GST-Nter1
GST-Nter2
GST-Cter3
GST-Cter2
GST-Cter1
GST-gp11K
WCL
Sur2
GST
1 2 3 4 5 6 7 8 9 10 11 12

Fig. 2.5. CR3 of MAV-1 E1A is essential for the interaction between Sur2 and MAV-1 E1A. A, MBMECs were infected with wt MAV-1, *dl*E105 (CR1Δ mutant), *dl*E102 (CR2Δ mutant) or *dl*E106 (CR3Δ mutant) at an MOI of 5 and harvested at 40 hours p.i. and aliquotted. Immunoprecipitation/Western blot analysis was carried out as in Fig. 2.3C on one aliquot of each infection. The IgG used in immunoprecipitation was also detected due to the cross-reaction with the secondary antibody used in Western blotting (∗, IgG heavy chain. ∗∗, IgG light chain). The arrowhead shows the Sur2 position. B, Western blots (without immunoprecipitation) of another aliquot of each infection were probed with the indicated primary antibodies.

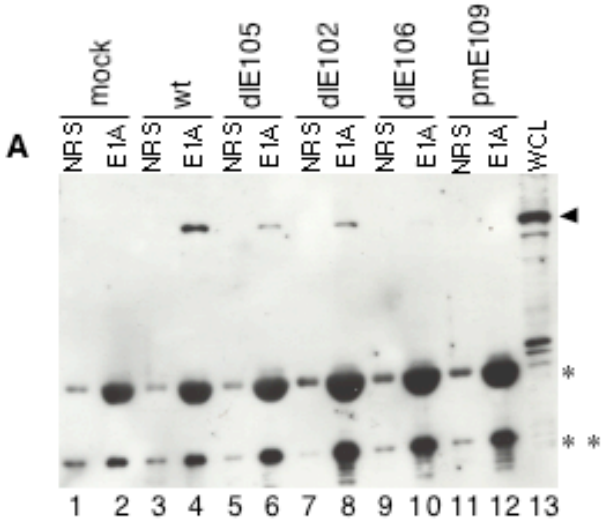
A
mock
wt
dlE105
dlE102
dlE106
pmE109
NRS
E1A
WCL
1 2 3 4 5 6 7 8 9 10 11 12 13
B
mock
wt
dlE105
dlE102
dlE016
pmE109
Sur2
β-actin
E3 gp 11K

Fig. 2.6. Cytopathic effects (CPE) in $Sur2^{+/+}$ and $Sur2^{-/-}$ MEFs upon MAV-1 infection. MEFs were either mock- or MAV-1-infected at the indicated MOI. Phase contrast pictures were taken at 7 days p.i. using an Olympus microscope (400 X). The scale bar is 50 μM.

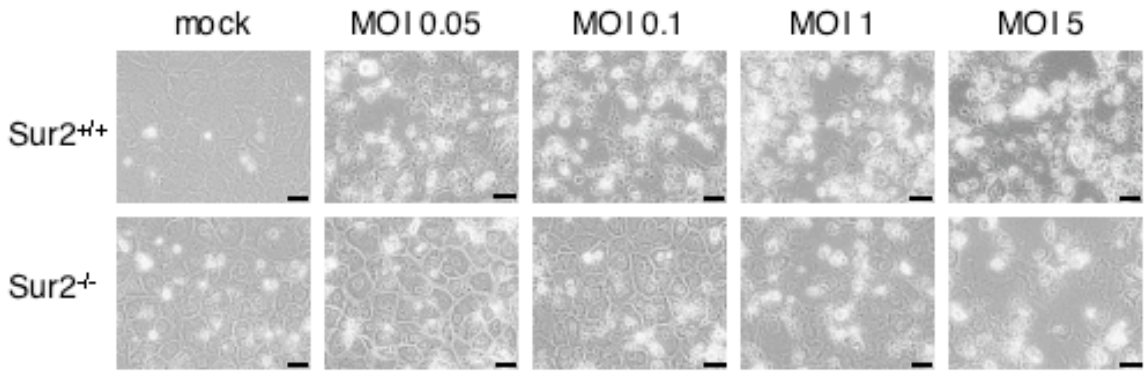
mock
MOI 0.05
MOI 0.1
MOI 1
MOI 5
Sur2+/+
Sur2-/-

Fig. 2.7. Multiplicity-dependence of MAV-1 viral yields on MEFs. A, growth curves of MAV-1 on $Sur2^{+/+}$ and $Sur2^{-/-}$ MEFs. $Sur2^{+/+}$ and $Sur2^{-/-}$ MEFs were infected with MAV-1 at the indicated MOIs and harvested at the indicated times. The viral yields were determined by plaque assays on 3T6 cells. Three independently infected cultures were assayed for each MOI. These experiments were repeated three times, with similar results (data not shown). B, growth curves of MHV-68 on $Sur2^{+/+}$ and $Sur2^{-/-}$ MEFs. $Sur2^{+/+}$ and $Sur2^{-/-}$ MEFs were infected with MHV-68 at an MOI of 0.01 and harvested at indicated times. The viral yields were determined by plaque assays on NIH3T3 cells. The legend for $Sur2^{+/+}$ MEFs and $Sur2^{-/-}$ MEFs is shown at the top and is the same for all panels.

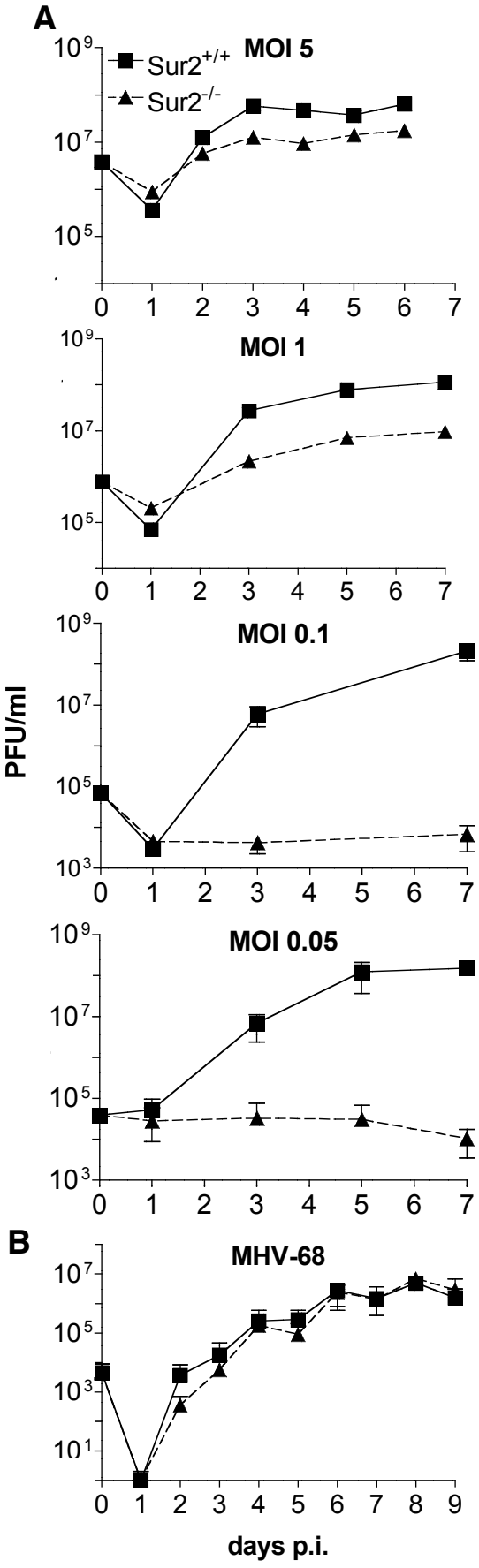
A
Sur2+/+
Sur2-/-
MOI 5
MOI 1
MOI 0.1
MOI 0.05
PFU/ml
B
MHV-68
days p.i.

Fig. 2.8. Multiplicity-dependent defects in viral DNA replication in $Sur2^{-/-}$ MEFs. Viral DNA was isolated from MAV-1 infected $Sur2^{+/+}$ (+/+) and $Sur2^{-/-}$ (-/-) MEFs at the indicated MOIs and times by the Hirt method. Equal amounts of DNA were digested with *Hin*d III, loaded on 0.7% agarose gels and transferred to membranes. The membranes were probed with MAV-1-specific DNA probes labeled with [α-^{32}P]-dATP. The sizes of the DNA fragments are indicated in kilobases. m, mock infected. These experiments were replicated three times with similar results (data not shown).

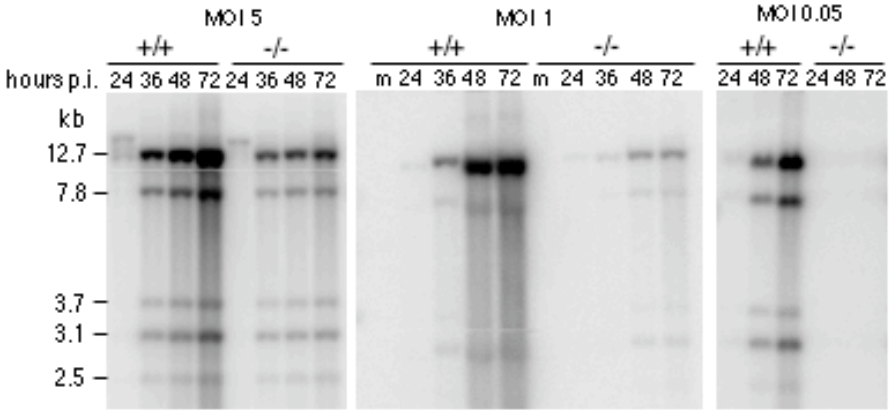
MOI 5
+/+
-/-
hours p.i. 24 36 48 72 24 36 48 72
MOI 1
+/+
-/-
m 24 36 48 72 m 24 36 48 72
MOI 0.05
+/+
-/-
24 48 72 24 48 72
kb
12.7
7.8
3.7
3.1
2.5

Fig. 2.9. Multiplicity-dependent defects in viral mRNA levels in $Sur2^{-/-}$ MEFs. A, Total RNA was isolated from MAV-1 infected $Sur2^{+/+}$ (+/+) and $Sur2^{-/-}$ (-/-) MEFs at the indicated MOIs and times. The multiplexed probe ("probe") shows the full-length probes (no RNase) for E1A, hexon and L32, as indicated by the tick marks. The size of probe protected from RNase treatment is shown by the arrows and asterisks for each gene. L32 was used as an internal loading control. These experiments were repeated three times with similar results (data not shown). B, Quantitation of RPAs. $Sur2^{+/+}$ and $Sur2^{-/-}$ MEFs were infected at an MOI of 0.05 and harvested at the indicated times. Viral genes E1A, E2A, E3gp11K, E4, and hexon were analyzed by RPAs. The amount of mRNA for each gene was determined by quantitation of band intensities in the autoradiograph using a phosphorimager and ImageQuaNT software and then normalized to L32 or β-actin controls, whose levels were set to 100%. C, $Sur2^{+/+}$ and $Sur2^{-/-}$ MEFs were infected at an MOI of 1, and viral genes were analyzed as panel B.

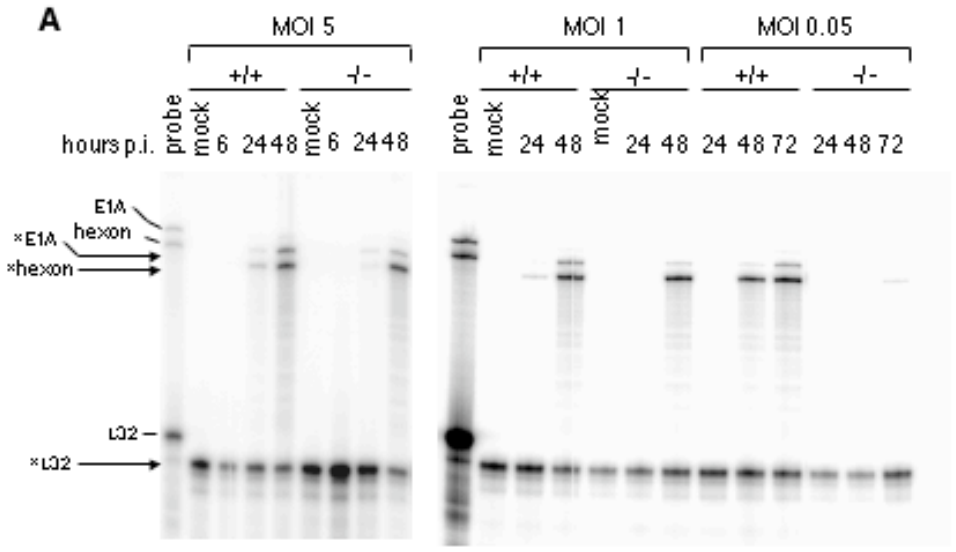
A
MOI 5
MOI 1
MOI 0.05
+/+
-/-
probe
mock
hours p.i.
6 24 48
24 48 72
E1A
hexon
×E1A
×hexon
L32
×L32

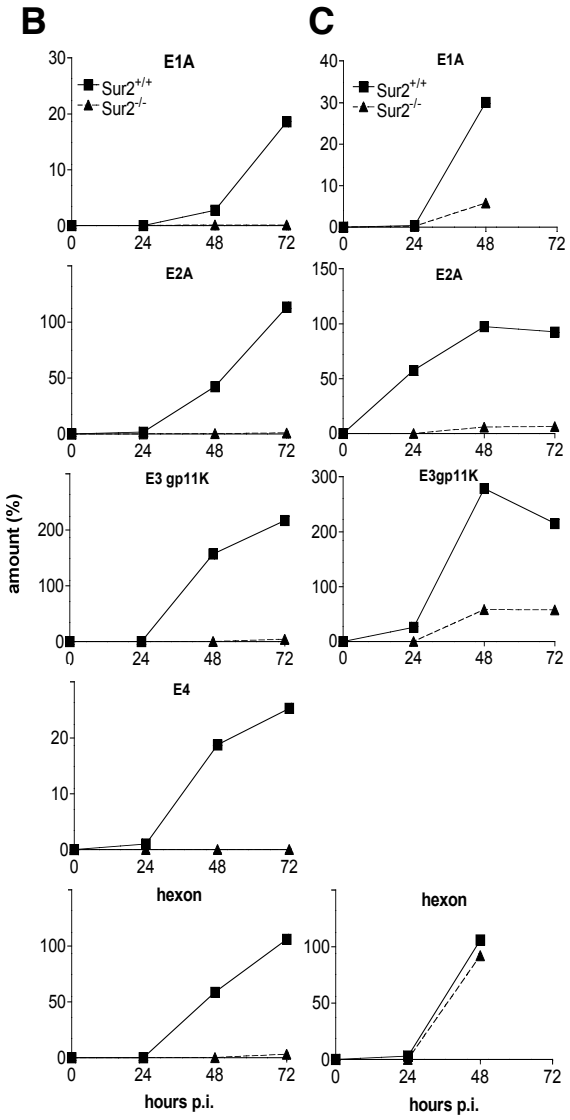
B
C
E1A
E2A
E3 gp11K
E4
hexon
E3gp11K
Sur2+/+
Sur2-/-
amount (%)
hours p.i.
0
24
48
72

Fig. 2.10. Differences in viral protein levels between infected $Sur2^{+/+}$ and $Sur2^{-/-}$ MEFs. A, MEFs were infected with MAV-1 at an MOI of 1 and harvested at the indicated times. Cell pellets were lysed in E3 lysis buffer (420 mM NaCl, 50 mM Tris-HCl [pH 7.4], 1% NP40). Protein concentrations were measured using a Bio-Rad protein assay kit. Equivalent amounts of protein except for the $Sur2^{+/+}$ MEF 5 and 7 days p.i. samples were loaded. For those tow samples, only 39% and 32%, respectively, were recovered and loaded. Samples were electrophoresced on an 8%-15% gradient SDS-polyacylamide gel and analyzed by Western blotting using antibodies as indicated at the right. β-actin was assayed as a loading control. B, Quantitation of Western blots. The band intensities were quantitated by densitometry and normalized to β-actin levels for each sample.

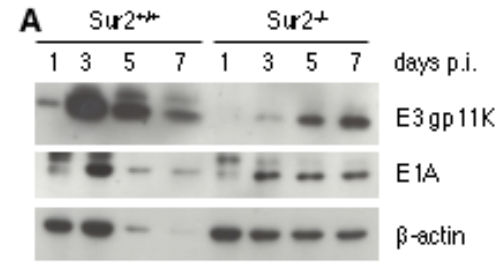
A
Sur2+/+
Sur2-/-
1 3 5 7 1 3 5 7
days p.i.
E3gp11K
E1A
β-actin

B

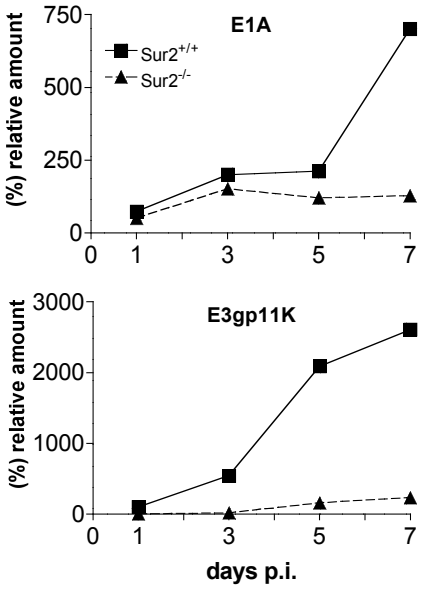
E1A
Sur2+/+
Sur2-/-
(%) relative amount
750
500
250
0
0 1 3 5 7
E3gp11K
(%) relative amount
3000
2000
1000
0
0 1 3 5 7
days p.i.

CHAPTER 3

E1A-CR3 INTERACTION-DEPENDENT AND -INDEPENDENT FUNCTIONS OF mSUR2 IN VIRAL REPLICATION OF EARLY REGION 1A MUTANTS OF MOUSE ADENOVIRUS TYPE 1 [1]

[1] L. Fang, K. R. Spindler. Submitted to Journal of Virology.

ABSTRACT

Conserved region 3 (CR3) of early region 1A (E1A) of mouse adenovirus type 1 (MAV-1) interacts with mSur2, a subunit of the Mediator complex, and mSur2 is required for efficient wt MAV-1 replication due at least in part to the requirement of mSur2 for viral early gene transcription (L. Fang, J. L. Stevens, A. J. Berk, K. R. Spindler, J. Virol. Control number: JVI01111-04). In this work, we further studied the contributions of E1A to mSur2 function in MAV-1 replication using E1A mutant viruses. At an MOI of 1, viruses containing an intact CR3 (wt MAV-1, CR1Δ mutant, and CR2Δ mutant) replicated better in $Sur2^{+/+}$ mouse embryonic fibroblasts (MEFs) than in $Sur2^{-/-}$ MEFs. In contrast, viruses lacking CR3 (E1A null mutant, and CR3Δ mutant) replicated no better in $Sur2^{+/+}$ than in $Sur2^{-/-}$ MEFs. This result supports the hypothesis that the E1A CR3-mSur2 interaction is important for MAV-1 replication. However, at an MOI of 0.05, viruses lacking CR3 (E1A null mutant and CR3Δ mutant) showed replication defects in $Sur2^{-/-}$ MEFs compared to $Sur2^{+/+}$ MEFs, suggesting an E1A CR3 interaction-independent function of mSur2 in MAV-1 replication in cell culture. Paradoxically, CR1Δ, CR2Δ, and CR3Δ mutant viruses replicated slightly more efficiently than wt MAV-1 and E1A null mutant viruses in $Sur2^{-/-}$ MEFs at an MOI of 0.05. The defects of E1A expression of wt MAV-1 in $Sur2^{-/-}$ MEFs were rescued by co-infection with CR3Δ mutant virus, as measured by Western blots and RNase protection assays. This suggests that an inhibiting effect on wt E1A protein expression and/or E1A function might account for the severe viral replication defect of wt MAV-1 in $Sur2^{-/-}$ MEFs at low MOIs. Moreover, titrations of viral yields from infected brains of four inbred strains of mice showed that E1A null and CR3Δ mutant viruses have a significant defect in viral replication compared to wt MAV-1 in all these strains of mice. This result

supports the hypothesis that the MAV-1 E1A-mSur2 interaction is important in MAV-1 replication in mice.

INTRODUCTION

Study of mouse adenovirus type 1 (MAV-1) infection in its natural host facilitates understanding the pathogenesis of adenoviruses. MAV-1 early region 1A (E1A) is a virulence factor in viral infection in mice, as demonstrated by LD_{50} experiments (28). However, the molecular functions of MAV-1 E1A in viral infection have not been fully investigated. Previously we showed that mSur2, a subunit of Mediator complex, interacts with MAV-1 E1A conserved region 3 (CR3) and that mSur2 is required for efficient MAV-1 replication (8). The Mediator complex connects transcriptional regulators to the basal RNA polymerase II transcriptional machinery and is important for efficient transcription activation (3, 5, 34). Experimental evidence has demonstrated that an interaction between a transcription activation domain and Mediator promotes transcription preinitiation complex assembly on promoter DNA (6). The human adenovirus (hAd) large E1A protein also binds to Sur2 via CR3 (5, 36). The conservation in human and mouse adenoviruses of the ability of E1A to bind to Sur2 indicates the importance of E1A CR3-Sur2 interaction in adenovirus pathogenesis.

Wild type (wt) MAV-1 exhibits a replication defect in $Sur2^{-/-}$ MEFs in a multiplicity-dependent manner (8). The severe viral replication defect at low input MOIs (MOI of 0.05 or 0.1) can be partially overcome by higher input MOIs (MOI of 1 or 5). The defective viral replication is due at least in part to a defect in viral early gene transcription. This result supports the proposed model that adenovirus E1A protein transactivates viral early genes by recruiting Mediator complex through E1A CR3-Sur2 interaction (6, 36). In the work reported here, we further test this model using MAV-1 E1A mutant viruses. Our data suggest that mSur2 has

broader functions in MAV-1 replication in cell culture than just binding to E1A CR3. In addition, the defective viral replication of E1A null and CR3Δ mutant viruses in four different inbred stains of mice indicates that the MAV-1 E1A CR3-mSur2 interaction is important for viral replication in mice.

MATERIALS AND METHODS

Cells and Viruses. Mouse NIH3T6 fibroblast cells were maintained in Dulbecco's modified Eagle's medium (DMEM) supplemented with 5% heat-inactivated calf serum. MAV-1 E1A-expressing 37.1 cells (29) were maintained in DMEM containing 5% heat-inactivated calf serum and 200 μg/ml G418. Prior to viral infection, 37.1 cells were treated with 1.25 x 10^{-5} M dexamethasone (Sigma). The details of generation of $Sur2^{+/+}$ and $Sur2^{-/-}$ mouse embryonic fibroblast cells (MEFs) were described previously (8). They were maintained in DMEM containing 10% fetal bovine serum. Wt MAV-1 was the standard MAV-1 stock originally obtained from S. Larsen (1). *pm*E109 is a MAV-1 E1A null mutant virus; *dl*E105, *dl*E102, and *dl*E106 viruses are MAV-1 E1A CR1 deletion (CR1Δ), CR2 deletion (CR2Δ), and CR3 deletion (CR3Δ) mutants, respectively (29).

Mice. All animal work complied with all relevant federal guidelines and institutional policies. SJL/J and BALB/cJ mice were purchased from Jackson Laboratory. 129/J mice were obtained from Taconic Company. IFN-α/β$R^{-/-}$ (IFNAR) mice (21) are on a 129 Sv/Ev background and were a kind gift from Kate Ryman, who originally obtained them from Barbara Sherry (24). All mice were male and 3-5 weeks old. Mice were maintained in microisolator cages and infected with wt MAV-1, *pm*E109, or *dl*E106 at a dose of 100 PFU by i.p. injection in

a volume of 0.1 ml conditioned medium. Infected mice were euthanized by inhalation of CO_2 at 8 days post infection (p.i.), and the brains were harvested and stored in –20º C until use.

Antibodies. Mouse monoclonal antibody (mAb10B10) against MAV-1 E1A and mouse monoclonal antibody (mAb11H9) against MAV-1 E3gp11k were described previously (8). Anti-MAV-1 E1A (AKO7-147) rabbit polyclonal antibodies were as described (29). Mouse monoclonal antibody against β-actin of *Arabidopsis thaliana*, which cross-reacts with mouse β-actin, was obtained from Dr. Richard Meagher at University of Georgia and used at a 1:500 dilution for Western blots.

Viral growth curves. $Sur2^{+/+}$ and $Sur2^{-/-}$ MEFs were infected with either wt MAV-1 or mutant viruses at an MOI of 0.05 or 1. Plaque assays were carried out on 37.1 cells as described previously (38). Briefly, cells were harvested at various times p.i. by scraping in their medium. The cell suspensions were subjected to three cycles of freezing and thawing and the cell debris was spun out of the supernatant. Tenfold serial dilutions of supernatants were plated in triplicate on 37.1 cells, and plaques were counted 9 days after plating.

Determination of virus loads in mouse brains. A total weight of 0.1 g of brain tissue from an individual mouse was put into a tube filled with sterile glass beads and homogenized in a volume of 1 ml of phosphate-buffered saline (PBS) using a Beadbeater (Biospec Products) running at top speed for 1 min intervals for a total of 3 min. The homogenates were aspirated off of the beads and spun in a microcentrifuge at 700 x g for 5 min at room temperature. The supernatants were 10-fold serially diluted and titrated by plaque assays on 37.1 cells (38). Wt MAV-1 was used a positive control. Counts of fewer than 20 plaques per 60 mm-diameter plate were considered unreliable. Therefore, 2×10^3 PFU/g of tissue was calculated as the detection limit.

Southern blots. Sur2$^{+/+}$ and Sur2$^{-/-}$ MEFs were infected at an MOI of 0.05 or 1, and harvested at various times p.i. by scraping the cells off the plates. Viral DNA was isolated by the method of Hirt (12). Equal amounts of DNA samples were digested with *Hin*d III and RNase A and electrophoresed on a 0.7% agarose gel. The DNA was transferred to a positively charged nylon membrane (Boehringer) by capillary transfer. The membrane was prehybridized in 10 ml of PerfectHyb solution (Sigma) at 65ºC for 2 h. Then an MAV-1 genomic DNA-specific [γ–^{32}P]-labeled probe as described (8) was added to 10 ml PerfectHyb solution to hybridize at 65ºC for 5-18 h. The membranes were washed and exposed to a phosphorimager (8).

Ribonuclease protection assays (RPAs). Sur2$^{+/+}$ and Sur2$^{-/-}$ MEFs were infected at an MOI of 0.05. Total RNA was extracted using TRI reagent (Molecular Research Center, Inc.) following the manufacturer's instructions. Equimolar pools of linearized plasmid templates were used to make an [α-^{32}P] UTP-labeled multiplex RPA probe set using T7 or T3 polymerase transcription as described previously (8). One probe set included MAV-1 E1A, E4, and hexon, and mouse L32 and was labeled using T7 polymerase. The other probe set included MAV-1 E3gp11K, and E2A, and mouse β-actin and was labeled using T3 polymerase. The RPAs were carried out as described by Hobbs et al. (13). Briefly, 10 μg of total RNA were hybridized with the probe sets overnight at 56ºC. Yeast tRNA was used as a negative control in RPAs. After digestion with RNase A and RNase T1, samples were ethanol precipitated and electrophoresed on 5% polyacrylamide/8M urea gels. After drying, protected mRNA signals were visualized using a phosphorimager, and quantitation was performed by normalizing the mRNA species of interest to L32 or β-actin signals.

Rescue experiment by co-infection. Sur2$^{-/-}$ MEFs were singly infected with wt MAV-1 (MOI 0.1), CR1, CR2, or CR3Δ (MOI 0.1), or co-infected with wt MAV-1 (MOI 0.05) and

CR1Δ (MOI 0.05), wt MAV-1 (MOI 0.05) and CR2Δ (MOI 0.05), or wt MAV-1 (MOI 0.05) and CR3Δ (MOI 0.05) on 100 mm plates. As controls for infection, $Sur2^{+/+}$ MEFs were singly infected at MOI of 0.1 with wt MAV-1, CR1Δ, CR2Δ, or CR3Δ. Cells were harvested, pelleted, and stored at –20º C until use. The cell pellets were lysed on ice for 30 min in 20 μl E3 lysis buffer (420 mM NaCl, 50 mM Tris-HCl [pH 7.5], 1% NP-40) containing protease inhibitor cocktail (1: 50) (Sigma) and 1 mM PMSF. Twenty μl of 50 mM Tris-HCl [pH 7.5] was added to the lysates. The lysates were centrifuged at 12000 x g for 15 min at 4º C, and 13 μl of 4X sample loading buffer (17) was added to the 40 μl supernatants and boiled for 10 min. Fifteen μl of each sample was analyzed by Western blots.

Western blots. Protein samples were resolved on a 6%-18% gradient SDS-polyacrylamide gel and electrotransferred onto PVDF membranes at 120 volts for 3 hrs. The membranes were blocked by incubation at room temperature for 1 h in TBS-Tween (150 mM NaCl, 10 mM Tris [pH 7.4], 0.1% Tween-20) containing 5% nonfat dry milk. Anti-rabbit (1:12,000 from Amersham Biosciences) or anti-mouse (1:12,000 from Amersham Biosciences) IgG-HRP conjugated antibody was used as the secondary antibody. Immunoblots were developed using SuperSignal West Pico Chemiluminescent Substrate (Pierce Biotechnology, Inc.).

RESULTS

Functions of mSur2 in MAV-1 E1A mutant virus replication. Infection of $Sur2^{+/+}$ and $Sur2^{-/-}$ MEFs with wt MAV-1 showed that mSur2 is required for efficient viral replication (8). Using E1A mutant viruses, we also showed that MAV-1 E1A is dispensable for viral replication in 3T6 cells infected at an MOI of 5 (38). Therefore, it was of interest to test whether mSur2 was

required for E1A mutant viruses to replicate. Since there is a multiplicity-dependent effect in $Sur2^{-/-}$ MEFs upon wt MAV-1 infection (8), it was important to ensure that equivalent input amounts of all the viruses were used. Accordingly, wt MAV-1, E1A null, CR1Δ, CR2Δ, CR3Δ mutants were titrated on 37.1 cells (a complementing cell line for E1A mutants) in the same experiment. To confirm equivalent input virus in subsequent infections based on these plaque assays, viral gene expression was analyzed using ribonuclease protection assays (RPAs). 37.1 cells were infected at an MOI of 0.05 using these viruses, and total RNAs were extracted at 24 hrs and 48 hrs post infection (p.i.). As shown in Fig. 3.1, viral E4 and hexon gene expression appeared similar in the wt and E1A mutant virus infections, indicating equivalent amounts of input virus. This was confirmed by quantitation using phosphorimager in comparison to the mouse L32 gene (data not shown).

Viral growth assays were performed to compare growth of wt and E1A mutants on $Sur2^{+/+}$ and $Sur2^{-/-}$ MEFs. $Sur2^{+/+}$ and $Sur2^{-/-}$ MEFs were infected by wt, E1A null mutant, CR1Δ mutant, CR2Δ mutant, or CR3Δ mutant viruses at an MOI of 1. Plaque assays on 37.1 cells were carried out to titrate the viral yields, and the results are shown in Fig. 3.2A. There was about a 10-fold difference in wt virus yield between $Sur2^{+/+}$ and $Sur2^{-/-}$ MEFs. This is consistent with previous results (8). There were about 5-fold lower yields of CR1Δ and CR2Δ viruses in $Sur2^{-/-}$ compared to $Sur2^{+/+}$ MEFs. MAV-1 E1A CR3 is required for interacting with mSur2 (8). These data, taken together with the wt MAV-1 result, indicate that mSur2 is important for these viruses, which all contain CR3, to replicate. No significant difference was detected in the yields of E1A null mutant or CR3Δ viruses between $Sur2^{+/+}$ and $Sur2^{-/-}$ MEFs, indicating that mSur2 is not required for them to replicate, at least at an input MOI of 1. Together the viral replication data of

viruses containing CR3 (wt, CR1Δ, CR2Δ) and viruses lacking CR3 (E1A null and CR3Δ) indicate that E1A CR3-mSur2 interaction was important for MAV-1 replication.

We previously observed multiplicity-dependent defects in viral replication in $Sur2^{-/-}$ MEFs upon wt MAV-1 infection (8). The severe defects at a low input MOI of wt virus can be partially overcome at a higher input MOI. Therefore, we tested whether there was a multiplicity-dependent effect in viral replication of E1A mutant viruses by using a low input MOI. $Sur2^{+/+}$ and $Sur2^{-/-}$ MEFs were infected at an MOI of 0.05, and viral yields were analyzed by plaque assays on 37.1 cells. There were viral replication defects for all strains of viruses in $Sur2^{-/-}$ MEFs compared to $Sur2^{+/+}$ MEFs at an MOI of 0.05 (Fig. 3.2B). The wt MAV-1 replication was severely restricted in $Sur2^{-/-}$ MEFs, since the viral yields were the same as the level of input viruses. This was consistent with previous results for wt MAV-1 growth in $Sur2^{-/-}$ MEFs titrated on 3T6 cells (8). The E1A null mutant showed the same severe viral replication restriction in $Sur2^{-/-}$ MEFs as wt MAV-1. There were 1 to 2 log units lower yields for CR1Δ, CR2Δ, and CR3Δ mutant viruses in $Sur2^{-/-}$ MEFs compared to $Sur2^{+/+}$ MEFs. These data indicate that mSur2 was important for efficient viral replication for all the E1A mutant viruses at an MOI of 0.05. For each virus (wt and E1A mutants), the severity of viral replication defect in $Sur2^{-/-}$ MEFs at an MOI of 0.05 was partially overcome at an MOI of 1. Thus there is a multiplicity-dependent effect for all these viruses. However, E1A null and CR3Δ mutants, which lack CR3 and therefore lack the ability to interact with mSur2, also showed viral replication defects in $Sur2^{-/-}$ MEFs at an MOI of 0.05. Therefore, E1A null and CR3Δ mutant viruses are dependent on mSur2 for replication at an MOI of 0.05. But this is independent of an E1A CR3-mSur2 interaction since these viruses lack CR3. Surprisingly, CR1Δ, CR2Δ, and CR3Δ mutant viruses replicated slightly better than wt MAV-1 and E1A null mutant in $Sur2^{-/-}$ MEFs at an MOI of 0.05.

Multiplicity-dependent defects in viral DNA replication in E1A mutant-infected Sur2$^{-/-}$ MEFs. Wt MAV-1 infection of Sur2$^{-/-}$ MEFs shows reduced accumulation of viral DNA compared to infection of Sur2$^{+/+}$ MEFs (8), indicating that mSur2 is important for viral DNA replication. To determine whether for E1A mutant infections the accumulated viral DNA levels correlated with reduced viral yields in Sur2$^{-/-}$ MEFs compared to Sur2$^{+/+}$ MEFs, Sur2$^{-/-}$ and Sur2$^{+/+}$ MEFs were infected at an MOI of 0.05 or 1 with wt MAV-1 and E1A mutant viruses. Viral DNAs were isolated by the method of Hirt (12), digested with *Hin*dIII, and analyzed by Southern blots (Fig. 3.3). Consistent with previous results (8), we did not detect viral DNA in wt MAV-1-infected Sur2$^{-/-}$ MEFs at an MOI of 0.05 (lanes 4-6, bottom panel), and we detected a reduced amount of viral DNA at an MOI of 1 compared to Sur2$^{+/+}$ MEFs (compare lanes 4-6 to lanes 1-3, top panel). Little viral DNA was detected in Sur2$^{-/-}$ MEFs infected with E1A null mutant at an MOI of 0.05 (lanes 16-18, bottom), but the viral DNA levels were comparable between Sur2$^{+/+}$ and Sur2$^{-/-}$ MEFs at an MOI of 1 (lanes 16-18 and 13-15, top). The defects of viral DNA accumulation in Sur2$^{-/-}$ MEFs compared to Sur2$^{+/+}$ MEFs were more severe at an MOI of 0.05 than at an MOI of 1 for CR1Δ, CR2Δ, and CR3Δ mutant viruses, respectively, though we detected low levels of viral DNA at an MOI of 0.05. Therefore, the multiplicity-dependent defects in viral DNA replication in Sur2$^{-/-}$ MEFs seen with wt virus were also observed with E1A mutant viruses. At an MOI of 1, we noted that viral DNA levels in Sur2$^{-/-}$ MEFs were comparable to those in Sur2$^{+/+}$ MEFs for E1A null and CR3Δ virus infection (Fig. 3.3, lanes 7-18, top panel). This result was consistent with plaque assay results (Fig. 3.2A). The low levels of viral DNA in Sur2$^{-/-}$ MEFs infected with CR1Δ, CR2Δ, or CR3Δ mutant viruses at an MOI of 0.05, taken together with the lack of viral DNA detected in Sur2$^{-/-}$ MEFs infected with wt MAV-1 or E1A null mutant, were also consistent with viral replication data (Fig. 3.2).

Importance of mSur2 for viral mRNA expression in E1A mutant infections. mSur2 is important for efficient wt MAV-1 replication, and the defect in viral replication is due at least in part to a defect in viral early gene transcription (8). We tested whether there was a defect in viral mRNA expression in E1A mutant virus infections of $Sur2^{-/-}$ MEFs that correlated with the viral replication and DNA accumulation defects. $Sur2^{+/+}$ and $Sur2^{-/-}$ MEFs were infected with wt or E1A mutant MAV-1 at an MOI of 0.05. Viral early genes (E1A, E2A, E3, E4) and one viral late gene, hexon, were analyzed by RPAs (Fig. 3.4). The wt E1A was detected only in wt MAV-1-infected $Sur2^{+/+}$ MEFs at 2 and 3 days p.i. The CR1, CR2, and CR3 deletion E1A mRNAs expressed from the E1A mutant-infected cells cannot be detected by the MAV-1 E1A probe in these RPAs. The mRNA levels of all the assayed viral genes were markedly reduced in $Sur2^{-/-}$ MEFs compared to $Sur2^{+/+}$ MEFs for wt virus and each mutant virus, indicating that mSur2 is important for viral gene transcription in both wt MAV-1 and E1A mutant infections. The viral mRNA levels were severely diminished or not detectable in $Sur2^{-/-}$ MEFs upon wt MAV-1 infection, results which were consistent with previous data (8). Similar to wt virus, there were severely diminished or non-detectable levels of viral mRNAs in $Sur2^{-/-}$ MEFs infected with the E1A null mutant. However, we detected low levels of viral mRNAs, particularly E4 and hexon, in $Sur2^{-/-}$ MEFs infected with CR1Δ, CR2Δ, or CR3Δ mutant viruses. These data were consistent with viral replication and viral DNA accumulation defects observed in Figs. 3.2 and 3.3.

CR1Δ, CR2Δ, and CR3Δ mutant viruses are able to rescue wt MAV-1 in $Sur2^{-/-}$ MEFs. Wt MAV-1 replication is severely restricted and there are no detectable levels of viral DNA, viral mRNAs, or viral proteins (E1A or E3gp11K) in $Sur2^{-/-}$ MEFs at low MOIs (MOI of 0.05) (8). However, CR1Δ, CR2Δ, and CR3Δ mutants did replicate in $Sur2^{-/-}$ MEFs, though not as efficiently as in $Sur2^{+/+}$ MEFs (Fig. 3.2). We also detected low levels of viral DNA and viral

mRNAs in Sur2$^{-/-}$ MEFs infected with CR1Δ, CR2Δ, or CR3Δ mutant viruses (Figs. 3.3 and 3.4). We speculated that there might be a negative regulatory factor that inhibited the replication of wt MAV-1, but not CR1Δ, CR2Δ, or CR3Δ mutant viruses in Sur2$^{-/-}$ MEFs. To test this hypothesis, we examined whether the CR3Δ mutant could rescue viral replication of wt MAV-1 in Sur2$^{-/-}$ MEFs in a co-infection experiment. Although we cannot distinguish plaques between wt MAV-1 and CR3Δ infection, by using Western blots we can distinguish wt and CR3Δ E1A protein expression using a monoclonal antibody that only recognizes the wt E1A protein. A mouse monoclonal antibody for E3gp11K recognizes E3 proteins from both wt- and CR3Δ mutant-infected cells. Sur2$^{-/-}$ MEFs were infected with wt MAV-1 or CR3Δ at an MOI of 0.1, or co-infected with wt MAV-1 and CR3Δ (MOI of 0.05 each). Sur2$^{+/+}$ MEFs were singly infected as controls. As shown in Fig. 3.5A lanes 1 and 2, E3gp11K protein was detected at 5 days p.i. in Sur2$^{+/+}$ MEFs infected with wt MAV-1 or CR3Δ. These data demonstrated that the cells were successfully infected. Wt E1A protein recognized by the monoclonal antibody was also detected (Fig. 3.5A, lane 1). As expected, we did not detect any CR3Δ mutant E1A protein in Sur2$^{+/+}$ MEFs infected with CR3Δ (Fig. 3.5A, lane 2, and Fig. 3.5B, lanes 4-5, bottom panel) even after a long exposure (data not shown), demonstrating that the monoclonal antibody only recognized wt E1A protein, not CR3Δ mutant E1A protein. We further showed that CR3Δ E1A protein was expressed from CR3Δ-infected Sur2$^{+/+}$ MEFs (Fig. 3.5B, lanes 4-5, top panel) by using rabbit polyclonal antibody (AKO7-147) against MAV-1 E1A that can recognize both wt and CR3Δ E1A. The reduced amount of E1A protein at 7 days p.i. in Sur2$^{+/+}$ MEFs infected with wt MAV-1 (Fig. 3.5B, lane 3) is due to the cytopathic effects at late times in infections, as observed previously (8). There were no detectable levels of E1A or E3gp11K protein in Sur2$^{-/-}$ MEFs infected with wt MAV-1 (Fig. 3.5A, lane 3, and Fig. 3.5B, lanes 6-7), consistent with previous

data (8). In contrast, there were low levels of E3gp11K protein at 7 days p.i. in Sur2$^{-/-}$ MEFs infected with CR3Δ (Fig. 3.5A, lane 4), correlating with better replication of CR3Δ compared to wt MAV-1 in Sur2$^{-/-}$ MEFs (Fig. 3.2B). In Sur2$^{-/-}$ MEFs co-infected with wt MAV-1 and CR3Δ, we detected wt E1A protein (Fig. 3.5A, lane 5, and Fig. 3.5B bottom, lanes 10-11). This result demonstrated that co-infection with CR3Δ rescued the E1A protein expression in wt virus-infected Sur2$^{-/-}$ MEFs.

In addition, we tested whether co-infection could rescue the transcription defects of wt E1A in Sur2$^{-/-}$ MEFs. Sur2$^{+/+}$ and Sur2$^{-/-}$ MEFs were infected with wt MAV-1, CR3Δ, or co-infected as in Fig. 3.5A. The wt E1A mRNA was analyzed by RPAs. Wt E1A mRNA was detected in Sur2$^{+/+}$ infected cells (Fig. 3.5C, lanes 1-3). As expected, there was no wt E1A mRNA in CR3Δ-infected cells (Fig. 3.5C, lanes 4-6). We detected wt E1A mRNA expression in co-infected Sur2$^{-/-}$ MEFs (Fig. 3.5C, lanes 14 and 15) but not in wt virus-infected Sur2$^{-/-}$ MEFs (Fig. 3.5C, lanes 8 and 9), demonstrating that co-infection rescued the defects of wt E1A expression at the transcription level. In addition, the wt viral DNA replication defect in Sur2$^{-/-}$ MEFs ((8) and Fig. 3.3) was rescued by co-infection with the CR3Δ mutant virus (data not shown). These data indicated that the CR3Δ mutant virus was able to rescue wt MAV-1 replication in Sur2$^{-/-}$ MEFs.

We also tested whether CR1Δ and CR2Δ mutants could rescue wt MAV-1 viral replication in Sur2$^{-/-}$ MEFs as did the CR3 mutant. Sur2$^{+/+}$ MEFs and Sur2$^{-/-}$ MEFs were singly infected or co-infected as indicated in Fig. 3.5D. E3gp11K viral proteins were expressed from virus-infected Sur2$^{+/+}$ MEFs, demonstrating successful viral infections (Fig. 3.5D, lanes 1-3). The monoclonal antibody against E1A recognized wt E1A, CR1Δ, and CR2Δ mutant E1A with

distinguishable positions in the membrane, as shown in Fig. 3.5D, lanes 1-3. CR1Δ E1A protein ran slightly higher than wt E1A protein, as previously reported (29). We detected E3gp11K proteins and CR1Δ E1A, CR2Δ E1A protein in $Sur2^{-/-}$ MEFs (Fig. 3.5D, lanes 5-6), correlating with better replication of CR1Δ and CR2Δ mutants compared to wt MAV-1 in $Sur2^{-/-}$ MEFs (Fig. 3.2B). There was no detectable wt E1A protein in wt MAV-1 infected $Sur2^{-/-}$ MEFs (Fig. 3.5D, lane 4). In contrast, we detected wt E1A proteins in co-infected $Sur2^{-/-}$ MEFs (Fig. 3.5D, lanes 7 and 8). The data indicated that like the CR3Δ mutant, the CR1Δ and CR2Δ mutants could rescue wt MAV-1 viral replication in $Sur2^{-/-}$ MEFs.

Replication defects of E1A null mutant and CR3Δ mutant viruses in mice. We examined whether the in vitro findings regarding mSur2 have parallels in infections of inbred mice. MAV-1 E1A is dispensable for viral replication in 3T6 cells at an MOI of 5 (38). In addition, there was only 1 log unit difference in growth of viruses between wt MAV-1 and E1A null mutant in $Sur2^{+/+}$ MEFs at MOIs of 0.05 and 1, and no significant different between wt MAV-1 and CR1Δ, CR2Δ, or CR3Δ mutant viruses in $Sur2^{+/+}$ MEFs at an MOI of 0.05 or 1 (Fig. 3.2). However, the E1A gene product is a virulence factor in MAV-1 infection in Swiss outbred mice (28) and inbred SJL/J mice (31), as demonstrated by LD_{50} experiments. The presence of the immune response in mice and the actual target cell types that MAV-1 infects in mice (endothelial cells and macrophage/mononuclear lineage) compared to those used in cell culture (fibroblast cells) were our rationale for investigating the role of the E1A-mSur2 interaction in mice. Since the mSur2 knockout is embryonic lethal in mice (J. L. Stevens and A. J. Berk, personal communication), we used an indirect approach to address the importance of E1A-mSur2 interaction in mice. Because E1A null mutant and CR3Δ mutant viruses lack the E1A CR3-mSur2 interaction (8), we tested whether there were viral replication defects of these viral

mutants in inbred mice. Four different inbred strains of mice (SJL/J, BALB/c, 129/J, and IFNAR [deficient in type I IFN signaling]) were infected intraperitoneally with wt MAV-1, E1A null mutant, or CR3Δ at 100 PFU. Mouse brains were harvested at 8 days p.i., and titrated for viral yields on 37.1 cells. As shown in Fig. 3.6A, the viral yields of both E1A mutants were reduced compared to wt MAV-1 in all four strains of mice. These results were consistent with higher LD_{50}s of E1A null mutant and CR3Δ mutant viruses in outbred mice (28). Viral loads in the brains of SJL/J mice were about two log units lower for E1A null and CR3Δ mutant viruses compared to wt MAV-1 ($P < 0.0001$, and $P = 0.0001$, respectively). Viral yields from wt MAV-1-infected BALB/c mice were 2 log units lower compared to SJL/J mice, consistent with BALB/c mice being resistant to MAV-1 infection (10, 31). We did not detect any infectious viruses in brains of E1A null- or CR3Δ-infected BALB/c mice. 129/J mice are the parental strain of IFNAR mice, which are deficient for the interferon-α/β receptor. The viral replication patterns in 129/J mice were similar to SJL/J mice, with about 2 log units lower virus yields from E1A null and CR3Δ mutant viruses compared to wt MAV-1 infection. There were also about 2 log units difference between viral yields of CR3Δ and wt MAV-1 infection in IFNAR mice ($P = 0.003$).

Previously we showed that the defective viral replication of MAV-1 in $Sur2^{-/-}$ MEFs compared to $Sur2^{+/+}$ MEFs is due at least in part to the reduced viral mRNA expression, indicating that mSur is important for viral gene transcription in vitro (8). We tested whether there was a defect in viral mRNA expression of E1A null and CR3Δ mutant viruses compared to wt MAV-1 in mice. SJL/J mice were infected intraperitoneally with wt MAV-1, E1A null, or CR3Δ at 100 PFU. Mouse brains were harvested at 8 days p.i., and total RNA was isolated for RPAs analysis of the viral mRNA levels. Viral mRNAs (E4, hexon, E3, and E2A) were detected from

wt MAV-1-infected mouse brains, but not from E1A null- or CR3Δ- infected mouse brains (Fig. 3.6B). Therefore, the defective viral mRNA expression of E1A null and CR3Δ may account at least in part for the reduced viral replication of E1A null and CR3Δ in mice.

DISCUSSION

The cellular protein mSur2 interacts with MAV-1 E1A, CR3 is required for the protein-protein interaction, and mSur2 is required for efficient wt MAV-1 replication in cell culture (8). Here we expanded the study of mSur2 function using E1A mutant viruses, We found that similar to wt virus (8), the E1A mutants exhibited a multiplicity-dependent effect, that is, they were more defective in $Sur2^{-/-}$ MEFs at low input MOIs than in high MOIs (Fig. 3.2). The viral replication defects at an MOI of 0.05 were partially overcome for wt MAV-1, CR1Δ, and CR2Δ at an MOI of 1 (Fig. 3.2), but completely overcome for E1A null and CR3Δ. The viral DNA levels (Fig. 3.3) of each mutant virus also showed more severe defects at an MOI of 0.05 compared to MOI of 1.

hAd E1A CR3 binds Sur2 to recruit Mediator complex (5, 36). It has been proposed that hAd E1A transactivates transcription of viral early genes by recruiting Mediator to the DNA promoters via E1A CR3-Sur2 interaction (5, 6, 36). The MAV-1 viral yield data at an MOI of 1 (Fig. 3.2A) perfectly supported this proposed model. MAV-1 E1A CR3 is required for interacting with mSur2 (8). Since wt MAV-1, CR1Δ, and CR2Δ mutant viruses contain an intact CR3 domain, presumably there is E1A CR3-mSur2 interaction in $Sur2^{+/+}$ MEFs upon infection. In contrast, E1A null and CR3Δ lack the CR3 domain. As expected, we observed a replication defect in $Sur2^{-/-}$ MEFs (absence of CR3-mSur2 interaction) infected with CR3-containing viruses (wt, CR1Δ, and CR2Δ) compared to $Sur2^{+/+}$ MEFs (presence of CR3-mSur2 interaction). Similarly, as expected, in E1A null- or CR3Δ-infection we observed no replication difference

between $Sur2^{+/+}$ and $Sur2^{-/-}$ MEFs. Therefore, our data using E1A mutant viruses indicated that E1A CR3-mSur2 interaction was important for MAV-1 replication.

Strikingly, at an MOI of 0.05, we observed a different viral replication pattern upon E1A null and CR3Δ infection compared to MOI of 1. Instead of the equally efficient replication of each virus seen at an MOI of 1 in $Sur2^{+/+}$ and $Sur2^{-/-}$ MEFs, at an MOI of 0.05 there were viral replication defects in $Sur2^{-/-}$ MEFs compared to $Sur2^{+/+}$ MEFs. The viral DNA and viral mRNA levels in E1A null and CR3Δ infection (Fig. 3.3 and Fig. 3.4) were consistent with the pattern in their viral yields (Fig. 3.2). Since MAV-1 replication apparently is not exclusively dependent on E1A CR3-mSur2 interaction (Fig. 3.2B, E1A null and CR3Δ data), these results suggested that mSur2 must have a broader function in viral replication in cell culture at an MOI of 0.05 than just the consequences of its binding to E1A CR3. The defects of viral replication of E1A null and CR3Δ in $Sur2^{-/-}$ MEFs (Fig. 3.2) were due at least in part to a defect in transcription of viral early genes (Fig. 3.4). The physiological functions of Sur2 might have direct and/or indirect effects on MAV-1 replication. Further study of Sur2 functions may help to understand the E1A CR3-mSur2 interaction-independent mechanisms.

The fact that the E1A null mutant was able to replicate in $Sur2^{-/-}$ MEFs at an MOI of 1 (Fig. 3.2A) demonstrated that there was an E1A-independent, mSur2-independent viral replication pathway. hAd E1A CR3 is primarily responsible for transactivating transcription of viral early genes (5, 6, 36). It has been proposed that recruiting Mediator complex to enhance the efficiency of transcription via E1A CR3-Sur2 interaction is the primary molecular mechanism of function of the interaction (5, 6, 36). Our previous (8) and current studies of MAV-1 infection using $Sur2^{-/-}$ MEFs also support this proposed model. However, neither hAd E1A nor MAV-1 E1A is absolutely required for viral replication at high input MOIs (8, 9, 22, 27). hAd E4 orf6/7

can functionally compensate for the loss of function of E1A (23, 26). Cellular E1A-like molecules (14, 18, 19) in the host cells may also support E1A null mutant viral replication. Human C/EBPβ has been shown to have E1A-like activity (30). It interacts with hSur2 (20), and hAd E1A protein can totally block C/EBPβ-hSur2 interaction (20). It is possible that MAV-1 E4 orf d, which has 17% identity and 43% similarity to hAd E4 orf 6/7 protein (L. Fang and K. R. Spindler, unpublished data), and/or mouse C/EBPβ could compensate for the loss of function of MAV-1 E1A in viral replication in E1A mutants. Moreover, our data presented in this paper suggest mSur2 has an E1A CR3 interaction-independent function. Further study of the functions of MAV-1 E4, mouse C/EBPβ, and mSur2 may help to elucidate the molecular mechanisms of multiple replication pathways of MAV-1.

We also noted that CR1Δ, CR2Δ, and CR3Δ mutant viruses replicated slightly better than wt MAV-1 and the E1A null mutant in $Sur2^{-/-}$ MEFs at an MOI of 0.05 (Fig. 3.2B). The viral DNA (Fig. 3.3), viral mRNA levels (Fig. 3.4), and viral protein levels (Fig. 3.5, single virus infected samples) were consistent with the virus replication data. The severely restricted viral replication of E1A null mutant in $Sur2^{-/-}$ MEFs at an MOI of 0.05 suggested that both MAV-1 E1A and mSur2 were critical for viral replication. However, it is paradoxical that wt MAV-1 has more severely restricted replication than CR1Δ, CR2Δ, or CR3Δ mutant viruses. One model to explain this is pictured in Fig. 3.7. There may be a negative regulator that inhibits wt E1A functions during wt MAV-1 infection in $Sur2^{-/-}$ MEFs. Consistent with this are previous data showing that the steady-state levels of viral early mRNAs (E4, E1B, and E1A) in CR1Δ, CR2Δ, or CR3Δ mutant-infected 3T6 cells at an MOI of 5 are higher than in wt MAV-1-infected cells (38). Wt MAV-1 E1A may associate directly or indirectly with an inhibitor activity to repress viral gene expression, including its own. hAd wt E1A represses transcription from viral (2, 35,

37) and cellular enhancers (11, 15, 32, 33). We postulate that the inhibiting effect could be relieved by CR1Δ, CR2Δ, and CR3Δ mutant E1A proteins, for example if the mutant E1A proteins have conformational changes such that they cannot be influenced by the negative regulator. In this case in the absence of mSur2, wt MAV-1 E1A would repress the transcription of viral early genes, including E1A itself, directly or indirectly through recruiting some repressor-like activity. However, due to conformational changes of CR1Δ, CR2Δ, and CR3Δ mutant E1A proteins, the repressor-like activity would not be associated, and viral early genes could be transcribed in the mutant virus infections. Interestingly, our co-infection data indicated that CR1Δ, CR2Δ, and CR3Δ mutant viruses could rescue the viral replication of wt MAV-1 in $Sur2^{-/-}$ MEFs. The rescued wt E1A protein expression (Fig. 3.5A, and 3.5D) and mRNA expression (Fig. 3.5C) are consistent with a model where there is an inhibiting effect (at least in part) on wt E1A transcription and translation. HAd E1A protein binds CtBP, a transcriptional co-repressor (4, 25). Even though the C-terminus of MAV-1 E1A lacks the conserved motif PXDLS that is required for interaction with CtBP, and thus is unlikely to bind to a mouse homolog of CtBP, it is possible that MAV-1 E1A could bind to a cellular protein that contains CtBP-like activity. We are currently investigating a cellular protein that potentially interacts with the C-terminus of MAV-1 E1A.

MAV-1 E1A is a virulence factor in mice (28), but the mechanism of E1A virulence has not been elucidated. The discovery of the MAV-1 E1A CR3-mSur2 interaction enabled us to begin to examine the E1A functions in MAV-1 pathogenesis in mice. Due to the unavailability of Sur2 knockout mice, we used an indirect assay, MAV-1 E1A mutants, to test the importance of the function of E1A-mSur2 interaction in mice. SJL/J mice are susceptible, and BALB/c mice are resistant to MAV-1 infection (31). 129/J mice are immunocompetent parent strain for IFNAR

mice, which are immunodeficient, lacking the interferon-α/β receptor. In all four strains of mice, the E1A null mutant and CR3 mutant viruses replicated at significantly reduced levels compared to wt MAV-1 (Fig. 3.6A). This suggests that the reduced viral replication was due to a defect in the mutant viruses themselves, rather than host-specific factors. There is no E1A-mSur2 interaction in E1A null mutant- or CR3 mutant-infected mouse brain microvascular endothelial cells (8). Endothelial cells are a target cell type in MAV-1-infected mice (7, 16). We further showed that there is defective viral mRNA expression of E1A null mutant and CR3Δ viruses in mouse brains (Fig. 3.6B), which correlated with the viral replication defects (Fig. 3.6A). This defect in viral mRNA expression might be due to the lack of E1A CR3-mSur2 interaction, since Sur2 is primarily responsible for transactivating transcription of viral genes through interaction with E1A CR3 (34). Though we cannot rule out the possibility that other functions of E1A CR3 besides its interaction with mSur2 may also cause the viral replication defects in mice, the results suggest that E1A CR3-mSur2 interaction is critical for viral replication in mice and thereby contributes to E1A being a virulence factor in mice. An MAV-1 mutant that is only defective in binding to mSur2 may address this question directly.

ACKNOWLEDGMENTS

We thank Amanda Welton for excellent technical assistance and Jason Weinberg for assistance with RPAs. We thank Arnie Berk for helpful discussions. We thank Mike Imperiale for suggestion of the co-infection experiments and critical review of the manuscript. This work was supported by NIH grant R01 AI023762 to K.R.S.

REFERENCES

1. **Ball, A. O., C. W. Beard, P. Villegas, and K. R. Spindler.** 1991. Early region 4 sequence and biological comparison of two isolates of mouse adenovirus type 1. Virology **180:**257-265.

2. **Borelli, E., R. Hen, and P. Chambon.** 1984. Adenovirus-2 E1A products repress enhancer-induced stimulation of transcription. Nature **312:**608-612.

3. **Boube, M., L. Joulia, D. L. Cribbs, and H.-M. Bourbon.** 2002. Evidence for a mediator of RNA polymerase II transcriptional regulation conserved from yeast to man. Cell **110:**143-151.

4. **Boyd, J. M., T. Subramanian, U. Schaeper, M. La Regina, S. Bayley, and G. Chinnadurai.** 1993. A region in the C-terminus of adenovirus 2/5 E1a protein is required for association with a cellular phosphoprotein and important for the negative modulation of T24-*ras* mediated transformation, tumorigenesis, and metastasis. EMBO J. **12:**469-478.

5. **Boyer, T. G., M. E. D. Martin, E. Lees, R. P. Ricciardi, and A. J. Berk.** 1999. Mammalian Srb/Mediator complex is targeted by adenovirus E1A protein. Nature **399:**276-279.

6. **Cantin, G. T., J. L. Stevens, and A. J. Berk.** 2003. Activation domain-mediator interactions promote transcription preinitiation complex assembly on promoter DNA. Proc. Natl. Acad. Sci. USA **100:**12003-12008.

7. **Charles, P. C., J. D. Guida, C. F. Brosnan, and M. S. Horwitz.** 1998. Mouse adenovirus type-1 replication is restricted to vascular endothelium in the CNS of susceptible strains of mice. Virology **245:**216-228.

8. **Fang, L., J. L. Stevens, A. J. Berk, and K. R. Spindler.** 2004. Requirement of Sur2 for efficient mouse adenovirus type 1 replication. J. Virol.**:***in press*.

9. **Gaynor, R. B., and A. J. Berk.** 1983. Cis-acting induction of adenovirus transcription. Cell **33:**683-693.

10. **Guida, J. D., G. Fejer, L.-A. Pirofski, C. F. Brosnan, and M. S. Horwitz.** 1995. Mouse adenovirus type 1 causes a fatal hemorrhagic encephalomyelitis in adult C57BL/6 but not BALB/c mice. J. Virol. **69:**7674-7681.

11. **Hen, R., E. Borelli, and P. Chambon.** 1985. Repression of the immunoglobulin heavy chain enhancer by the adenovirus-2 E1A products. Science **230:**1391-1394.

12. **Hirt, B.** 1967. Selective extraction of polyoma DNA from infected mouse cell cultures. J. Mol. Biol. **26:**365-369.

13. **Hobbs, M. V., W. O. Weigle, D. J. Noonan, B. E. Torbett, R. J. McEvilly, R. J. Koch, G. J. Cardenas, and D. N. Ernst.** 1993. Patterns of cytokine gene expression by CD4+ T cells from young and old mice. J. Immunol. **150:**3602-3614.

14. **Imperiale, M. J., H.-T. Kao, L. T. Feldman, J. R. Nevins, and S. Strickland.** 1984. Common control of the heat shock gene and early adenovirus genes: evidence for a cellular E1A-like activity. Mol. Cell. Biol. **4:**867-874.

15. **Janaswami, P. M., D. V. R. Kalvakolanu, Y. Zhang, and G. C. Sen.** 1992. Transcriptional repression of interleukin-6 gene by adenoviral E1A proteins. J. Biol. Chem. **267:**24886-24891.

16. **Kajon, A. E., C. C. Brown, and K. R. Spindler.** 1998. Distribution of mouse adenovirus type 1 in intraperitoneally and intranasally infected adult outbred mice. J. Virol. **72:**1219-1223.

17. **Laemmli, U. K.** 1970. Cleavage of structural proteins during the assembly of the head of bacteriophage T4. Nature **227:**680-685.

18. **Lee, H. J., J. K. Lee, S. Miyake, and S. J. Kim.** 2004. A novel E1A-like inhibitor of differentiation (EID) family member, EID-2, suppresses transforming growth factor (TGF)-beta signaling by blocking TGF-beta-induced formation of Smad3-Smad4 complexes. J Biol Chem **279:**2666-72.

19. **MacLellan, W. R., G. Xiao, M. Abdellatif, and M. D. Schneider.** 2000. A novel Rb- and p300-binding protein inhibits transactivation by MyoD. Mol Cell Biol **20:**8903-15.

20. **Mo, X., E. Kowenz-Leutz, H. Xu, and A. Leutz.** 2004. Ras induces mediator complex exchange on C/EBP beta. Mol. Cell **13:**241-250.

21. **Müller, U., U. Steinhoff, L. F. L. Reis, S. Hemmi, J. Pavlovic, R. M. Zinkernagel, and M. Aguet.** 1994. Functional role of type I and type II interferons in antiviral defense. Science **264:**1918-1921.

22. **Nevins, J. R.** 1981. Mechanism of activation of early viral transcription by the adenovirus E1A gene product. Cell **26:**213-220.

23. **O'Connor, R. J., and P. Hearing.** 2000. The E4-6/7 protein functionally compensates for the loss of E1A expression in adenovirus infection. J. Virol. **74:**5819-5824.

24. **Ryman, K. D., W. B. Klimstra, K. B. Nguyen, C. A. Biron, and R. E. Johnston.** 2000. Alpha/beta interferon protects adult mice from fatal Sindbis virus infection and is an important determinant of cell and tissue tropism. J. Virol. **74:**3366-3378.

25. **Schaeper, U., J. M. Boyd, S. Verma, E. Uhlmann, T. Subramanian, and G. Chinnadurai.** 1995. Molecular cloning and characterization of a cellular phosphoprotein that interacts with a conserved C-terminal domain of adenovirus E1A involved in

negative modulation of oncogenic transformation. Proc. Natl. Acad. Sci. USA **92:**10467-10471.

26. **Schaley, J., R. J. O'Connor, L. J. Taylor, D. Bar-Sagi, and P. Hearing.** 2000. Induction of the cellular E2F-1 promoter by the adenovirus E4-6/7 protein. J. Virol. **74:**2084-2093.

27. **Shenk, T., N. Jones, W. Colby, and D. Fowlkes.** 1979. Functional analysis of adenovirus-5 host-range deletion mutants defective for transformation of rat embryo cells. Cold Spring Harbor Symp. Quant. Biol. **44:**367-375.

28. **Smith, K., C. C. Brown, and K. R. Spindler.** 1998. The role of mouse adenovirus type 1 early region 1A in acute and persistent infections in mice. J. Virol. **72:**5699-5706.

29. **Smith, K., B. Ying, A. O. Ball, C. W. Beard, and K. R. Spindler.** 1996. Interaction of mouse adenovirus type 1 early region 1A protein with cellular proteins pRb and p107. Virology **224:**184-197.

30. **Spergel, J. M., W. Hsu, S. Akira, B. Thimmappaya, T. Kishimoto, and S. Chen-Kiang.** 1992. NF-IL6, a member of the C/EBP family, regulates E1A-responsive promoters in the absence of E1A. J. Virol. **66:**1021-1030.

31. **Spindler, K. R., L. Fang, M. L. Moore, C. C. Brown, G. N. Hirsch, and A. K. Kajon.** 2001. SJL/J mice are highly susceptible to infection by mouse adenovirus type 1. J. Virol. **75:**12039-12046.

32. **Stein, R. W., M. Corrigan, P. Yaciuk, J. Whelan, and E. Moran.** 1990. Analysis of E1A-mediated growth regulation functions: binding of the 300-kilodalton cellular product correlates with E1A enhancer repression function and DNA synthesis-inducing activity. J. Virol. **64:**4421-4427.

33. **Stein, R. W., and E. B. Ziff.** 1987. Repression of insulin gene expression by adenovirus type 5 E1A proteins. Mol. Cell. Biol. **7:**1164-1170.

34. **Stevens, J. L., G. T. Cantin, G. Wang, A. Shevchenko, A. Shevchenko, and A. J. Berk.** 2002. Transcription control by E1A and MAP kinase pathway via Sur2 mediator subunit. Science **296:**755-758.

35. **Velcich, A., and E. Ziff.** 1985. Adenovirus E1A proteins repress transcription from the SV40 early promoter. Cell **40:**705-716.

36. **Wang, G., and A. J. Berk.** 2002. In vivo association of adenovirus large E1A protein with the human mediator complex in adenovirus-infected and -transformed cells. J. Virol. **76:**9186-9193.

37. **Wang, H. G., Y. Rikitake, M. C. Carter, P. Yaciuk, S. E. Abraham, B. Zerler, and E. Moran.** 1993. Identification of specific adenovirus E1A N-terminal residues critical to the binding of cellular proteins and to the control of cell growth. J. Virol. **67:**476-88.

38. **Ying, B., K. Smith, and K. R. Spindler.** 1998. Mouse adenovirus type 1 early region 1A is dispensable for growth in cultured fibroblasts. J. Virol. **72:**6325-6331.

Fig. 3.1. RPA analysis of mRNA levels from equal MOI E1A mutant infections. 37.1 cells were infected with wt MAV-1 (wt), E1A null mutant, CR1Δ, CR2Δ, or CR3Δ at an MOI of 0.05. Total RNA was isolated at indicated time points. The probe lane shows the full length of each probe in the set, including MAV-1 E4, E1A, and hexon, and mouse L32. The protected probe sizes are shown by arrows for each gene. L32 was used as an internal loading control. The wt E1A bands detected in all samples were from 37.1 cells, which are 3T6 cell derivatives that stably transfected with MAV-1 E1A (29). We quantitated the viral gene expression levels by phosphoimager, normalizing to L32 (data not shown). The results confirmed that the viral gene expression levels were similar among the viruses for E4 and hexon. E1A levels were similar as expected because it is constitutively expressed in the 37.1 cells.

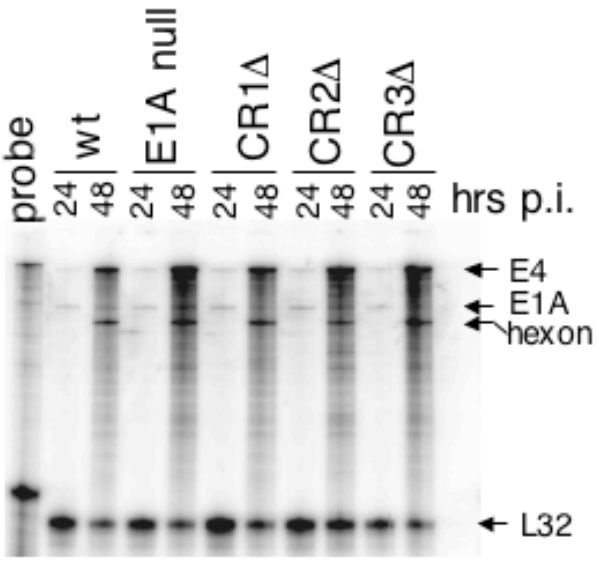
probe
wt
E1A null
CR1Δ
CR2Δ
CR3Δ
24
48
hrs p.i.
E4
E1A
hexon
L32

Fig. 3.2. Growth of MAV-1 E1A mutant viruses in $Sur2^{+/+}$ and $Sur2^{-/-}$ MEFs. The indicated cell types were infected with wt MAV-1, E1A null mutant, CR1Δ, CR2Δ, or CR3Δ at an MOI of 1 (A) or an MOI of 0.05 (B) and harvested at the indicated times. The viral yields were determined by plaque assays on 37.1 cells. The legend for $Sur2^{+/+}$ MEFs and $Sur2^{-/-}$ MEFs is shown at the top and is the same for all panels. The experiments were reproduced two additional times. Error bars are only distinguishable in a few samples (e.g. CR3Δ, MOI 0.05); other error bars were too small to be visualized.

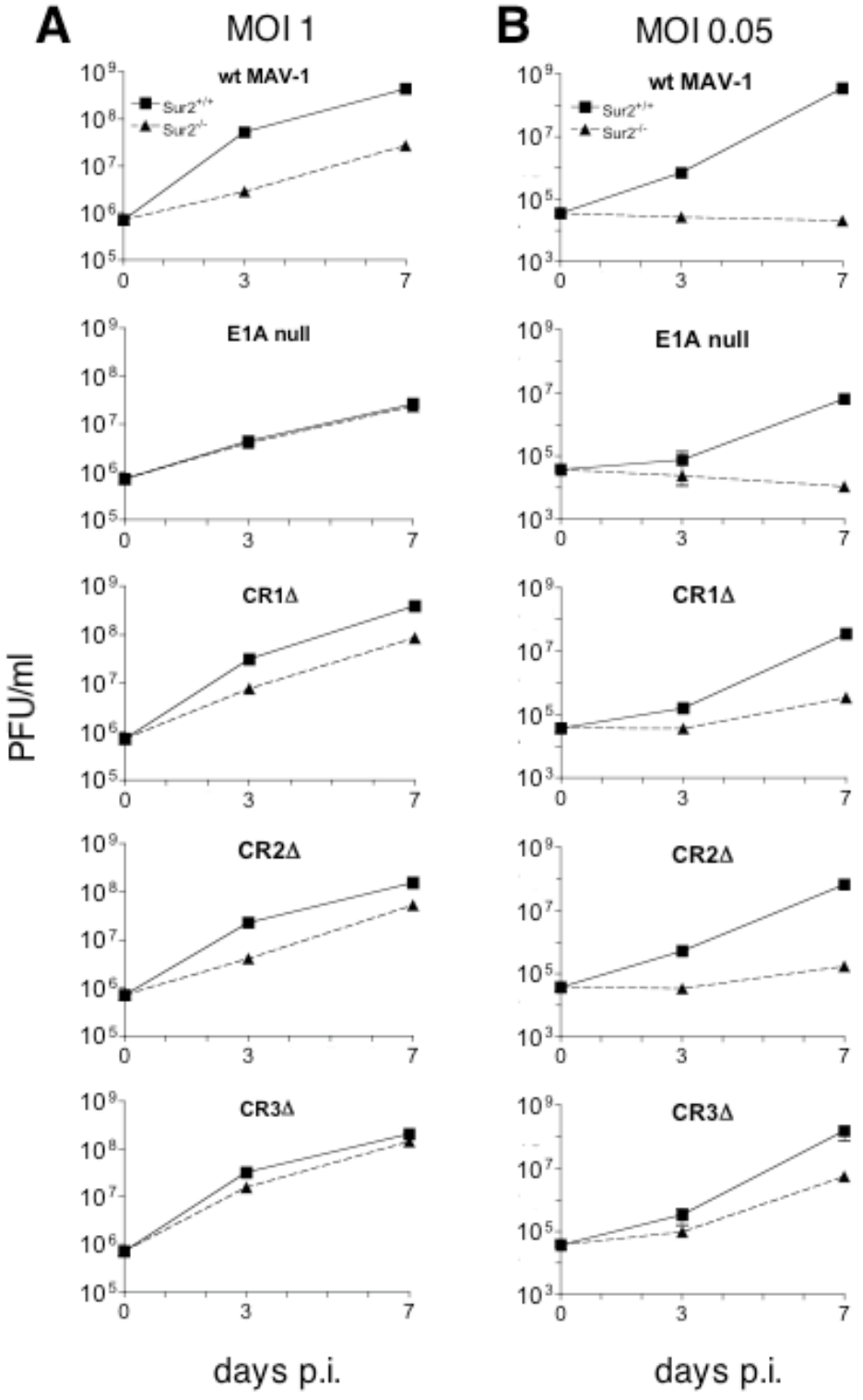
A
MOI 1
B
MOI 0.05
wt MAV-1
Sur2+/+
Sur2-/-
E1A null
CR1Δ
CR2Δ
CR3Δ
PFU/ml
days p.i.
days p.i.

Fig. 3.3. Multiplicity-dependent defects in viral DNA replication of wt MAV-1 and E1A mutant viruses in $Sur2^{-/-}$ MEFs. $Sur2^{+/+}$ (+/+) and $Sur2^{-/-}$ (-/-) MEFs were infected with wt MAV-1, E1A null mutant, CR1Δ, CR2Δ, or CR3Δ at an MOI of 0.05 or 1. Viral DNA was isolated at the indicated times by the Hirt method (12). Equal amounts of DNA were digested with *Hin*dIII and Southern blotted with MAV-1-specific DNA probes. DNA fragment sizes are indicated in kilobases on the right.

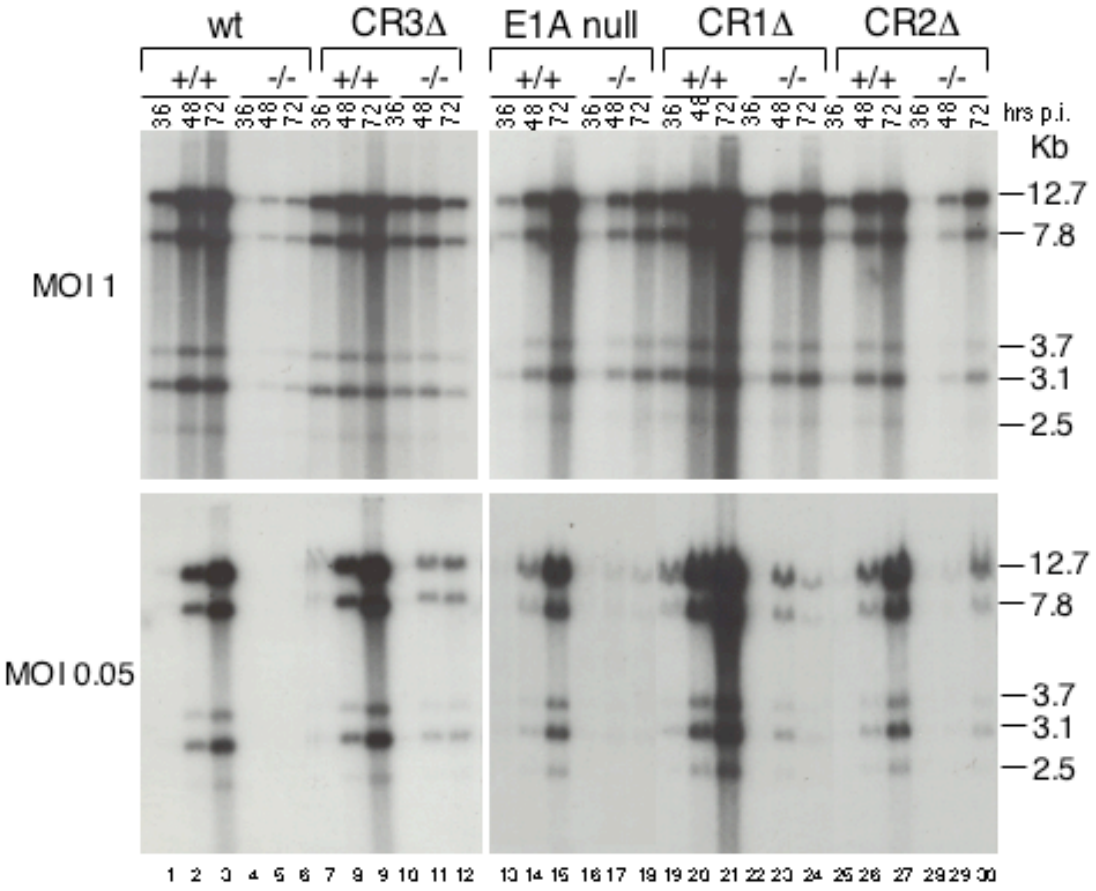
wt
CR3Δ
E1A null
CR1Δ
CR2Δ
+/+
-/-
36 48 72
hrs p.i.
Kb
12.7
7.8
3.7
3.1
2.5
MOI 1
MOI 0.05
1 2 3 4 5 6 7 8 9 10 11 12 13 14 15 16 17 18 19 20 21 22 23 24 25 26 27 28 29 30

Fig. 3.4. Importance of mSur2 for viral mRNA expression in E1A mutant infections. $Sur2^{+/+}$ (+/+) and $Sur2^{-/-}$ (-/-) MEFs were infected with wt MAV-1, E1A null mutant, CR1Δ, CR2Δ, or CR3Δ at an MOI of 0.05. Total RNA was isolated at the indicated times. The sizes of probes protected from RNase treatment are shown by the arrows for each gene at the right side. Even with longer exposure, we did not observe wt E1A expression in the E1A mutant-infected samples (data not shown). L32 and β-actin were used as internal loading controls. Yeast tRNA was used as a negative control. m, DNA size marker; probe, full length probe set (no RNase).

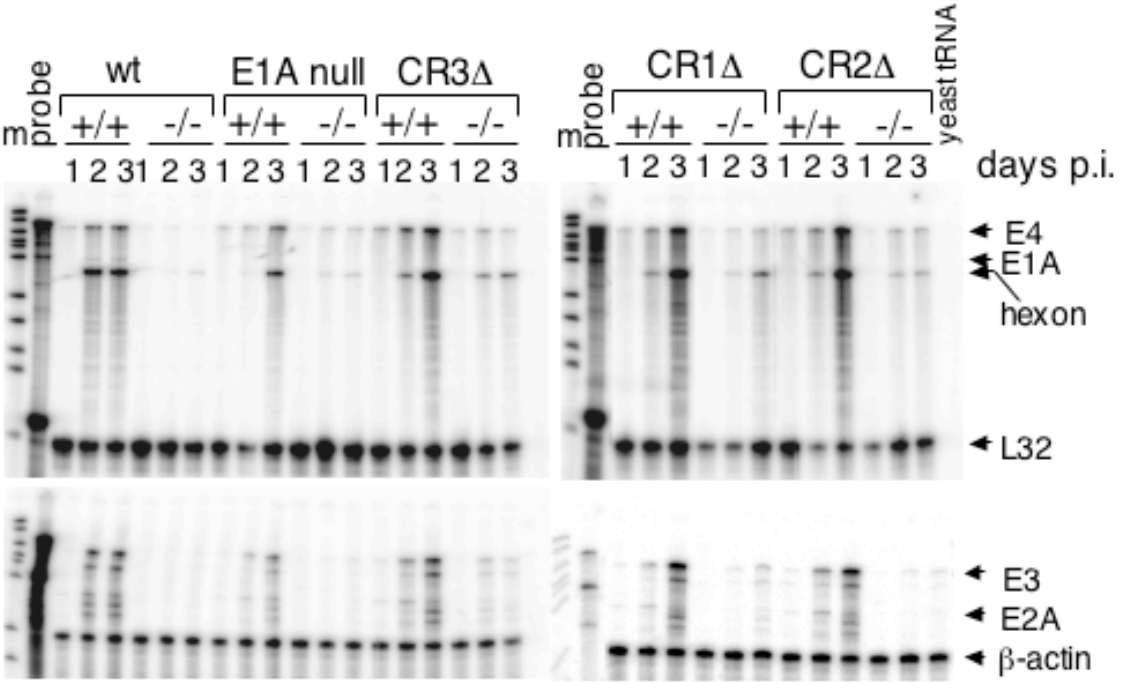
mprobe
wt
E1A null
CR3Δ
+/+
-/-
1 2 31 2 3 1 2 3 1 2 3 12 3 1 2 3
mprobe
CR1Δ
CR2Δ
yeast tRNA
1 2 3 1 2 3 1 2 3 1 2 3
days p.i.
E4
E1A
hexon
L32
E3
E2A
β-actin

Fig. 3.5. The defect in wt E1A expression in $Sur2^{-/-}$ MEFs was rescued by co-infection. A, $Sur2^{+/+}$ and $Sur2^{-/-}$ MEFs were infected with wt MAV-1 or CR3Δ at an MOI of 0.1, or co-infected with wt MAV-1 and CR3Δ (both at an MOI of 0.05). Cells were harvested at 7 days p.i. and lysed in E3 lysis buffer. Samples were analyzed by SDS-PAGE on an 8%-15% gradient gel and Western blotting using antibodies as indicated at the right: monoclonal mAb10B10 was the E1A antibody and mAb11H9 was the E3gp11K antibody. β-actin was assayed as a loading control. B, $Sur2^{+/+}$ and $Sur2^{-/-}$ MEFs were infected and processed as in panel A. Rabbit polyclonal antibody against MAV-1 E1A (AKO7-147) was used in the top panel to detect the CR3Δ mutant E1A, and monoclonal antibody (mAb10B10) against MAV-1 E1A was used in the bottom panel to detect wt E1A. C, Total RNAs were isolated from infected cells (same as panel A) at indicated times, and RPAs using the probe set that includes viral gene E1A, E4, and hexon, and mouse L32 were carried out. The sizes of protected probes are shown by the arrows at the right side. L32 were used as an internal loading control. D, $Sur2^{+/+}$ and $Sur2^{-/-}$ MEFs were singly infected with wt MAV-1 (lane1, 4), CR1Δ (lane 2, 5), or CR2Δ (lane 3, 6) at an MOI of 0.1, or co-infected with wt MAV-1 and CR1Δ (both at an MOI of 0.05) (lane 7), or wt MAV-1 and CR2Δ (both at an MOI of 0.05) (lane 8). Cells were harvested at 7 days p.i. and processed as in panel A with mAb10B10 for E1A and mAb 11H9 for E3gp11K.

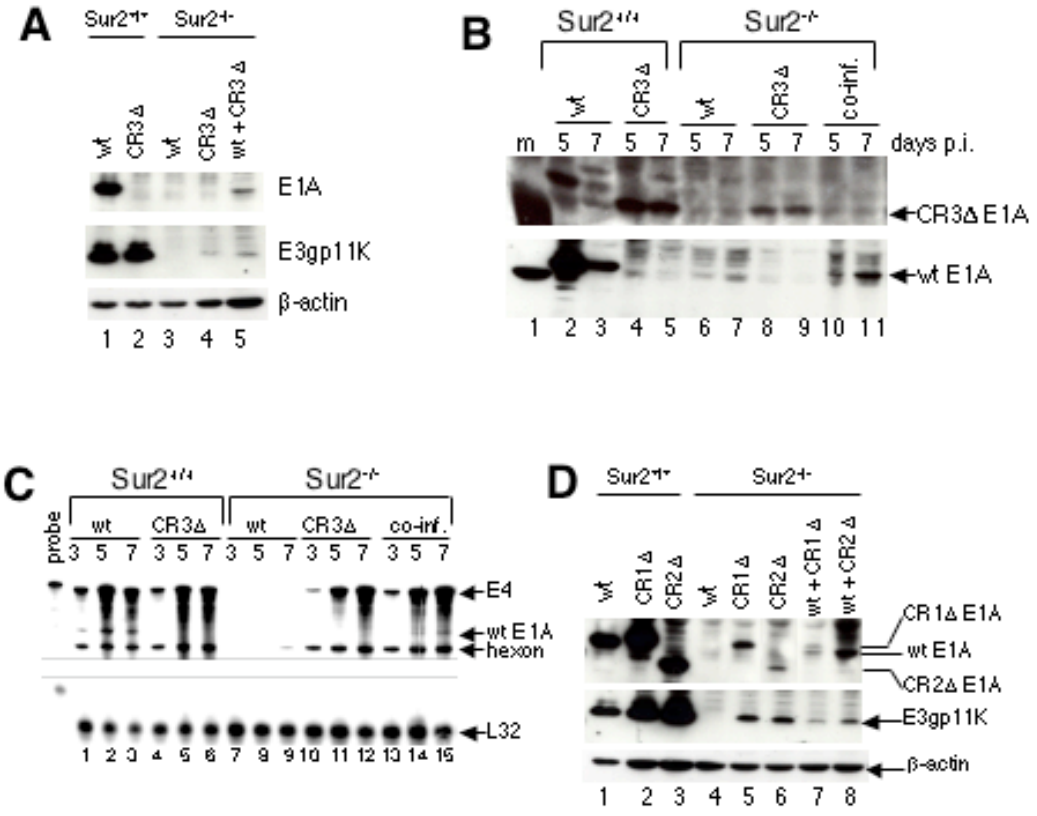
A
Sur2+/+
Sur2+/-
wt
CR3Δ
wt
CR3Δ
wt + CR3Δ
E1A
E3gp11K
β-actin
1 2 3 4 5
B
Sur2+/+
Sur2-/-
wt
CR3Δ
wt
CR3Δ
co-inf.
m 5 7 5 7 5 7 5 7 5 7 days p.i.
CR3Δ E1A
wt E1A
1 2 3 4 5 6 7 8 9 10 11
C
Sur2+/+
Sur2-/-
probe
wt
CR3Δ
wt
CR3Δ
co-inf.
3 5 7 3 5 7 3 5 7 3 5 7 3 5 7
E4
wt E1A
hexon
L32
1 2 3 4 5 6 7 8 9 10 11 12 13 14 15
D
Sur2+/+
Sur2+/-
wt
CR1Δ
CR2Δ
wt
CR1Δ
CR2Δ
wt + CR1Δ
wt + CR2Δ
CR1Δ E1A
wt E1A
CR2Δ E1A
E3gp11K
β-actin
1 2 3 4 5 6 7 8

Fig. 3.6. Viral replication defects of E1A null and CR3Δ mutants in mice. A, Four strains of mice (SJL/J, BALB/c, 129/J, and IFNAR) were infected by the intraperitoneal route with wt MAV-1, E1A null mutant, or CR3Δ at 100 PFU. Brains were harvested at 8 days p.i., and homogenates were titrated for viruses by plaque assays on 37.1 cells. Each symbol represents an individual mouse. The dotted line at 2 x 10^3 represents the lower limit of detection of the assay. Data points below the limit of detection were excluded from t statistical calculations. *, P <0.0001, and P = 0.002 for E1A null mutant titers compared to wt MAV-1 titers in SJL/J, and 129/J mice, respectively. **, P = 0.0001, P = 0.02, and P = 0.003 for CR3Δ titers compared to wt MAV-1 titers in SJL/J, 129/J, and IFNAR mice, respectively. B, SJL/J mice were infected by the intraperitoneal route with wt MAV-1, E1A null mutant, or CR3Δ at 100 PFU. Brains were harvested at 8 days p.i. Total RNA was isolated, and RPAs were carried out using probe sets as in Fig. 3.4.

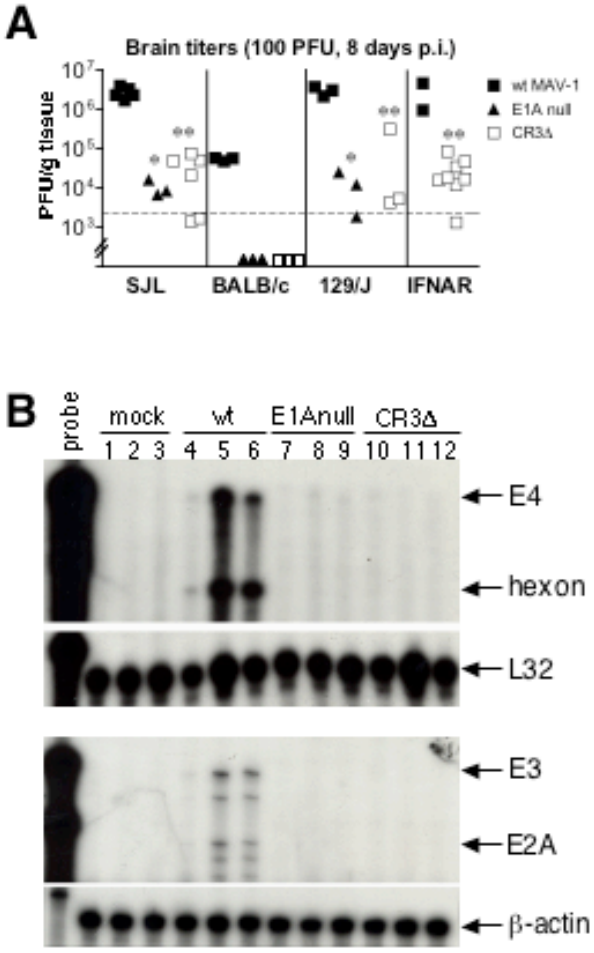
A
Brain titers (100 PFU, 8 days p.i.)
PFU/g tissue
wt MAV-1
E1A null
CR3Δ
SJL
BALB/c
129/J
IFNAR
B
probe
mock
wt
E1Anull
CR3Δ
1 2 3 4 5 6 7 8 9 10 11 12
E4
hexon
L32
E3
E2A
β-actin

Fig. 3.7. Model of restricted viral replication of wt MAV-1 in $Sur2^{-/-}$ MEFs. We propose that there is a negative regulator (triangle) that inhibits wt E1A function during wt MAV-1 infection. This negative regulator might directly or indirectly associate with E1A protein. In the presence of Sur2 ($Sur2^{+/+}$ MEFs), the interaction between MAV-1 E1A and Sur2 is the predominant mechanism to transactivate viral genes and is important for efficient viral replication, and the inhibitor has little influence. In contrast, in the absence of Sur2 ($Sur2^{-/-}$ MEFs), due to the lack of E1A-Sur2 interaction, the negative regulator inhibits E1A functions, resulting in the restricted viral replication of wt MAV-1 at low MOIs. We propose that the negative regulator would not inhibit the function of mutant E1As (CR1Δ, CR2Δ, and CR3Δ) due to conformational changes resulting from the deletions. Therefore, these mutant viruses would replicate in $Sur2^{-/-}$ MEFs. The presence of a negative regulator is consistent with co-infection experiments in which wt E1A expression was rescued by CR1Δ, CR2Δ, and CR3Δ mutant viruses.

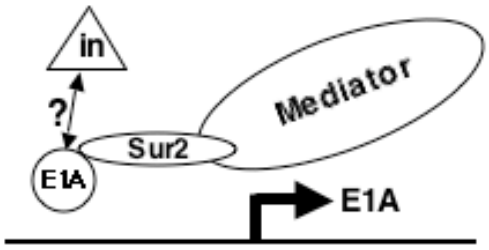
in
?
Mediator
Sur2
E1A
E1A

CHAPTER 4

LACK OF ALTERED CELLULAR ADHESION MOLECULE EXPRESSION ON MOUSE BRAIN MICROVASCULAR ENDOTHELIAL CELLS INFECTED WITH MOUSE ADENOVIRUS TYPE I

[1] L. Fang, K. R. Spindler. To be submitted.

ABSTRACT

We investigated the roles of cell adhesion molecules of endothelial cells (ECs) in the pathogenesis of mouse adenovirus type 1 (MAV-1). Vascular endothelial cells play a crucial role in inflammation and immune responses by expressing various cell adhesion molecules. The expression levels of VCAM-1, ICAM-1, and E-selectin on one established cell line, mouse brain microvascular endothelial cell (MBMEC), was examined by flow cytometry. VCAM-1 and ICAM-1 were induced on MBMECs by lipopolysacchride (LPS), tumor necrosis factor α (TNF-α), and interferon γ (IFN-γ), but not by MAV-1 infection. We did not detect E-selectin expression on MBMECs, even treated with LPS, TNF-α, or IFN-γ. The data suggest that MAV-1 infection does not directly induce the expression of cellular adhesion molecules on endothelial cells in the mouse brain.

INTRODUCTION

Viruses are dependent on the biochemical processes and structural characteristics of the cells that they infect (1). In addition to viral receptors, intracellular factors can be involved in determining tissue or cell tropism. Cell-type tropism is undoubtedly one determining factor for the pathogenic outcome of the infection. Vascular endothelium, especially endothelium lining the microvessels of brain and spinal cord, is one of the major sites of MAV-1 infection in vivo (7, 10). The endotheliotropic characteristic of MAV-1 is different from hAd, which is an epitheliotropic virus (9). MAV-1 causes dose-dependent encephalomyelitis and inflammatory cell accumulation in the brain blood vessels (6, 12, 13, 17). The endothelium forms a continuous lining of the cardiovascular system, strategically positioned as an interface between the blood and all other tissues (4). It serves and participates in highly active metabolic and regulatory

functions including control of primary hemostasis, blood coagulation and fibrinolysis, platelet and leukocyte interactions with the vessel wall, interaction with lipoprotein metabolism, and regulation of vascular tone (4). The large- and small-vessel ECs differ not only in their growth requirements and prostaglandin secretion, but also most importantly in the production, expression, regulation and function of cell surface adhesion molecules. Factor VIII-related antigen, alkaline phosphatase, CD31, endoglin, specific binding to lectins, uptake of acetylated LDL, and prostacyclin synthesis are generally regarded as endothelial cell markers (15), although there are some variations due to different species, tissues and/or cell culture in vitro.

Unlike most organ systems, the central nervous system (CNS) is separated from the blood by a protective cellular barrier, the blood-brain barrier (BBB) (5). ECs of brain capillaries are connected together by tight junctions with extremely high electrical resistance and are important for maintaining the intactness of the BBB. ECs express cell adhesion molecules, which play a critical role in the inflammatory response (3, 11). ICAM-1, an adhesion molecule that belongs to the immunoglobulin gene superfamily, is a major ligand for lymphocyte function-associated antigen 1 (LFA-1, CD18/CD11a). ICAM-1 is responsible for leukocyte binding to endothelial cells via LFA-1, playing a central role in the inflammatory reaction as a signaling and co-stimulatory molecule on T-lymphocytes.

Another important adhesion molecule involved in inflammatory brain reactions is the vascular cell adhesion molecule 1 (VCAM-1), which binds its ligand, β1-integrin very late antigen 4 (VLA-4). Endothelial VCAM-1 can mediate adhesion of lymphocytes and macrophages via their integrin receptors. Selectins seem to be critically important in inflammation, and their lectin domain is responsible for adhesion (8). E-selectin is not constitutively expressed by resting endothelial cells, but its membrane expression and synthesis

can be induced by pro-inflammatory cytokines such as TNF-α and IL-1. It is mainly involved in endothelial-neutrophil interactions.

The observation of accumulated inflammatory cells in brain blood vessels in MAV-1 infection (6, 12, 13, 17) suggests that cellular adhesion molecules play a role in MAV-1-induced encephalomyelitis in mice. More interestingly, an E3 null mutant virus (*pm*E304) causes less inflammatory reaction in brain than wt MAV-1 infection at a dose of 10^3 PFU at 8 days p.i. in outbred Swiss mice (6), suggesting an anti-inflammatory role of E3 gene products. We tested whether MAV-1 infection alters the expression of cellular adhesion molecules in vitro.

MATERIALS AND METHODS

Cells and Viruses. Mouse NIH 3T6 fibroblast cells were maintained in Dulbecco's modified Eagle's medium (DMEM) supplemented with 5% heat-inactivated calf serum. Mouse brain microvascular endothelial cells (MBMECs) were obtained from Dr. Howard Fox at the Scripps Research Institute and maintained in complete MBMVEC medium purchased from Cell Applications, Inc. J774A.1 cells (mouse macrophage cell line) were maintained in 1X DMEM with 10% heat-inactivated calf serum. SHMECs (mouse microvascular heart endothelial cell line) were obtained from Dr. Robert Auerbach at the University of Wisconsin and maintained in 1X DMEM with 10% fetal bovine serum. Wild type (wt) MAV-1 was the standard MAV-1 stock originally obtained from S. Larsen (2).

Antibodies. Antibodies against VCAM (Cat# 553330), ICAM (Cat# 553250), and E-selectin (Cat# 553749) were purchased from BD Pharmingen. FITC-conjugated anti-rat IgG antibody was from Sigma (used at 1:500 dilution). FITC-conjugated anti-hamster IgG antibody

(Cat# 554011) was purchased from Pharmingen. Antibody isotype controls rat IgG2a (kappa) and Armenian Hamster IgG (group 1, kappa) were from Pharmingen.

Immunofluorescence staining. Cells were cultured on 8-well chamber slides (Falcon) and treated with lipopolysaccharide (LPS, Sigma) for 3 or 6 hours. Cells were fixed with 4% paraformaldehyde for 30 min at room temperature and then incubated with primary antibody (anti-VCAM, anti-ICAM, or anti-E-selectin) for 2 hours at room temperature at the indicated concentrations. Chamber slides were washed three times in 1X PBS for 5 min. FITC-conjugated anti-rat IgG antibody was incubated with cells for 2 hours at room temperature. Slides were observed by fluorescence microscopy.

Uptake of DiL-Ac-LDL assay. Cells were cultured on 8-well chamber slides (Falcon), incubated with 10 μg/ml DiI-Ac-LDL (acetylated low density lipoprotein, Biomedical Technologies, Stoughton, MA, U.S.A.) at 37º C for 40 min, and observed by fluorescence microscopy.

Flow cytometry analysis. MBMECs were cultured in 6-well plates and either mock- or virus-infected at an MOI of 0.05, 1, or 5. Cells were trypsinized and stained with primary antibody (anti-VCAM, anti-ICAM, or anti-E-selectin) for 2 hours at 4º C. Isotype control antibodies were used as negative controls. Cells treated with IFN-γ (Sigma) and TNF-β (Sigma) were used as positive controls. After washing, cells were incubated with FITC-conjugated anti-rat antibody for 2 hours at 4º C. Flow cytometry analysis was done in a FACScan machine and data were analyzed using FlowJo software.

RESULTS

Induced expression of ICAM, VCAM, not E-selectin by LPS. Endothelial cells have been demonstrated to play crucial roles in inflammation and immune responses by expressing various cell adhesion molecules such as ICAM-1, VCAM-1, and E-selectin. We tested whether these three cellular adhesion molecules were expressed on MBMECs. MBMECs were cultured on chamber slides or 6-well plates and treated with LPS for 3 or 6 hrs. Immunofluorescence staining or flow cytometry were carried out to analyze the expression levels of adhesion molecular levels. In the absence of LPS treatment, we detected no ICAM-1 or E-selectin, and only levels of VCAM-1 slightly above background (Figs. 4.1 and 4.2). Upon stimulation with LPS, both ICAM-1 and VCAM-1 surface expression were increased (Figs. 4.1 and 4.2), but we did not detect any E-selectin expression (data not shown). Using flow cytometry analysis, we observed strong constitutive expression of VCAM-1 without LPS treatment, and again there was no detected expression of ICAM-1 or E-selectin on MBMECs. After stimulation with LPS, the mean fluorescence intensity (MFI) of VCAM-1 was increased from 57 to 97 (Fig. 4.3C, 4.3D), and the MFI of ICAM-1 was increased from 3 to 9 (Fig. 4.3F, 4.3G). E-selectin was not detected after LPS treatment (Fig. 4.3I, 4.3J).

The expression of VCAM-1 and ICAM-1 on the surface of MBMECs were induced by either TNF-α or IFN-γ. The expression of cellular adhesion molecules can be induced by cytokines. We tested whether VCAM-1, ICAM-1, and E-selectin could be induced by TNF-α or IFN-γ on the surface of MBMECs. The cultured MBMECs were treated with either TNF-α or IFN-γ and flow cytometry analysis was carried out to examine the expression levels of VCAM-1, ICAM-1, and E-selectin. There was no detectable E-selectin on MBMECs (data not shown). In

contrast, VCAM-1 and ICAM-1 expression were increased dramatically with TNF-α treatment (Fig. 4.4A, 4.4C). VCAM-1 expression was increased with IFN-γ treatment (Fig. 4.4B). There was little induction of ICAM-1 expression with low dose IFN-γ treatment (data not shown), but increased expression of ICAM-1 was observed using a five-fold higher dose of IFN-γ treatment (Fig. 4.4D). Therefore, our data showed that cytokines TNF-α and IFN-γ induce the expression of VCAM-1 and ICAM-1 on MBMECs.

Lack of uptake of Dil-Ac-LDL by MBMECs. The ability to take up acetylated LDL is one endothelial cell characteristic and we tested whether MBMECs had this characteristic. Mouse macrophage cell line J744A.1 was used as a positive control and mouse 3T6 fibroblast cells as a negative control. In addition, we tested another cultured endothelial cell line, mouse heart microvascular endothelial cells, SHMEC. Macrophage cell line J744A.1 showed strong fluorescence signals upon Dil-Ac-LDL treatment (Fig. 4.5). In contrast, there was no fluorescence signal in 3T6 cells (fibroblast cells), and there was little fluorescence in the two endothelial cell lines. This suggests that this LDL-uptake characteristic of endothelial cells has been lost during culture process for these two endothelial cell lines. In addition, we did not detect the expression of CD31 or endoglin on MBMECs by flow cytometry analysis (data not shown).

Lack of altered expression of cellular adhesion molecules on MBMECs infected with MAV-1. We tested whether MAV-1 infection could alter the expression levels of VCAM-1 or ICAM-1 on MBMECs. Cells were infected with wt MAV-1 at an MOI of 5 and analyzed by flow cytometry at different times post infection. There was little difference in VCAM-1 or ICAM-1 expression levels between mock- and virus-infected cells, whereas TNF-α increased the

expression of both (Fig. 4.6A, 4.6B). These data suggest that MAV-1 infection does not alter the expression levels of VCAM-1 or ICAM-1 on the surface of MBMECs.

DISCUSSION

Previously we observed the accumulation of inflammatory cells in the blood vessels of wt MAV-1-infected mouse brains (6, 12, 13, 17). Since cellular adhesion molecules are important for inflammatory cell attachment, and brain endothelial cells are the only cell type infected by MAV-1 in the brain, we hypothesized that MAV-1 infection might alter the expression levels of cellular adhesion molecules on brain endothelial cells. We first showed that cultured MBMECs maintained some features of endothelial cells, such as VCAM-1 expression, and inducible VCAM-1 and ICAM-1 expression upon stimulation by cytokines and LPS. We also noted that MBMECs lost certain endothelial cell features, such as LDL-uptake, expression of CD31 and endoglin. The loss of some endothelial cell markers during cell culture process is commonly observed for endothelial cells (4, 15). We tested the expression levels of VCAM-1 and ICAM-1 on the surface of MBMECs upon wt MAV-1 infection in cell culture, and found that MAV-1 infection did not alter their expression.

Due to the technical difficulties in isolating primary endothelial cells from mouse brains, we have not been able to test whether MAV-1 infection alters the expression of cellular adhesion molecules on primary cells. But the fact that MAV-1 infection did not change the expression levels of cellular adhesion molecules in cell culture could have several explanations. One is that VCAM-1 and ICAM-1 are not involved in the inflammatory cell accumulation caused by MAV-1 infection, and other cellular adhesion molecules that were not tested are affected by MAV-1 infection. Such other cellular adhesion molecules could include VCAM-2, ICAM-2, or ICAM-3. Alternatively, MAV-1 infection may not change the expression of any cellular adhesion

molecules directly. Since these adhesion molecules can be induced by cytokines (14-16), as shown in Fig. 4.4, the cytokine-induced cellular adhesion molecules might be sufficient to cause inflammatory cell accumulation in the blood vessels of mouse brains we observed in infected mice. Cytokine expression including IFN-γ is increased significantly in MAV-1 infected mouse brains (unpublished data) compared to mock-infected mouse brains. Since the data here were generated from in vitro (cell culture) experiments, it will be of interest to test whether the expression of cellular adhesion molecules is altered in virus-infected mice.

ACKNOWLEDGMENT

I thank Carla Pretto for excellent technical assistance. I thank Dr. Gary Huffnagle for help with flow cytometry analysis. I thank the Spindler lab members for comments on this manuscript. This work was supported by NIH grant R01 AI023762 to K.R.S.

REFERENCES

1. **Andino, R., N. Böddeker, D. Silvera, and A. V. Gamarnik.** 1999. Intracellular determinants of picornavirus replication. Trends in microbiology **7:**76.
2. **Ball, A. O., C. W. Beard, P. Villegas, and K. R. Spindler.** 1991. Early region 4 sequence and biological comparison of two isolates of mouse adenovirus type 1. Virology **180:**257-265.
3. **Bevilaqua, M. P.** 1993. Endothelial-leukocyte adhesion molecules. Annu. Rev. Immunol. **11:**767-804.
4. **Bicknell, R.** 1993. Heterogeneity of the endothelial cell. Behring Inst. Res. Commun. **92:**1-7.
5. **Bilzer, T., and L. Stitz.** 1996. Immunopathogenesis of virus diseases affecting the central nervous system. Crit. Rev. Immunol. **16:**145-222.
6. **Cauthen, A. N., C. C. Brown, and K. R. Spindler.** 1999. In vitro and in vivo characterization of a mouse adenovirus type 1 early region 3 mutant. J. Virol. **73:**8640-8646.
7. **Charles, P. C., J. D. Guida, C. F. Brosnan, and M. S. Horwitz.** 1998. Mouse adenovirus type-1 replication is restricted to vascular endothelium in the CNS of susceptible strains of mice. Virology **245:**216-228.
8. **Geng, J. G., M. P. Bevilaqua, K. L. Moore, and T. M. McIntyre.** 1990. Rapid neutrophil adhesion to activated endothelium mediated by p-selectin. Nature **343:**757-760.
9. **Horwitz, M. S.** 2001. Adenoviruses, p. 2301-2326. *In* D. M. Knipe and P. M. Howley (ed.), Fields Virology, 4th ed, vol. 2. Lippincott Williams & Wilkins, Philadelphia.

10. **Kajon, A. E., C. C. Brown, and K. R. Spindler.** 1998. Distribution of mouse adenovirus type 1 in intraperitoneally and intranasally infected adult outbred mice. J. Virol. **72:**1219-1223.

11. **Malik, A. B., and S. K. Lo.** 1996. Vascular endothelial adhesion moleculaes and tissue inflammation. Pharmacological Rev. **48:**213-229.

12. **Moore, M. L., C. C. Brown, and K. R. Spindler.** 2003. T cells cause acute immunopathology and are required for long-term survival in mouse adenovirus type 1-induced encephalomyelitis. J. Virol. **77:**10060-10070.

13. **Moore, M. L., E. L. McKissic, C. C. Brown, J. E. Wilkinson, and K. R. Spindler.** 2004. Fatal disseminated mouse adenovirus type 1 infection in mice lacking B cells or Bruton's tyrosine kinase. *J. Virol.* **in press**.

14. **Parr, M. B., and E. L. Parr.** 2000. Interferon-gamma up-regulates intercellular adhesion molecule-1 and vascular cell adhesion molecule-1 and recruits lymphocytes into the vagina of immune mice challenged with herpes simplex virus-2. Immunology **99:**540-5.

15. **Ruszczak, Z., and R. A. Schwartz.** 1996. Vascular endothelium in the regulation of immune response. Res. Comm. Molec. Pathol. Pharm. **94:**3-21.

16. **Shen, J., T. T. SS, L. Schrieber, and N. J. King.** 1997. Early E-selectin, VCAM-1, ICAM-1, and late major histocompatibility complex antigen induction on human endothelial cells by flavivirus and comodulation of adhesion molecule expression by immune cytokines. J Virol **71:**9323-32.

17. **Spindler, K. R., L. Fang, M. L. Moore, C. C. Brown, G. N. Hirsch, and A. K. Kajon.** 2001. SJL/J mice are highly susceptible to infection by mouse adenovirus type 1. J. Virol. **75:**12039-12046.

Fig. 4.1. Immunofluorescence staining for VCAM-1 on MBMECs. MBMECs were treated with 1 μg/ml LPS for 3 (A-F) or 6 hours (G-I). FITC-conjugated anti-rat IgG was used as a secondary antibody. Multiple fields were photographed at 100X from the same chamber well; representive fields are shown. Cells that were treated with LPS for 3 hrs and stained with secondary antibody only (2nd Ab alone) were used as a background control (A). -LPS, no LPS treatment (B, C). +LPS, with LPS treatment (D-I). Scale bar, 50 μm.

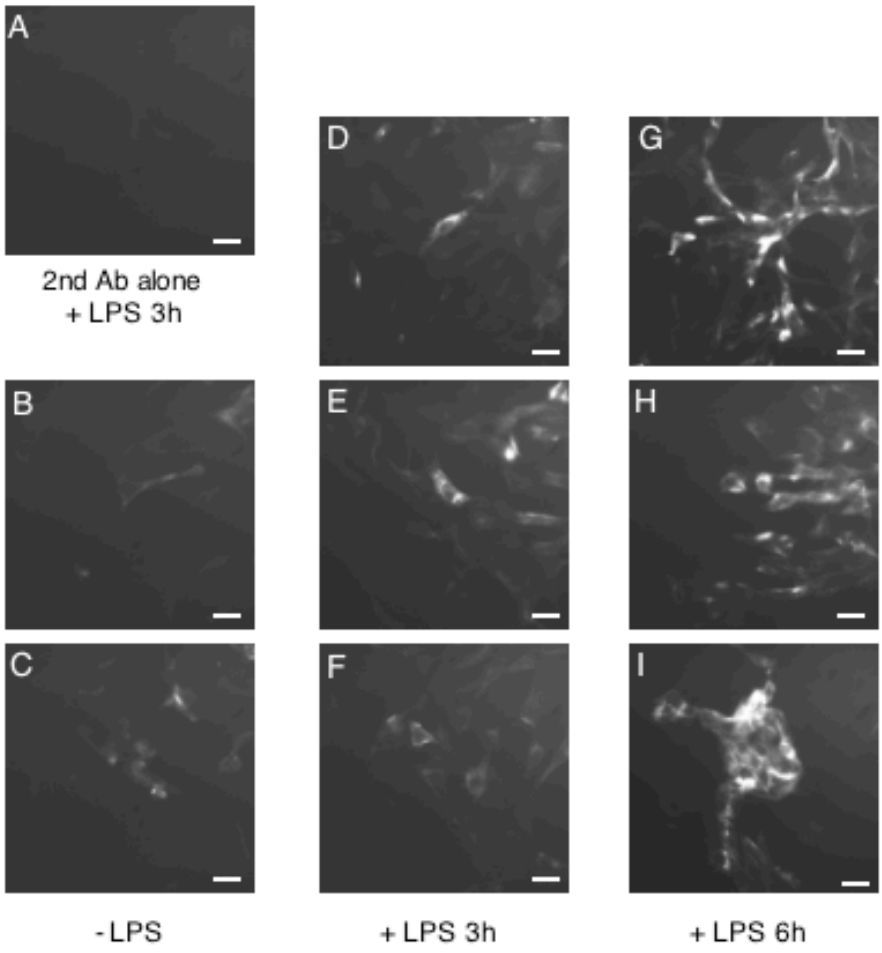
A
2nd Ab alone
+ LPS 3h
D
G
B
E
H
C
F
I
- LPS
+ LPS 3h
+ LPS 6h

Fig. 4.2. Immunofluorescence staining for ICAM-1 on MBMECs. MBMECs were treated with 1 μg/ml LPS for 3 (A-G) or 6 hours (H-K). FITC-conjugated anti-rat IgG was used as a secondary antibody. Multiple fields were photograghed at 100X from the same chamber well; representative fields are shown here. Cells that were treated with LPS for 3 hrs and stained with secondary antibody only (2nd Ab alone) were used as a background control (A). -LPS, no LPS treatment (B, C). +LPS, with LPS treatment (D-K). Scale bar, 50 μm.

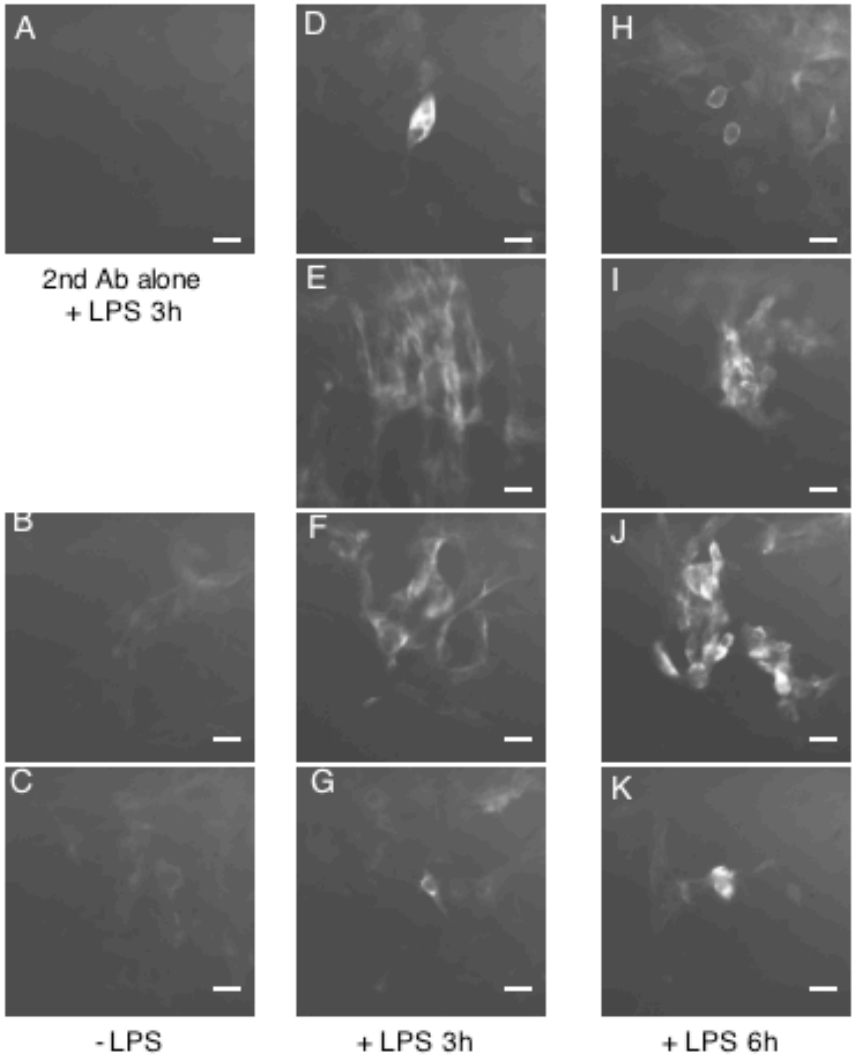
A
D
H
2nd Ab alone
+ LPS 3h
E
I
B
F
J
C
G
K
- LPS
+ LPS 3h
+ LPS 6h

Fig. 4.3. Flow cytometry analysis of LPS induction of VCAM-1 and ICAM-1, but not E-selectin, surface expression on MBMECs. Cells were cultured to 100% confluence and treated with 1 μg/ml LPS for 6 hours. Cells were harvested and stained with primary antibodies against VCAM-1 (panels C, D, and E), ICAM-1 (panels F, G, and H), or E-selectin (panels I, J and K) as indicated. The flow cytometry data are presentated as histograms. Panels A and B, ovals (85% of total cells) show the cells that were gated for the 0 and 6 hrs FACS analysis, respectively. The x-axis represents forward scatter (FSC), the y-axis represents side scatter (SSC). Panels C, D, F, G, I, and J, the dark gray lines in represent the isotype antibody controls, and the light gray lines represent the antibody-stained samples as indicated at the left side. The x-axis represents the fluorescence intensity. The bars represent the percentage of gated cells with the fluorescence intensity larger than the defined levels. Overlays of the histograms for 0 h and 6 h samples are shown for direct comparison (panels E, H, and K).

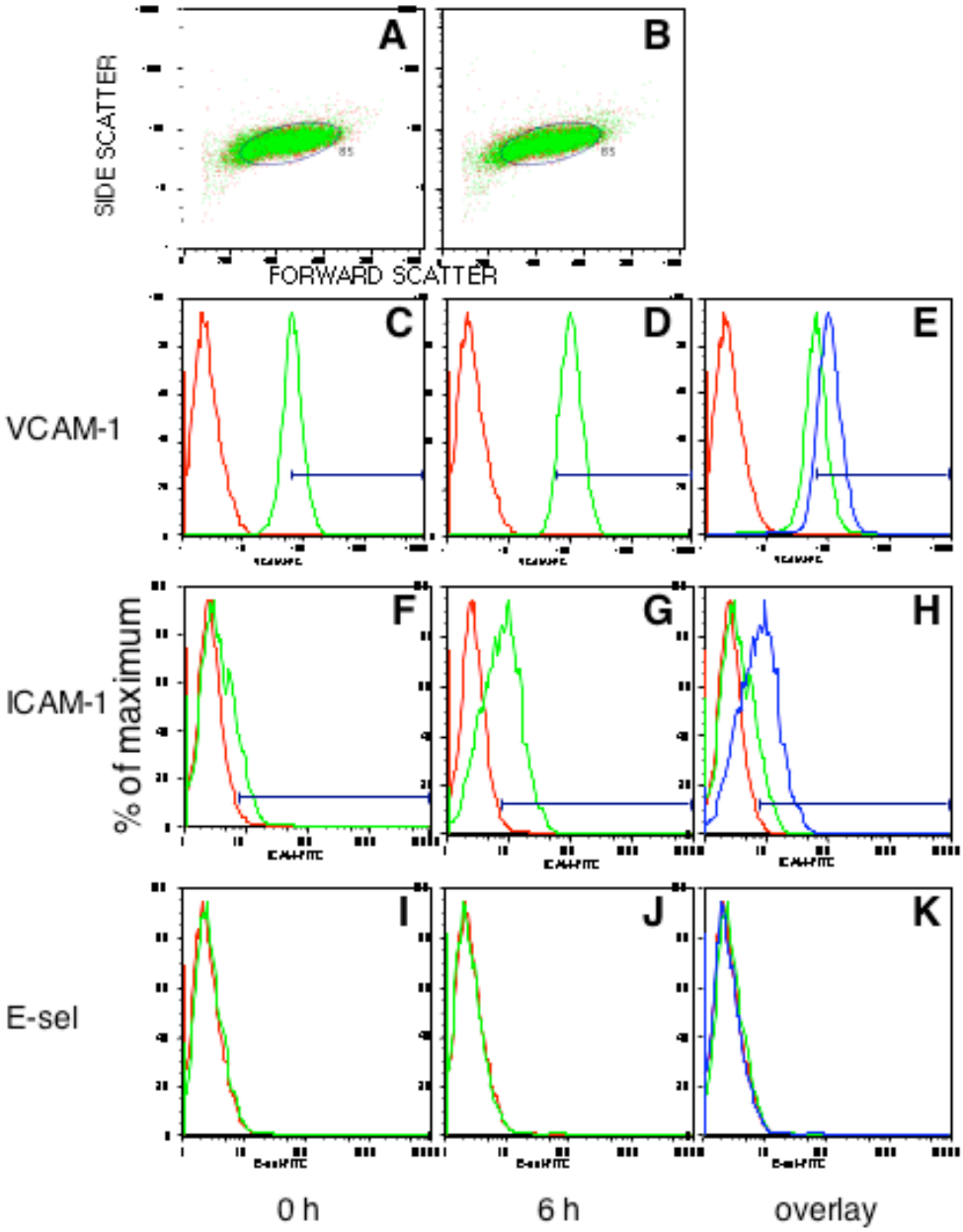
A
B
SIDE SCATTER
FORWARD SCATTER
C
D
E
VCAM-1
F
G
H
ICAM-1
% of maximum
I
J
K
E-sel
0 h
6 h
overlay

Fig. 4.4. Flow cytometry analysis of TNF-α and IFN-γ induction of VCAM-1 and ICAM-1 expression on MBMECs. Cells were cultured to 100% confluence and treated with either TNF-α or IFN-γ, and harvested at different time points as indicated. Cells were stained with antibodies against VCAM-1 or ICAM-1 and followed by flow cytometry analysis. Isotype antibody controls were used as negative controls. The mean fluorescence intensities (MFI) are shown in the upper right. A, VCAM-1 expression of cells treated with 10 ng/μl TNF-α for the indicated times. B, VCAM-1 expression treated with 20 units/ml IFN-γ for indicated times. C, ICAM-1 expression of cells treated with 10 ng/μl TNF-α. D, ICAM-1 expression of cells treated with 100 units/ml IFN-γ.

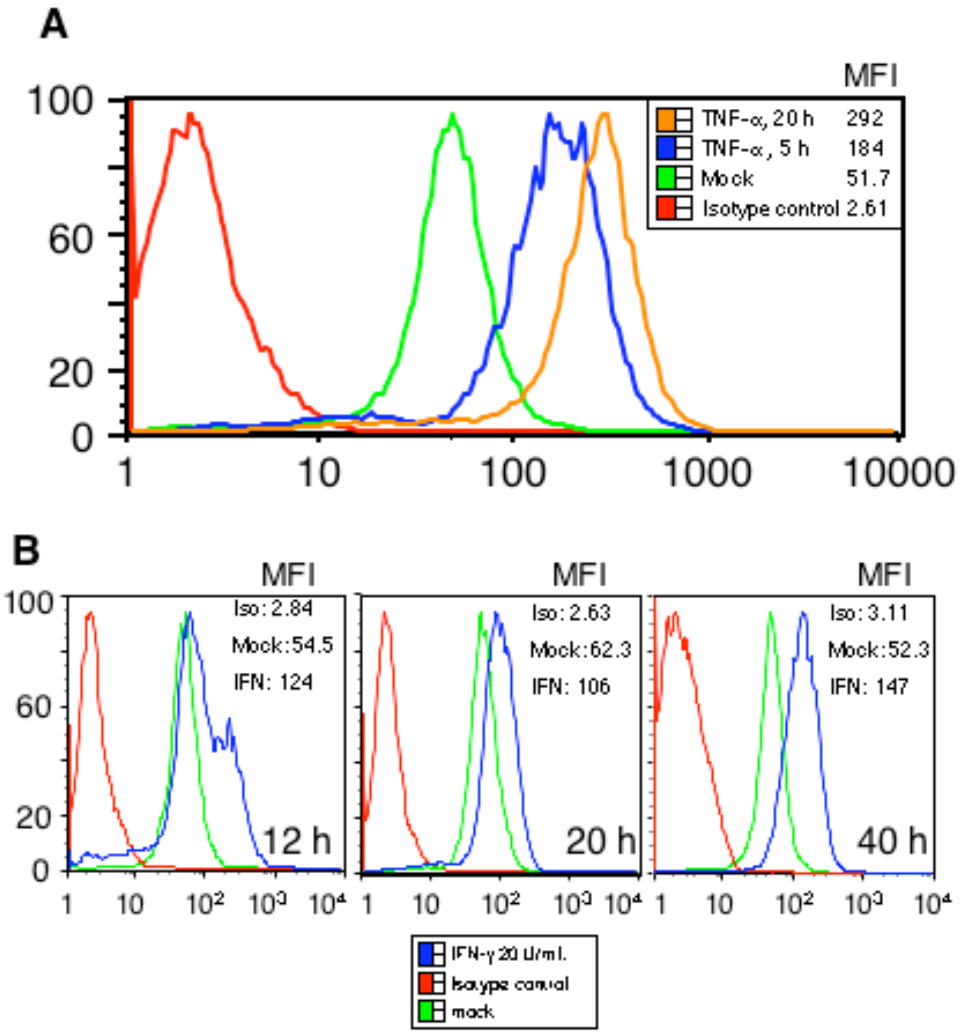
A
MFI
100
60
20
0
1
10
100
1000
10000
TNF-α, 20 h 292
TNF-α, 5 h 184
Mock 51.7
Isotype control 2.61
B
MFI
MFI
MFI
Iso: 2.84
Mock: 54.5
IFN: 124
12 h
Iso: 2.63
Mock: 62.3
IFN: 106
20 h
Iso: 3.11
Mock: 52.3
IFN: 147
40 h
IFN-γ 20 U/ml.
Isotype control
mock

C

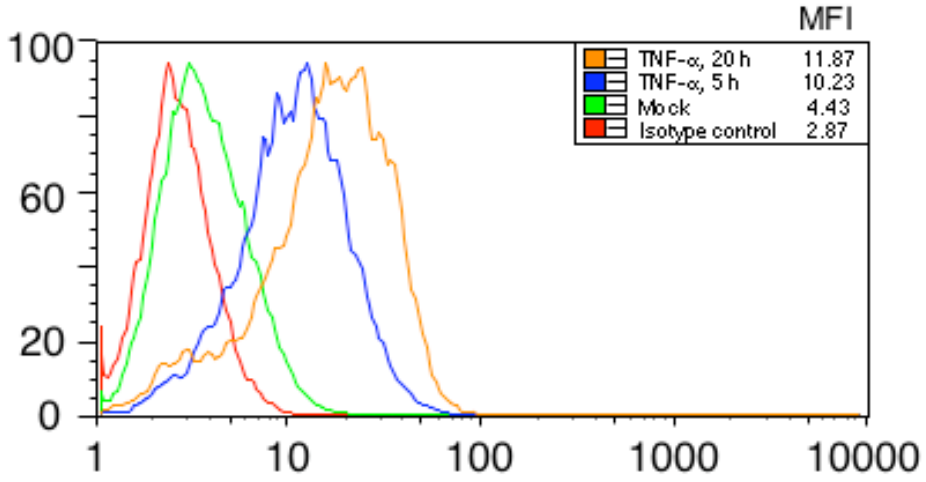
MFI
TNF-α, 20 h 11.87
TNF-α, 5 h 10.23
Mock 4.43
Isotype control 2.87
100
60
20
0
1
10
100
1000
10000

D

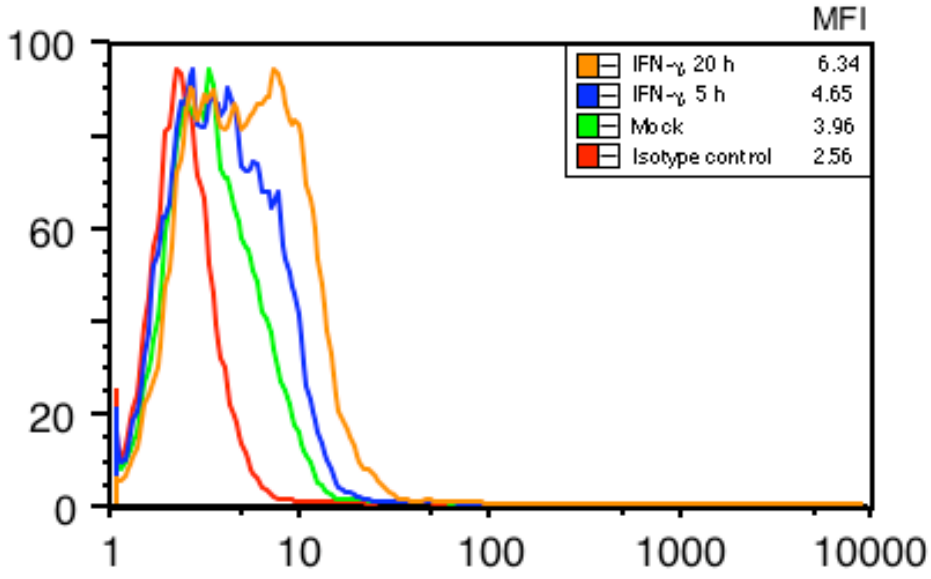
MFI
IFN-γ, 20 h 6.34
IFN-γ, 5 h 4.65
Mock 3.96
Isotype control 2.56
100
60
20
0
1
10
100
1000
10000

Fig. 4.5. DiI-Ac-LDL staining. 3T6 (fibroblast cells), MBMEC (brain endothelial cells), SHMEC (heart endothelial cells), J774A.1 (macrophage cells) were incubated with 10 μg/ml DiI-Ac-LDL for 40 min at 37º C and observed by fluorescence microscopy (Leika). One representative picture of each is shown (200X). Scale bar, 50 μm.

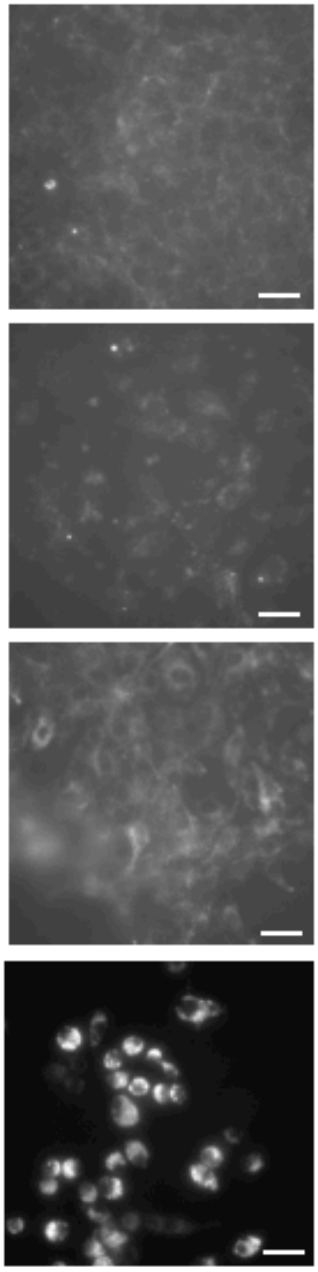
3T6
MBMEC
SHMEC
J774A.1

Fig. 4.6. Effects of MAV-1 infection on VCAM-1 or ICAM-1 surface expression on MBMECs. Cells were infected with wild type MAV-1 at an MOI of 5 and harvested at the indicated times post infection. Cells were stained with antibodies against VCAM-1 or ICAM-1, and analyzed by flow cytometry. Isotype antibody controls were used as negative controls. Cells treated with 10 ng/ml TNF-α were used as positive controls. A, histograms of flow cytometry data. B, the mean fluorescence intensities from samples in panel A.

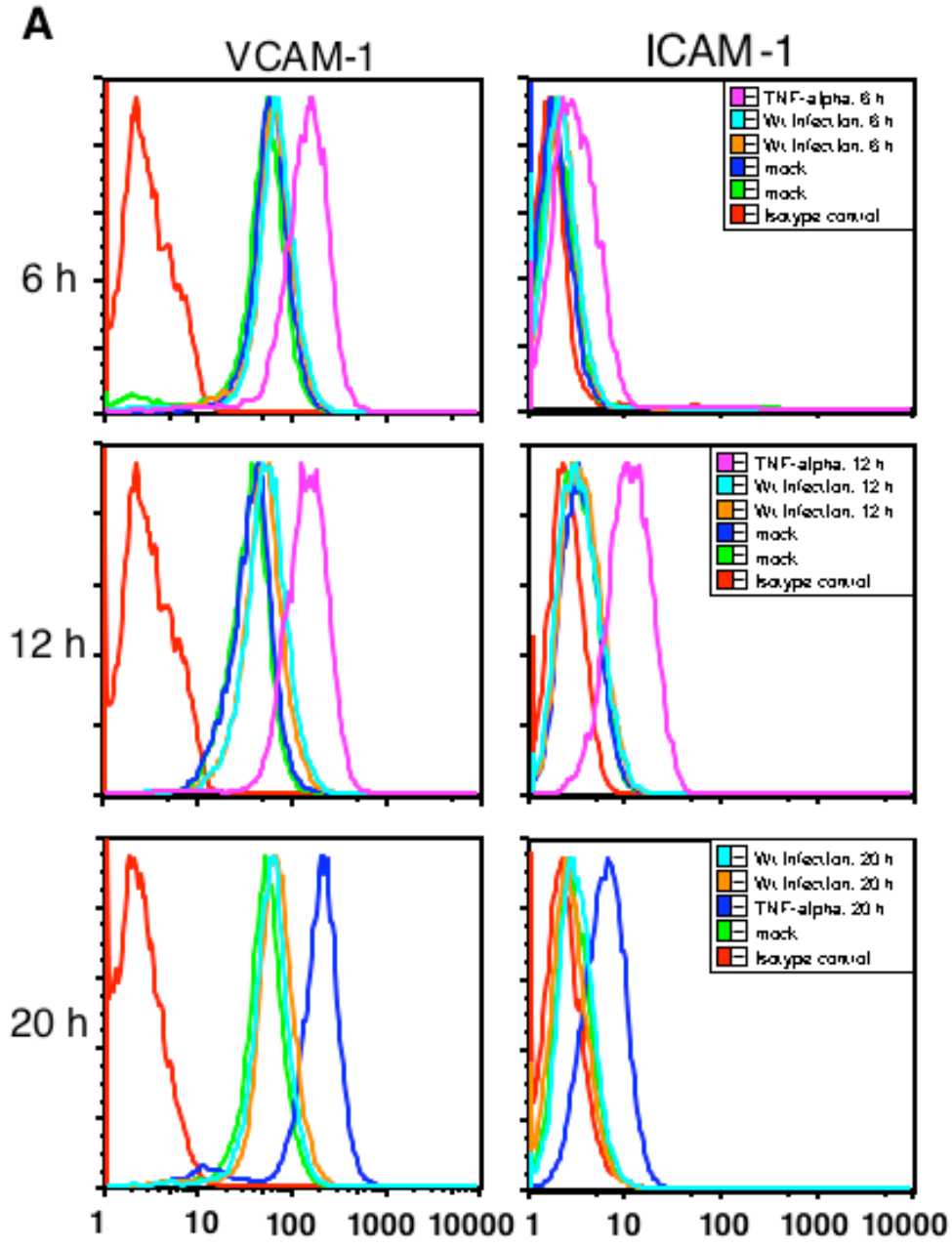
A
VCAM-1
ICAM-1
6 h
12 h
20 h
TNF-alpha, 6 h
Wt Infection, 6 h
Wt Infection, 6 h
mock
mock
Isotype control
TNF-alpha, 12 h
Wt Infection, 12 h
Wt Infection, 12 h
mock
mock
Isotype control
Wt Infection, 20 h
Wt Infection, 20 h
TNF-alpha, 20 h
mock
Isotype control
1
10
100
1000
10000
1
10
100
1000
10000

B

	VCAM-1			ICAM-1		
MFI	6 h	12 h	20 h	6 h	12 h	20 h
isotype	3.39	3.53	2.47	2.36	2.68	2.62
mock	55.4	39.6	56	2.43	3.54	3.16
mock	65.5	42.3	N.A.	1.98	3.65	N.A.
infected	70.2	55.8	64.5	2.33	3.81	3.16
infected	74.2	60.4	73.8	2.32	3.71	2.86
TNF-α	163	164	208	3.57	12.5	6.18

MFI, mean fluorescence intensity
N.A., not assayed.

CHAPTER 5

DISCUSSION

We identified mSur2 as a protein that interacts with MAV-1 E1A (Chapter 2). The CR3 domain of MAV-1 E1A is required for this protein-protein interaction, as is true of the hAd E1A-Sur2 interaction. Study of mSur2 functions showed that it is important for efficient MAV-1 replication. Our data using E1A mutant viruses and $Sur2^{-/-}$ MEFs suggest that mSur2 may function through both E1A CR3 interaction-dependent and -independent pathways (Chapter 3). This raises many interesting questions.

In order to address more definitively the important function of E1A CR3-mSur2 interaction in MAV-1 replication, it will be useful to generate either an MAV-1 E1A mutant virus that is only defective in binding mSur2 or a cell line/mice with mutant mSur2 that is only defective in binding E1A CR3. It is known that the zinc finger motif in CR3 of E1A protein is critical for binding to Sur2 (1, 3). hAd E1A with a single amino acid mutation in the CR3 domain is defective in binding Sur2 protein. Like hAd, E1A CR3 of MAV-1 has a zinc finger motif. Ideally, we will generate an E1A mutant virus with a single amino acid mutation in the CR3 domain that only lacks the ability to bind to mSur2. Since we do not know what amino acid in CR3 that would be, first we would need to test multiple sites in an in vitro binding assay, such as GST pulldown assay like that used in Chapter 2. Four conserved cysteine sites, which are essential for the zinc finger motif, are of particular interest to test initially. Based on the GST pulldown results, we would generate a series of mutant viruses in the CR3 domain. Each mutant virus would only have a single amino acid mutation and would be defective in binding to mSur2. If all of these mutants show essentially the same growth defect, it would strongly argue that the defect is due to the lack of CR3-mSur2 interaction.

Since the Sur2 knock-out is embryonic lethal in mice (Jennitte L. Stevens and Arnold J. Berk, personal communication), we cannot directly study functions of Sur2 in MAV-1

replication in mice. Study of mice infected with *pm*E109 and *dl*E106 mutant viruses that are not able to bind to mSur2 is not a direct assay to test Sur2 function. Therefore, it will be ideal to have conditional Sur2 knockout mice to study. One approach would to use a lentivirus-based vector to deliver siRNAs to knock down the Sur2 expression in the mouse brains. Lentiviral vectors have been successfully used to deliver genes in mice (18, 19). More importantly, they can be genetically engineered to target specific cell types, for instance, endothelial cells (5). Once these mice are available, we can study the Sur2 functions in mice. Alternatively, when we know which domain of mSur2 interacts with E1A CR3, we could knock out the specific binding domain of mSur2, instead of the full gene, in mice. This partially deleted mSur2 in mice might not be embryonic lethal. Then these specific domain mSur2 knockout mice will be useful to address the functions of E1A CR3-mSur2 interaction in MAV-1 infection.

Strikingly, we observed that mSur2 was able to function in MAV-1 replication through an E1A CR3 interaction-independent pathway. Similar to this, E1A CR1 binding proteins, p300/CBP can stimulate hAd E1A CR1-dependent transactivation through an E1A CR1 interaction-independent pathway (12). It is of interest to investigate the E1A interaction-independent mechanisms. Study of physiological functions of Sur2 may address the molecular mechanisms of its action. Elk-1, a transcriptional factor, interacts with Sur2 and recruits Mediator complex in mouse embryonic stem (ES) cells (17). The interaction between Elk-1 and Sur2 is required for activating endogenous immediate early genes, such as egr-2, in response to the RTK-Ras-Raf-MEK-ERK signaling pathway (17). MAV-1 E1A also interacts with Sur2 (Chapter 2). We tested whether MAV-1 E1A interfered with Elk-1 function through competition with Elk-1 for binding to mSur2. $Sur2^{+/+}$ and $Sur2^{-/-}$ MEFs were infected with wt MAV-1 at an MOI of 1 and incubated with media containing 2% FBS for 24 hours, then with media containing

0.1% FBS for another 24 hours. Total RNAs were isolated after cells were induced with 20% FBS for different times. RNase protection assays (RPAs) were carried out to quantify the serum-induced egr-2 mRNA levels (Fig. 5.1A). The viral mRNAs were assayed to confirm successful viral infection (Fig. 5.1B). In the mock-infected samples, egr-2 levels were transiently increased and reached peak levels between 30 to 60 min after serum addition to serum-starved $Sur2^{+/+}$ MEFs, consistent with published results (17). There was about 3 to 5-fold more egr-2 mRNA in $Sur2^{+/+}$ than $Sur2^{-/-}$ MEFs. This is not as dramatic as the difference between $Sur2^{+/+}$ and $Sur2^{-/-}$ ES cells (17). This suggested that there might be some transcription factors not expressed in ES cells but expressed in MEFs that can partially compensate the loss of function of mSur2. In the wt MAV-1-infected $Sur2^{+/+}$ MEFs, the serum-induced egr-2 mRNA levels were reduced compared to mock-infected $Sur2^{+/+}$ MEFs. There was little difference in egr-2 mRNA levels between virus- and mock-infected $Sur2^{-/-}$ MEFS. These data showed that wt MAV-1 infection could reduce the serum-induced transcription of egr-2. However, preliminary data showed that infections of E1A mutant viruses in $Sur2^{+/+}$ MEFs also decrease the serum-induced egr-2 mRNA levels as did wt MAV-1 infection (Fig. 5.2), which suggested that E1A was not responsible for the down-regulation of the serum-induced egr-2 expression. However, the serum-induced egr-2 expression is dependent on Sur2 (17, and Fig. 5.1 and 5.2). Therefore, we found a function of Sur2 that is independent of E1A. Since MAV-1 infection (including wt and E1A mutants) decreased the serum-induced egr-2 mRNA levels, it is of interest to investigate which viral gene(s) is responsible for this down-regulation. There are MAV-1 E3 null mutant, and E1B null mutant viruses available that we can test whether E3 and/or E1B are involved in this down-regulation of serum-induced egr-2.

We have also identified several other potential MAV-1 E1A interacting proteins from GST pull-down assays. There are at least two potential MAV-1 E1A interacting proteins, Mybbp1a (Myb binding protein 1a) and GCN1, that have not been shown to interact with hAd E1A. We are currently verifying the interactions between these two cellular proteins with MAV-1 E1A.

MAV-1 targets endothelial cells and the mononuclear/macrophage lineage in mice, and mouse brain and spleen are two major sites for MAV-1 replication. Although the mechanism of endothelial tropism of MAV-1 has not been fully elucidated, study of MAV-1 infection in its targeted cells will help address some unresolved questions. MAV-1 infection of a variety of cell types (renal, renal adenosarcoma, connective tissue, and embryonic origin) does not affect the surface expression of mouse class I major histocompatibility complex (MHC) (10). The recent discovery of mouse brain microvascular endothelial cells (ECs) as the major MAV-1 target cell type renders the possibility that only a unique cell type exists in which MAV-1 infection alters the expression of class I MHC. MHC class II molecules can be induced on other cell types by interferon (IFN) -γ. There is relatively little information concerning the role of brain capillary EC expression of MHC molecules during viral infection (2). In mice susceptible to Theiler's virus-induced demyelination, but not in resistant mice, expression of MHC class II on cerebrovascular ECs was observed 24 hours after IFN-γ treatment (20). Animal strain variations in levels of inducible MHC antigens on rat cerebral ECs have also been described (11). In a study of experimental allergic encephalomyelitis (EAE), the investigative analog to human multiple sclerosis, MHC class II expression correlated with strain-specific susceptibility to EAE (8). However, MHC class II expression has not been evaluated in MAV-1 infection.

MAV-1 E1A mutants grow like wt virus in mouse fibroblast cells (3T6 cell line) at an MOI of 5. Besides using a low multiplicity infection to see phenotypic differences between wt and mutant viruses (Chapter 2), using a cell line that closely resembles the natural target of the virus may be more informative to elucidate E1A functions. In fact, *pm*E109 (E1A null mutant) showed a severe replication defect in mouse brain microendothelial cells (MBMECs) compared to wt MAV-1 at an input MOI of 0.05 (Martin L. Moore and Katherine R. Spindler, unpublished data). We tested another cell line IBE (immortalized brain endothelial) cells, which were derived from tsA58 Large T transgenic mice (9). Unfortunately, MAV-1 did not grow efficiently in this cell line.

MAV-1 causes encephalomyelitis in mice (7, 13, 16). We consistently observe increased inflammatory cell accumulation in the blood vessels of wt MAV-1 virus-infected brains (4, 13, 14). More interestingly, there was less inflammatory reaction in brains infected with an E3 null mutant (*dl*E314) compared to wt MAV-1 (4). Because of the important functions of cellular adhesion molecules in inflammatory cell recruitment, we hypothesized that wt MAV-1 infection in endothelial cells in mouse brains may increase the expression of cellular adhesion molecules on the cell surface, which in turn facilitate the accumulation of inflammatory cells in blood vessels. MBMECs displayed some EC characteristics but not all (Chapter 4). It has been observed that the cultured endothelial cells may lose their cell type features due to continuous passage of cells in culture (15). However, using MBMECs as an in vitro model, we found no increased expression of VCAM-1 or ICAM-1 on the cell surface upon MAV-1 infection (Chapter 4). It is of interest to test whether MAV-1 infection can alter the expression levels of cellular adhesion molecules after IFN-γ and/or TNF-α stimulation. In addition, we are in the

process of isolating primary brain microvesular endothelial cells, which might give different results from cultured MBMECs.

REFERENCES

1. **Berk, A. J., T. G. Boyer, A. N. Kapanidis, R. H. Ebright, N. N. Kobayashi, P. J. Horn, S. M. Sullivan, R. Koope, M. A. Surby, and S. J. Triezenberg.** 1998. Mechanisms of viral activators. Cold Spring Harb. Symp. Quant. Biol. **63:**243-252.

2. **Bilzer, T., and L. Stitz.** 1996. Immunopathogenesis of virus diseases affecting the central nervous system. Crit. Rev. Immunol. **16:**145-222.

3. **Boyer, T. G., M. E. D. Martin, E. Lees, R. P. Ricciardi, and A. J. Berk.** 1999. Mammalian Srb/Mediator complex is targeted by adenovirus E1A protein. Nature **399:**276-279.

4. **Cauthen, A. N., C. C. Brown, and K. R. Spindler.** 1999. In vitro and in vivo characterization of a mouse adenovirus type 1 early region 3 mutant. J. Virol. **73:**8640-8646.

5. **De Palma, M., M. A. Venneri, and L. Naldini.** 2003. In vivo targeting of tumor endothelial cells by systemic delivery of lentiviral vectors. Hum. Gene. Ther. **14:**1193-206.

6. **Fang, L., J. L. Stevens, A. J. Berk, and K. R. Spindler.** 2004. Requirement of Sur2 for efficient mouse adenovirus type 1 replication. J. Virol.**:***in press.*

7. **Guida, J. D., G. Fejer, L.-A. Pirofski, C. F. Brosnan, and M. S. Horwitz.** 1995. Mouse adenovirus type 1 causes a fatal hemorrhagic encephalomyelitis in adult C57BL/6 but not BALB/c mice. J. Virol. **69:**7674-7681.

8. **Jemison, L. M., S. K. Williams, N. Prayoonwiwat, and M. Rodriguez.** 1993. Interferon-gamma-inducible endothelial cell class II major histocompatibility complex

expression correlates with strain- and site-specifc susceptibility to experimental allergic encephalomyelitis. J. Neuroimmunol. **47:**15-25.

9. **Kanda, S., E. Landgren, M. Ljungström, and L. Claesson-Welsh.** 1996. Fibroblast growth factor receptor 1-induced differentiation of endothelial cell line established from TsA58 large T transgenic mice. Cell Growth Differ. **7:**383-395.

10. **Kring, S. C., and K. R. Spindler.** 1996. Lack of effect of mouse adenovirus type 1 infection on the cell surface expression of major histocompatibility complex class I antigens. J. Virol. **70:**5495-5502.

11. **Linke, A. T., and D. K. Male.** 1994. Strain-specifc variation in constitutive and inducible expression of mhc class ii, class i and icam-1 on rat cerebral endothelium. Immunology **82:**88-98.

12. **Mannervik, M., and G. Akusjarvi.** 1997. The transcriptional co-activator proteins p300 and CBP stimulate adenovirus E1A conserved region 1 transactivation independent of a direct interaction. FEBS Lett. **414:**111-6.

13. **Moore, M. L., C. C. Brown, and K. R. Spindler.** 2003. T cells cause acute immunopathology and are required for long-term survival in mouse adenovirus type 1-induced encephalomyelitis. J. Virol. **77:**10060-10070.

14. **Moore, M. L., E. L. McKissic, C. C. Brown, J. E. Wilkinson, and K. R. Spindler.** 2004. Fatal disseminated mouse adenovirus type 1 infection in mice lacking B cells or Bruton's tyrosine kinase. J. Virol. **78**:5584-5590.

15. **Ruszczak, Z., and R. A. Schwartz.** 1996. Vascular endothelium in the regulation of immune response. Res. Comm. Molec. Pathol. Pharm. **94:**3-21.

16. **Spindler, K. R., L. Fang, M. L. Moore, C. C. Brown, G. N. Hirsch, and A. K. Kajon.** 2001. SJL/J mice are highly susceptible to infection by mouse adenovirus type 1. J. Virol. **75:**12039-12046.

17. **Stevens, J. L., G. T. Cantin, G. Wang, A. Shevchenko, A. Shevchenko, and A. J. Berk.** 2002. Transcription control by E1A and MAP kinase pathway via Sur2 mediator subunit. Science **296:**755-758.

18. **Tiscornia, G., O. Singer, M. Ikawa, and I. M. Verma.** 2003. A general method for gene knockdown in mice by using lentiviral vectors expressing small interfering RNA. Proc. Natl. Acad. Sci. USA **100:**1844-1848.

19. **Tiscornia, G., V. Tergaonkar, F. Galimi, and I. M. Verma.** 2004. CRE recombinase-inducible RNA interference mediated by lentiviral vectors. Proc. Natl. Acad. Sci. USA **101:**7347-51.

20. **Welsh, J., B. Sapatino, B. Rosenbaum, R. Smith, and S. Linthicum.** 1993. Correlation between susceptibility to demyelination and interferon-gamma induction of major histocompatibility complex claas II antigens on murine cerebrovascular endothelial cells. J. Neuroimmunol. **48:**91-100.

Fig. 5.1. Wt MAV-1 infection down-regulated the serum induced egr-2 mRNA expression. $Sur2^{+/+}$ and $Sur2^{-/-}$ MEFs were infected with wt MAV-1 at an MOI of 1 and incubated with media containing 2% FBS for 24 hours, then with media containing 0.1% FBS for another 24 hours. Total RNAs were isolated after cells were induced with 20% FBS after the indicated times. A, RNase protection assays (RPAs) were carried out and ImageQuant software was used to quantify the serum-induced egr-2 mRNA levels. The egr-2 signals were normalized against mouse L32 signals. B, Viral mRNAs (E4, E1A, and hexon) were assayed using RPAs to confirm viral infection in $Sur2^{+/+}$ and $Sur2^{-/-}$ MEFs.

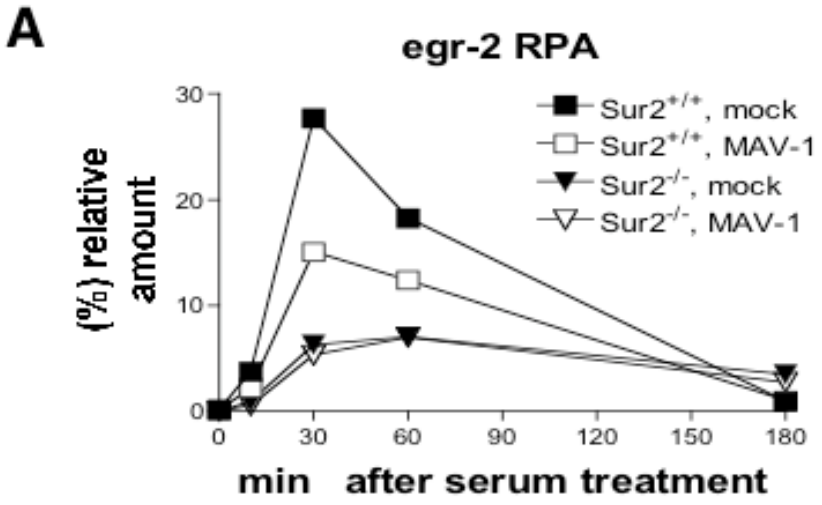
A
egr-2 RPA
{%} relative amount
30
20
10
0
0
30
60
90
120
150
180
min after serum treatment
Sur2+/+, mock
Sur2+/+, MAV-1
Sur2-/-, mock
Sur2-/-, MAV-1

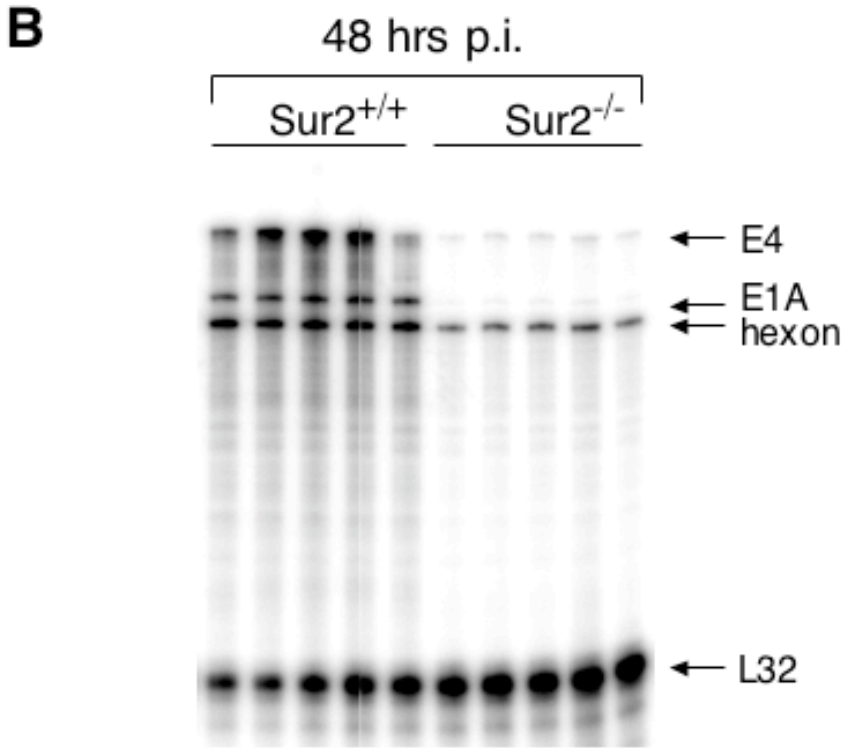
B
48 hrs p.i.
Sur2+/+
Sur2-/-
E4
E1A
hexon
L32

Fig. 5.2. Down-regulation of the serum induced egr-2 mRNA expression is MAV-1 E1A independent. Sur2$^{+/+}$ and Sur2$^{-/-}$ MEFs were infected with wt MAV-1, *pm*E109 (E1A null), *dl*E105 (CR1Δ), *dl*E102 (CR2Δ), or *dl*E106 (CR3Δ) at an MOI of 1 and incubated with media containing 2% FBS for 24 hours, then with media containing 0.1% FBS for another 24 hours. Mock-infected cells were used as negative controls. Total RNAs were isolated after cells were induced with 20% FBS after indicated times. A, RNase protection assays (RPAs) were carried out to analyze the serum-induced egr-2 mRNA levels. The sample in lane 11 was lost during experiments. B, ImageQuant software was used to quantify the serum-induced egr-2 mRNA levels. The egr-2 signals were normalized against mouse L32 signals. The sample numbers in panel B are same as the lane numbers in panel A.

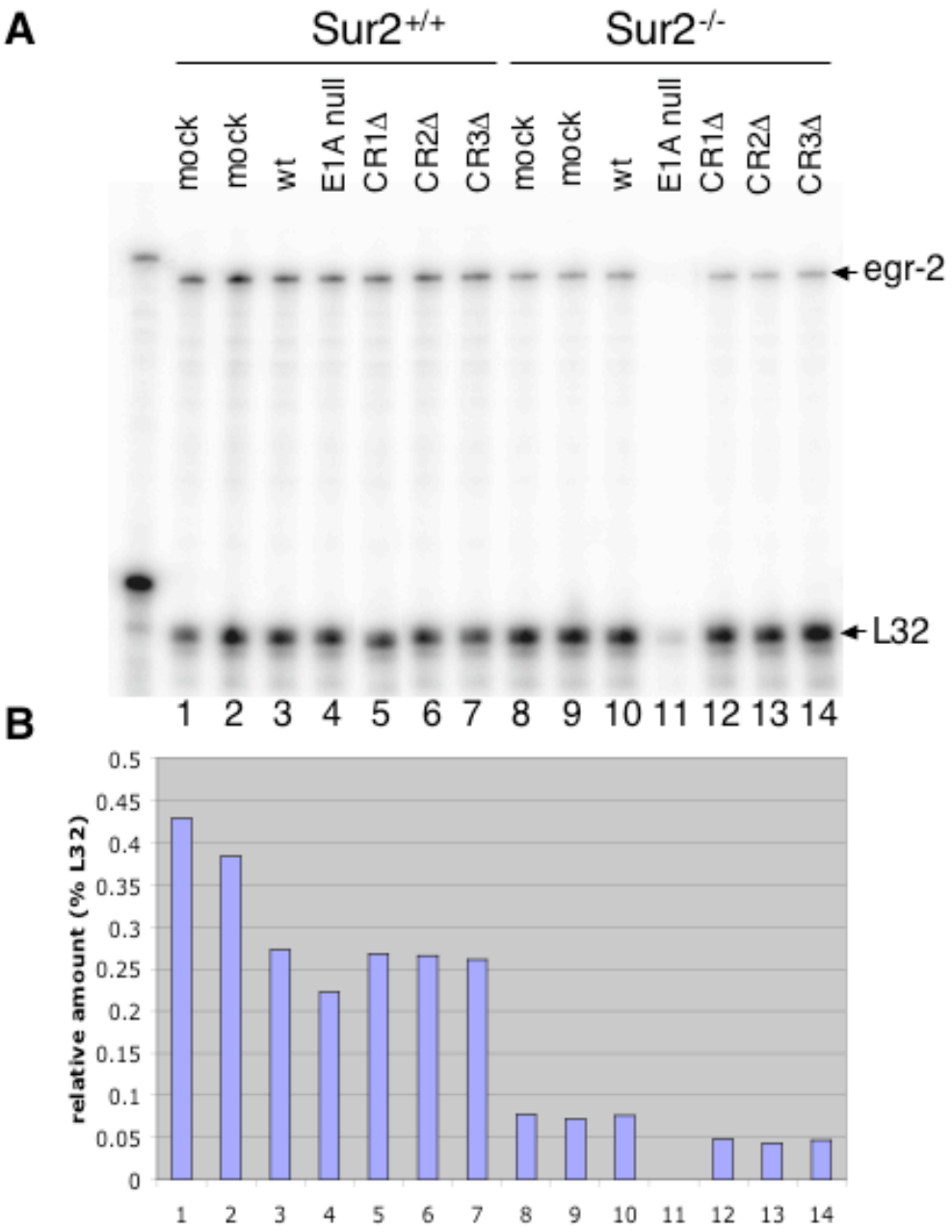
A
Sur2+/+
Sur2-/-
mock
mock
wt
E1A null
CR1Δ
CR2Δ
CR3Δ
mock
mock
wt
E1A null
CR1Δ
CR2Δ
CR3Δ
egr-2
L32
1 2 3 4 5 6 7 8 9 10 11 12 13 14
B
relative amount (% L32)
0.5
0.45
0.4
0.35
0.3
0.25
0.2
0.15
0.1
0.05
0
1 2 3 4 5 6 7 8 9 10 11 12 13 14